

The Formation and Structure
of the Basal Body (Centriole) from
the Rhesus Monkey Oviduct

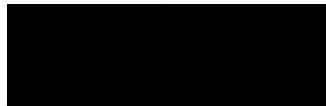
by

Richard G. W. Anderson, B.S.

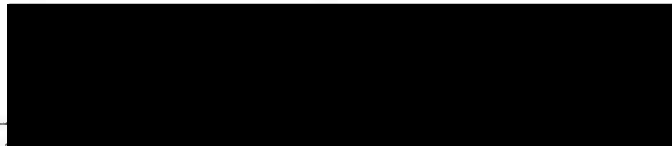
A THESIS
Presented to the Department of Anatomy
and the Graduate Division of the University of Oregon Medical School
in partial fulfillment of
the requirements for the degree of
Doctor of Philosophy

June 1970

APPROVED:



(Professor in Charge of Thesis)



(Chairman, Graduate Society)

This thesis is dedicated to

Barbara F. Anderson

Together we have learned to love and to understand
peace.

ACKNOWLEDGEMENTS

I would like to thank Dr. Robert M. Brenner for his guidance during the development of this thesis. Dr. Brenner's investigation of hormonally-driven ciliogenesis formed the foundation for my investigation, and his encouragement and foresight channeled my research efforts towards a worthwhile goal. It is to his credit that my initial naivete did not discourage him. I am thankful that my interest in differentiation and reproduction has increased as a result of our working relationship.

I owe a great deal to Dr. Robert L. Bacon, not only for stimulating my initial interests in developmental biology, but for giving me the opportunity to read, theorize, and develop an inquisitive mind. The numerous discussions which we had were fundamental to the development of my research interests. Thank you!

I would like to acknowledge the excellent technical assistance of Carole J. Kuster and Norma Hoskins. The excellent drawings were the product of my mind and the artistic talents of Joel H. Ito and Donna Ryan. Without the secretarial assistance of Sharon Maher, this thesis would not have been produced.

Finally, I would like to thank Drs. Wolf H. Fahrenbach, Nancy J. Alexander, Paul F. Parakkal, and Mary Bell. These people showed me that quality is as important to research as imagination.

TABLE OF CONTENTS

INTRODUCTION.....	1
MATERIALS AND METHODS.....	9
Experimental System.....	9
Labeling of the Fimbriae.....	9
Radioautography.....	10
Light Microscopy.....	10
Electron Microscopy.....	11
Analysis of Labeling.....	12
Enzyme Digestion and Chemical Treatments.....	12
Removal of Cell Components.....	12
Removal of Labeled Compounds.....	13
Construction of Model.....	14
Electron Microscopic Techniques.....	14
Fixation and Embedding.....	14
Coated Grid Preparation.....	16
Sectioning.....	17
Electron Microscopy.....	19
RESULTS.....	20
Basal Body Formation: Brief Summary.....	20
Centriolar Basal Body Formation: Detailed Analysis.....	23
Acentriolar Basal Body Formation: The Major Pathway.....	29
Procentriole Formation: Serial Section Analysis.....	38
Single Tube Formation.....	45

Basal Body Structure: Introduction.....	62
Basal Body Description.....	64
Basal Body Model.....	84
Enzyme Digestion Studies.....	88
Radioautography.....	98
DISCUSSION.....	104
Introduction.....	104
Basal Body Formation.....	104
Basal Body Structure.....	120
Basal Body Chemistry.....	127
SUMMARY.....	130
BIBLIOGRAPHY.....	131
APPENDIX.....	139

INTRODUCTION

Cell organelles and viruses, each composed of several different molecules, maintain their structure by a series of complex interactions between constituent macromolecules. Precisely how these molecules are arranged and what forces stabilize them are questions which have attracted a great deal of interest. The title of a recent review article, Self-assembly of biological structures (34), reflects the orientation of most investigators in this field. The collective aim of these investigators has been to dismantle the structure into its component molecules and then reassemble it in vitro under conditions created by the properties of the molecules and the chemical environment. The tacit assumption that underlies all of these studies is that the in vitro conditions reflect the cellular mechanism for generating these structures. However, all of these studies ignore the spatial and temporal constraints on cell processes which often make it impossible for a "self-assembly" system to be workable. For example, recent electron microscopy studies on virus formation and bacteriophage replication show that very definite morphological changes in the organization of the cell accompanies the generation of these structures (13, 52). This implies that certain undefined cellular conditions must be established before the viruses are synthesized. It is improbable that such conditions are reproducible in the test tube. The present study on the formation and structure of the oviduct basal body (centriole) strongly supports the conclusion that these organelles are not created by a self-assembly process.

The advantages of studying centriole formation as a model for

structure generation stems from the fact that this organelle is very complex. Not only are there several steps in its formation, but there are several distinct ways that it may be formed (1, 6, 10, 14, 15, 16, 17, 22, 23, 26, 28, 32, 33, 39, 40, 42, 43, 44, 51, 64, 65, 66). Thus, experimentally interrupting the generation process at any of the numerous stages of development is helpful in correlating morphological events with cell physiology under near in vivo conditions. Another advantage is that biochemical and morphological data about the generation, in addition to the chemical analysis of the isolated mature centriole, can give information about general structure formation that would not be detectable in the generation of a less complex organelle. Such information contributes to an understanding of how cells form and maintain their structural complexity.

The mature centriole is basically similar in structure, regardless of the cell type in which it is found (2, 4, 5, 11, 15, 18, 19, 20, 24, 25, 37, 46, 50, 64, 67); however, the structure has different names depending on its function, e.g., as a ciliary accessory in rat trachea (64) it is called a basal body, while a similar structure in unicellular ciliates is called a kinetosome (15). The geometric format is that of a cylinder, 500 m μ x 250 m μ , the wall of which is composed of nine symmetrically spaced tubules embedded in an electron dense material. Each of the nine tubules is partitioned into three compartments, giving the impression that there are three 200 Å subtubules to each of the nine tubules. The transverse axis of each triplet intersects the circumference of the lumen at $\sim 45^\circ$ near the base and $\sim 5^\circ$ near the apex (25). This means that in a three-

dimensional view the triplet set appears as a sheet of three sub-tubules which twists on its longitudinal axis as it extends from one end of the cylinder to the other. This twist establishes a structural polarity (to the organelle) which corresponds to a functional polarity; i.e., the end where the triplet angle is smaller always gives rise to the cilium while the other end produces the rootlet.

Attached to or associated with the centriole are certain accessory structures. The organization of these structures varies with the function of the centriole and with the animal species. Basal bodies in vertebrate ciliated cells characteristically have one or two basal feet extending laterally from their wall and a rootlet extending from the proximal end deep into the cytoplasm (18, 20, 37, 50, 64). Fibroblast centrioles contain vesicles within their lumen (67), and Paramecium kinetosomes have electron dense material, sometimes appearing to be helically arranged, in this compartment (15). A common accessory, which is very well developed in the protozoa Pseudotriconympha (25), is an arrangement of nine straight filaments radiating from a circular filament located in the center of the centriole lumen. Each of the straight filaments joins one of the triplet sets which gives the overall structure the appearance of a cartwheel. Finally, many unicellular animals such as Tetrahymena (1), Paramecium (15), or an apostome ciliate (10), have complex microtubule bundles associated with the kinetosome.

A survey of the literature reveals that new centrioles develop either in association with the parent centriole or from various precursor structures which develop independently. The former process is here

referred to as "centriolar" centriole formation while the latter is called "acentriolar" centriole formation. The centriolar process is characterized by the appearance of one or more small centrioles (procentrioles) at the proximal end of a diplosomal centriole (11, 42, 53, 64, 67) or parent kinetosome (1, 15, 32, 49). Procentrioles are smaller in diameter and shorter in length than the parent, and they lack accessory structures. In vertebrate cells, small electron dense aggregates (~80 m μ) are associated with their appearance (11, 42, 53, 67). Procentrioles lengthen and increase in diameter while still associated with the parent and finally break away to become a mature centriole. The number of centrioles formed simultaneously per parent centriole varies from one in diplosome replication (11, 42, 53, 64, 67) and kinetosome formation (1, 15, 32, 49) to twenty in atypical spermato-cytes of the snail Viviparus (23). Unicellular ciliates such as Paramecium (15) and Tetrahymena (1) have one additional variation. Their prokinetosome is only generated on one specific side of the parent, and this side is aligned with the anterior-posterior axis of the organism (15). Accessory structures are acquired by the centriole as the organelle assumes its functional role in the cell.

The term "acentriolar centriole generation" emphasizes that the beginning of centriole formation appears to be independent of any existing mature centriole although this structure may synthesize the procentriole precursor material (17, 64). These generative systems occur in cells which manufacture a large number of centrioles (200-300) in a relatively short period of time. This constraint results in the synthesis of various types of procentriole precursor material, although

some of the material may act as a procentriole organizer (65). Procentriole formation appears to be the condensation or rearrangement of this precursor material. The morphology of the material differs between species and can appear as electron dense aggregates of various sizes (6, 17, 22, 64, 65, 66); trellis-shaped membrane arrangements (39); spherical aggregates of tubes (40); cylindrical cores (33). The whole process seems to be very synchronous so that the stage of generation is uniform throughout the cell (33, 40). The maturation of the procentriole into the centriole occurs in association with the precursor material. The precursors are apparently consumed in the process (33, 65).

The protozoan Naegleria gruberi is capable of transforming from an amoeba without any diplosome into a flagellate with two basal bodies (14, 58). This transformation occurs without the appearance of any basal body precursor material - not even a procentriole! Likewise, artificially fertilized sea urchin eggs are able to generate new centrioles in the absence of an existing parent structure (16). In contrast, the basal bodies of the ciliated cells in rat trachea are generated by both the centriolar pathway and the acentriolar mechanism (64). These examples represent the extremes in capabilities that cells possess for the production of centrioles.

The nucleic acid chemistry of centrioles has attracted interest in recent years. Genetic and cytological studies on unicellular ciliates imply that centrioles are autonomous structures, possibly containing information for their own replication (1, 15, 49). However, the results of these biochemical studies have been inconclusive.

Three laboratories have isolated kinetosomes from the unicellular multiciliate Tetrahymena pyriformis (3, 27, 59). Their chemical analysis gave a DNA content varying from 0 to 3.1% dry weight, depending on the investigator and the method of extraction. The lack of reproducibility makes it difficult to come to a conclusion about the presence of DNA. Hufnagel isolated the pellicle of Tetrahymena and reports that there is 5×10^{-14} grams of DNA per pellicle; however, the buoyant density of this DNA is similar to nuclear DNA (29, 30). Possibly nuclear DNA contaminates the kinetosomes during the isolation procedure. Hufnagel suggests in a later study that the DNA from bacteria and other organisms which Paramecium ingest could be a contaminant (31).

In contrast to the varied results cited for DNA, the same investigators obtained similar values for the RNA content of these structures (2.5% dry weight) (3, 27, 59). These data are further supported by the fact that isolated kinetosomes are able to synthesize proteins under conditions which distinguish the system from cytoplasmic or mitochondrial protein synthesis (60).

Light radioautographic detection of H^3 -thymidine incorporation and characteristic fluorescent staining have provided convincing evidence for DNA in kinetosomes of Tetrahymena and Paramecium (48, 62). Both of the detection techniques are sensitive to DNase, but not RNase. Smith-Sonneborn and Plaut have demonstrated that the incorporation of H^3 -thymidine into the kinetosome is independent of the nucleus (63). Unfortunately, no one has been able to obtain electron microscopic radioautographic evidence for DNA in kinetosomes (47). This may be due to improper labeling and fixing techniques; however, since electron

microscopic methods better preserve the normal structure of the cell, the lack of labeling may mean that the light microscopic results are an artifact created by the harsh processing methods. In other words, nuclear or mitochondrial contamination could have been introduced.

Every cell with centrioles undergoes centriolar replication at some stage of its life cycle, and presumably there are some structural requirements which must be maintained in all of these processes. Some of the mechanisms may not be apparent in one cell system or another because they are obscured by the metabolic processes necessary to sustain life. However, cell systems which have a very definite morphological sequence leading to centriole formation offer an opportunity to understand the events in replication. In this type of cell, not only can the fine structure of the process be understood, but biochemical analysis is possible.

The present investigation was undertaken to extend our understanding of centriole formation by studying a cell which generates numerous basal bodies when it is properly stimulated. The fimbriated end of the rhesus monkey oviduct meets these requirements (7, 9). It completely deciliates following the removal of the ovaries, a process which results in the loss of all the basal bodies in these cells. The process can be reversed by injecting the animal with estradiol benzoate (15-30 $\mu\text{g}/\text{day}$ for four days). The reciliation is preceded by the formation of basal bodies, and the first stages of basal body formation are fairly synchronous.

This report begins by describing in detail the morphological events which occur in the formation of oviductal basal bodies. Samples

of tissue are examined on each of the five days it takes the cell to form a new complement of cilia, and an analysis of the chronology of events is made. Autoradiograms are used to identify the structures which incorporate tritiated nucleic acid precursors on specific days of the differentiation sequence. Enzyme digestion of tissue embedded in glycol methacrylate is used to elucidate the chemical composition of the precursor as well as the formed structure. Finally, a serial-sectioning and stereomicroscopic analysis of basal body structure is described. A scale model of a fully formed basal body has been constructed from this data.

MATERIALS AND METHODS

Experimental System

Rhesus monkeys - Macaca mulatta (Woodard Asiatic Corporation) - weighing 4-8 kilograms were ovariectomized at least 6 weeks before use to insure that the oviduct epithelium had returned to a basal state. The animals were hormonally stimulated by injecting intramuscularly 30 µg per day of estradiol benzoate (Schering Corporation) in sesame oil for 3 days. The animals received their injections twice daily; 15 µg in the morning and 15 µg in the evening.

After an appropriate time of stimulation, biopsies were taken by laparotomy from the fimbriated end of the oviduct and fixed immediately. The animal was then sutured and returned to an intensive care facility.

The surgery was handled by a separate staff of specially trained personnel. Sterile conditions were maintained at all times, and the animals were treated postoperatively with appropriate drugs to insure that their health remained normal.

Labeling of the Fimbriae

The fimbriae were labeled by performing a laparotomy and exposing the tissue to radioactive precursors. A sterile cup was placed in the abdominal cavity so that the fimbriated end of the oviduct could be placed in the container for extended periods of time. The cup was filled with 1 to 3 milliliters of sterile, radioactive solution, which had been prepared by diluting 1:10 stock solution of labeled compound with Lactated Ringer's solution (Abbot Company).

The administration of 100 µg/ml H^3 -thymidine, methyl-T, (Sp. Act. 16.1 C/mM, New England Nuclear Company) was performed on the

fourth and fifth days of estrogen stimulation. The left fimbriae were treated with the radioactive solution and the right fimbriae were exposed to a Ringer's solution control. The soaking periods were for 3 hours on each day, and a biopsy from each fimbriae was made after each soak. The animal was returned to Animal Care after the second soak, and on the tenth day of stimulation a final biopsy was made.

The fimbriae of a second animal were exposed to a 100 $\mu\text{g}/\text{ml}$ solution of H^3 -uridine (Sp. Act. 36.6 c/mM, New England Nuclear Corporation) on the fourth day of stimulation. The exposure period was for 60 minutes, and biopsies were made at 15 minutes, 30 minutes, and 60 minutes. A final biopsy was made on the seventh day.

Radioautography

Light Microscopy

Several sections, 1 μ thick, were cut from blocks of labeled fimbriae and mounted on subbed slides (.5% gelatin, .05% chrom Alum solution). Additional sections from a nonradioactive source were placed on the same slides so that a background check could be made for each slide.

The sections were stained with Weigert-Lillie stabilized iron chloride hematoxylin (80°C) for 1 hour before being coated with Kodak AR-10 stripping film. The slides were allowed to dry before being placed in a light-tight slide box containing a desiccant (W. A. Hammond Drierite Company). The boxes were stored in a 4°C refrigerator for 8 weeks.

The radioautograms were developed in D19-B developer (prepared from component chemicals) for 6 minutes at 18°C. After a rinse in

Sb5A (Acetic Acid-Ammonium Sulfate) the radioautograms were fixed for 5 minutes in Kodak Rapid Fixer. Photographs were made with an Aristophot camera mounted on a Leitz microscope. Polaroid P/N film was used.

Electron Microscopy

One per cent Parlodion (Mallinckrodt) was prepared by diluting a 4% stock solution with amyl acetate and then filtering it through a Millipore filter. Using the method of Salpeter (55), half-slides cleaned in 60°C Liquinox (Alconox, Inc.) and in acid (90% HNO₃-90% HCl, 1:1) were dipped in the 1% Parlodion and dried in a dust-free box overnight before use. The evaporation of the solvent left the slides covered with a removable Parlodion film.

Thin sections (800-1,000 Å) were floated on a saturated aqueous solution of uranyl acetate for 1 hour. After a half-hour rinse in Millipore filtered water they were transferred to a drop of water on a Parlodion covered slide. The slide, containing 1 or 2 sections, was dried on a hotplate. Each section was post-stained on the slide with lead citrate for 1.5 minutes.

After the staining, the slides were coated with a carbon film and then dipped in Ilford L-4 emulsion (37°C) diluted 13-35 with distilled water. The dipped slides were allowed to dry vertically for an hour, and then placed in light-tight boxes containing a desiccant (Drierite Company) and an atmosphere of argon. The boxes were stored for 3 and 6 month periods at 4°C.

D19B developer was used for 4 minutes (18°C) to develop the radioautograms. The slides were rinsed briefly in distilled water

before fixing in 20% sodium thiosulfate for 5 minutes.

After development, the Parlodion film containing the emulsion-covered sections was floated off the slides onto a distilled water bath. Two-hundred mesh grids were placed over the sections and the floating film with the grid-covered sections was picked up using a silicone-coated slide (Siliclad, Clay-Adams Company).

Analysis of Labeling

Grain counts were made by counting the number of grains associated with the basal body region per cell. Usually 300 cells were counted in each section, and the number of cells containing 0, 1, 2, 3, etc., grains were tabulated. Background counts in the basal body region were made on sections of unlabeled tissue samples. Multiple counts on each sample were made.

A normalized "t" test was used to test the hypothesis that the grain distribution in the nonradioactive controls was the same as the grain distribution in the radioactive samples. To test the effects of various enzyme pretreatments an analysis of variance was made using the total number of grains minus background for each section.

Enzyme Digestion and Chemical Treatments

Removal of Cell Components

Glycol methacrylate was used as the embedding media (35) for all of the following experiments. The permeability of this plastic to water-soluble chemicals permitted the specific removal of RNA, DNA, and proteins.

Sections were cut 800 - 1,000 Å thick and floated on the enzyme solutions, 1 section to each solution. In order to differentiate the

effects of the nuclease digestion procedure from the effects of variation in staining or section thickness, the first section of three serial sections was treated with DNase, the second with RNase, and the third with buffer. Individual sections were digested with Pronase and compared with untreated samples.

The enzymes used included .01% DNase (Worthington Company), .01% RNase (Worthington Company) and .01% Pronase (California Biochemical Company) in pH 7.1 Tris buffer. Nuclease digestions were at 37°C for 12 to 14 hours while protease digestions were for 5 minutes to 1 hour at 37°C.

The sections were rinsed by floating on distilled water for 1/2 to 1 hour. Then the sections were floated on 1% OsO₄ (Merck Company), prepared with cacodylate buffer (Table 1) for 1/2 hour. The sections were mounted on formvar-coated slot grids and stained with the following sequence: Lead citrate (10 sec.); Uranyl acetate (10 min.); Lead citrate (10 sec.).

Removal of Labeled Compounds

After the whole piece of tissue was fixed in a gluteraldehyde-formaldehyde fixative, it was cut into smaller pieces, and each sample was washed for 24 hours at 37°C with cacodylate buffer. A sample block of each labeling treatment was placed in either .01% DNase, .01% RNase, or buffer control for 48 hours at 37°C. The tissues were rinsed briefly in distilled water, postfixed in cacodylate buffered 1% OsO₄ for 2 hours and embedded in Araldite.

The DNase was prepared by dissolving 1 mg of enzyme in 3 ml of .1M phosphate buffer (pH 6.5) which contained .062 gr/50ml MgSO₄.

Phosphate buffer without $MgSO_4$ was used to prepare the RNAse (1 mg/2ml) while the $MgSO_4$ containing buffer was used as a control.

Construction of Model

The two scale models ($330 \text{ \AA} = 1 \text{ inch}$) of the basal body were constructed from polyethylene tubes and sheets. Linoleum was used as the base of the basal foot. The tubes were held in place by inserting them in holes which were drilled into a wooden platform at a 14° angle. Elmers glue was used to attach the various polyethylene sheets. One model, only containing the triplet tubes, was embedded in a plastic resin (R. B. Howell Company) and scale sections were cut on a band saw.

The photographs of the sectioned model were taken with a Hasselblad camera (250 mm, f 5.6 lens) using Kodak Pan-X film. The complete model was photographed with a Nikon F (55 mm, f 1.4 lens) camera using Kodak Tri-X film.

Electron Microscopic Techniques

Fixation and Embedding

Tissues were fixed in one of three types of fixatives (Table 1): cacodylate buffered .75% glutaraldehyde, a cacodylate buffered .75% glutaraldehyde-3% formaldehyde mixture, or 70% absolute alcohol - 30% glacial acetic acid mixture (Carnoy's fixative). Fixation in the aldehyde fixatives was for 30 minutes at room temperature while fixation in the alcohol-acetic acid fixative was for an hour at 0°C , followed by rehydration in a graded series of alcohols. All of the tissues were stored in cacodylate buffer and washed from 24 to 48 hours at 37°C in fresh buffer before embedding.

Araldite embedding was preceded by post-fixation with cacodylate

TABLE 1

Glutaraldehyde Fixative

0.75% Glutaraldehyde (Fisher Scientific Company)

1.00% Sodium cacodylate

4.50% Sucrose

0.05% Calcium chloride

0.05% Magnesium sulfate anhydrous

Glutaraldehyde-Formaldehyde Fixative

0.75% Glutaraldehyde

3.00% Paraformaldehyde (Fisher Scientific Company)

1.00% Sodium cacodylate

4.50% Sucrose

0.05% Calcium chloride

0.05% Magnesium sulfate anhydrous

Carnoy's Fixative

70.00% Absolute alcohol

30.00% Glacial acetic acid

Osmium Tetroxide Fixative

1.00% Osmium Tetroxide (Merck Company)

1.00% Sodium cacodylate

4.50% Sucrose

Cacodylate Buffer

1.00% Sodium cacodylate

4.50% Sucrose

buffered 1% OsO_4 for 2 hours at room temperature (Table 1). After a distilled water rinse the tissue was dehydrated to propylene oxide, using a graded series of alcohol solutions. A 1:1 followed by a 1:2 propylene oxide:araldite mixture facilitated the impregnation of the tissues with the resin. The tissue was then placed in an undiluted mixture of Araldite (Ladd Company) before the final positioning of the specimen in a Beem capsule filled with plastic. Polymerization was in a 60°C oven for two weeks.

Some tissue was embedded in the water miscible plastic glycol methacrylate (GMA) (35). The tissue was soaked in a series of polymer solutions designed to efficiently impregnate the tissue with plastic and reduce polymerization artifacts. The sequence of tissue treatments, conducted at 4°C , was: 80% GMA (Rohm and Haas Company) in water for 30 minutes; 96% GMA for 30 minutes; 30 minutes in a 7-parts GMA, 3-parts butyl methacrylate (BMA) mixture with 1% Benzyl Peroxide added to the BMA (Rohm and Haas Company) as a catalyst; overnight soaking in a prepolymer prepared by heating the GMA-BMA mixture to a critical temperature and then rapidly cooling it in an ice bath. The tissue was then placed in a gelatin capsule filled with prepolymer. After positioning the tissue, the capsule was placed in a holder and exposed to $>3160 \text{ \AA}$ ultraviolet light (W. P. Allen Company, England) for 5 to 7 days at 4°C .

Coated Grid Preparation

A formvar solution was prepared by dissolving .5 gm of formvar (Shawinigan Resin Company) in 100 ml of dioxane. After the formvar was completely dissolved, calcium hydride was added to absorb any

water in the solution. Before using, the solution was twice filtered through a Millipore filter (Solvinert filters, Millipore Company).

Slides cleaned with lens paper were dipped in the freshly filtered formvar and dried in a dust-free box overnight. A razor was used to free the edges of the formvar film from the slide. The films were then floated onto a water bath. Sonically cleaned grids were placed on the floating film, and the film with the grids was picked up with a Siliclad-treated slide. Slides with attached grids were stored in a slide box.

Sectioning

Sectioning was done with a Porter-Blum MT-2 ultramicrotome (Ivan Sorvall Company). Glass knives for thick sectioning were made with a Messer knife breaker (French Company). Thin sections were cut with DuPont diamond knives.

For the enzyme digestion procedure, serial sections, 800-1,000 Å were cut and floated on individual water troughs in order to maintain the sequence of the sections. After the digestion, the trapezoid-shaped sections were mounted on formvar-coated slot grids. The same end of the section was over the hole in each sample. The grids were stained and then placed in a vacuum evaporator. Carbon was evaporated onto the grids in quarter-second bursts at 60 amperes at an atmospheric pressure of 4×10^{-5} mm of mercury. The grids were then coated with silicon monoxide (Ladd Company); fifteen seconds of heating at 30 amperes, 4×10^{-5} mm of mercury.

A new technique was developed for doing the high resolution serial sectioning. To begin this procedure, a substratum was prepared

by dissolving 3 gm of gelatin in 100 ml of boiling water. The liquid gelatin was poured into a small petri dish and cooled to room temperature.

Serial sections were cut and transferred to the surface of the cooled, liquid gelatin with either a bamboo stick or a wire loop and then spread with trichloroethylene vapors. Large sections (1-2 mm sq.) were arranged into rows, to preserve the sequence of sectioning, and oriented with a hair to facilitate grid placement.

To gel the substratum the petri dish was placed in a refrigerator. The petri dish was then placed under a stereomicroscope and tilted approximately 45° to the plane of light produced by a fluorescent bulb, so that the sections showed their typical refractile colors.

The section to be mounted was centered in the field of the microscope and roughly oriented by rotating the dish. A grid was picked up with a pair of forceps and positioned so that the section was visible through the grid. The section and the grid were brought into register by manipulating the dish or the forceps. The front edge of the grid was placed on the gel in front of the section or ribbon, and then, while keeping the shadows cast by the grid bars aligned with the sections, the back edge was lowered slowly to the surface of the gel. Misplaced grids were picked up and new grids repositioned.

The gelatin was liquified in a 60°C oven, and the grids picked up with forceps. The excess gelatin was drained and the grid was floated for 30 minutes on a 2% solution of acetic acid (60°C) section-side down. After this, the grids were floated for several minutes on a bath of Tris buffer pH 7.1 (60°C) to neutralize the residual acidity. They were rinsed in distilled water (30 minutes, 60°C), dried in a grid

holder and stained. Sections survived the staining procedure best if they were rinsed gently and dried by touching their edges (not their surfaces) to filter paper. Mounted sections were stabilized with carbon.

Electron Microscopy

Electron micrographs were taken with a Philips 200 at either 40 or 60 k.v. (50 μ aperture). Stereo-photographs were obtained by photographing the specimen after tilting the stage forward and backwards 6°. Kodak 3 1/4" x 4" Electron Image plates were used, and they were developed in Kodak HRP developer. Printing was done with a Durst enlarger on variable contrast photographic paper.

Several photographs were printed using the image enhancing method described by Markham, et al. (38). Lantern slides (Kodak Company) of the desired negatives were printed, and these slides were projected onto a rotatable platform with a Durst enlarger. The image of the structure was positioned so that the center of the procentriole coincided with the center of the platform. Another lantern slide was positioned, the platform was rotated 40° and the slide was exposed for 1/9th the amount of time necessary to obtain a regular photograph. This procedure was repeated eight more times for a total of nine superimposed photographs. The slide was developed and the negative obtained was printed on variable contrast paper.

RESULTS

Basal Body Formation: Brief Summary

The rhesus monkey oviduct is an ideal system in which to study cell differentiation because the state of differentiation in each epithelial cell is under the control of estrogen. Oophorectomy or hypophysectomy will return the cells to an undifferentiated state, but when these animals are injected with estrogen - or an estrogen derivative - the epithelial cells divide, hypertrophy, and differentiate into either ciliated cells or secretory cells. The ciliated cells predominate, particularly in the fimbriae, where there are about 10 ciliated cells to each secretory cell. The formation of a fully ciliated cell takes about 6 days, with several well-defined morphological events preceding the final state (7, 8, 9). Basal body manufacture and cilia formation in the oviduct takes a considerably longer period of time than in such organisms as Paramecium or Tetrahymena (1, 15).

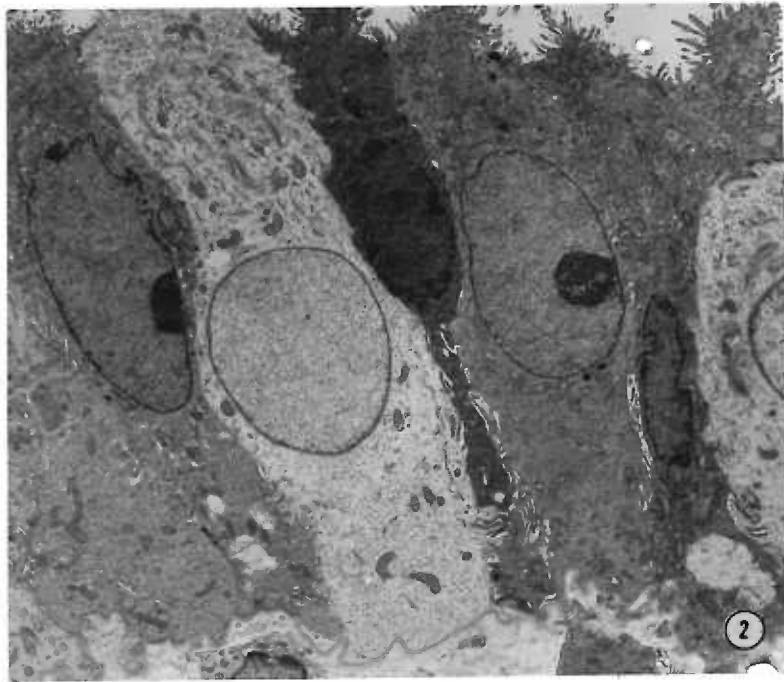
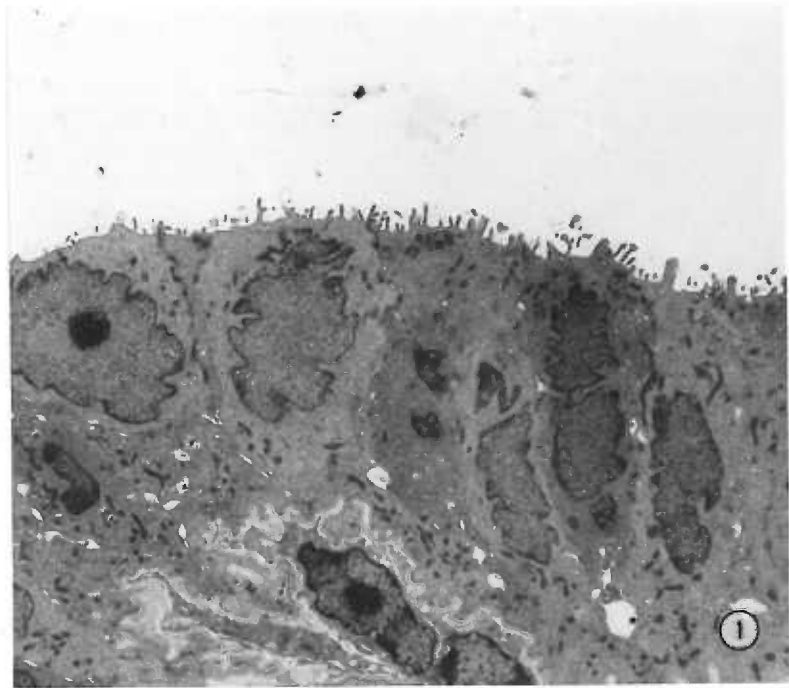
The major steps in acentriolar (i.e., without the involvement of a mature centriole) basal body formation in the rhesus monkey oviduct have been described by Brenner (7, 8, 9). The cuboidal epithelial cells present in the oophorectomized animal first divide and then hypertrophy within the first three days of estrogen treatment (Figs. 1, 2). In those columnar cells that will become ciliated there appear numerous 40-60 μ electron-dense granules on the third day of injections. These granules have been given various names by other investigators (6, 17, 22, 64, 65), but are best described as fibrous granules because of their 50 Å fibrillar component. The procentrioles begin to form in association with these fibrous granules, and simultaneously there

Figure 1. The epithelium of atrophied fimbriae. Future ciliated and secretory cells cannot be distinguished from each other.

Glutaraldehyde-formaldehyde, 5,920X

Figure 2. The epithelium of the fimbriae after four days of estrogen stimulation. The cells have become taller and have acquired many cytoplasmic organelles. Secretory cells are becoming recognizable as a result of an increase in density of their cytoplasm.

Glutaraldehyde-formaldehyde, 3,800X



appears a dense sphere (80 μ diameter) at the base of each procentriole. Each of these secondary bodies or deuterosomes (64) usually has the base of one or two procentrioles associated with it; occasionally four procentrioles radiate from one deuterosome. The procentrioles develop into basal bodies while maintaining these relationships and the fibrous granules disappear when the basal body is completely formed. Until cilia formation begins, each deuterosome remains attached to one basal body of the several with which it may have been initially associated. The basal bodies begin to acquire a single basal foot while migrating to the luminal surface of the cell, and as the cilium begins to grow, a rootlet is formed at the proximal end of each basal body. A new group of fibrous granules appear in the apical cytoplasm at the time of rootlet and cilia formation.

Acentriolar basal body formation is the major pathway for the production of these organelles, but as in the rat trachea (64), there is a second pathway of minor importance: centriolar basal body formation. The first morphologically distinguishable event in this progression is the migration of one or both diplosomal centrioles to the apical end of each cell after cell division. One of these centrioles usually produces a rudimentary cilium. At about the time the fibrous granules appear, procentrioles begin to bud at right angles from the basal end and midregion of these centrioles. The number of procentrioles which appear with each centriole varies from 1 to 10; the average is 4. Usually there are fibrous granules adjacent to the developing procentriole. The procentriole matures while in contact with the centriole, and the mature structure disassociates from the parent and mixes with

the other basal bodies. Centriolar basal body formation follows the same time course as the acentriolar pathway.

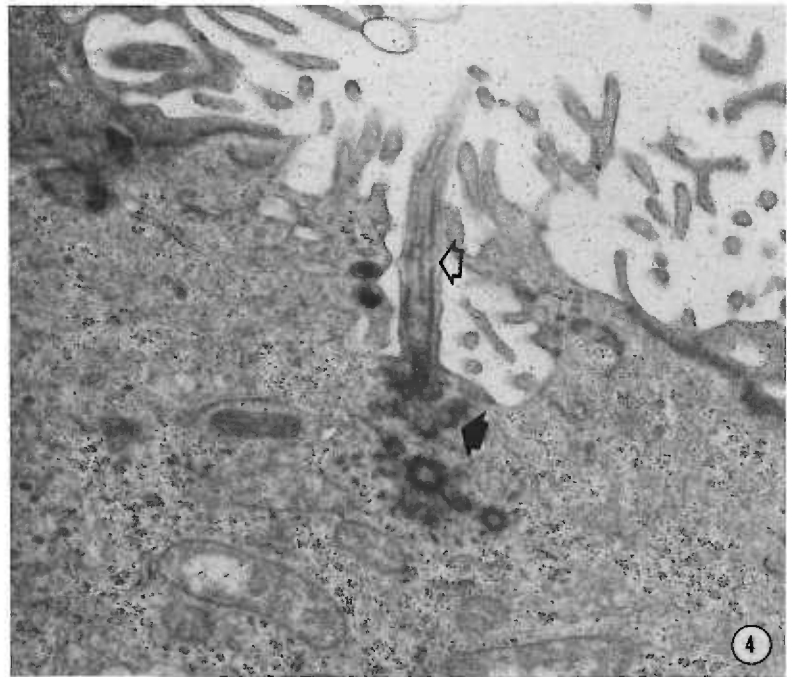
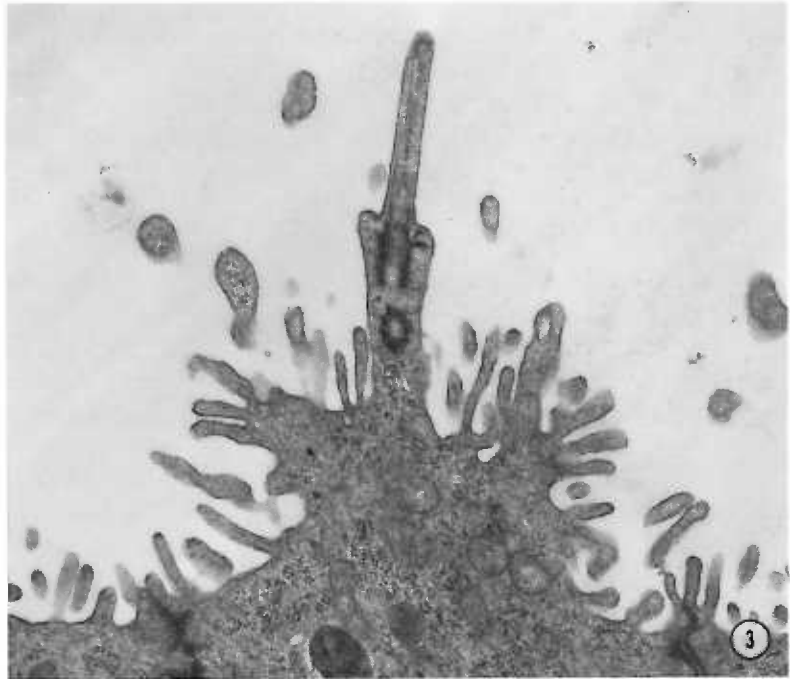
Centriolar Basal Body Formation: Detailed Analysis

It is not possible to distinguish between the secretory cells and the ciliated cells on the third day of estrogen stimulation (Figs. 1, 2). Both types of cells are becoming taller, and well developed Golgi, rough endoplasmic reticulum, polysomes and numerous mitochondria are evidence that the cell is actively synthesizing molecules necessary for differentiation. When examining a thin section of developing fimbriae, one frequently encounters cells which have 1 or 2 centrioles located in the apical region. The frequency of such observations indicates that every cell goes through this stage. The diplosomal pair are usually oriented at right angles to each other although various other orientations have been seen. Often one of the centrioles is acting as a basal body for a rudimentary cilium (Figs. 3, 4).

The structure of the centriole is similar to those found in other mammalian cells (2, 4, 5, 17, 42, 53, 67). Its basic geometric form is a cylinder measuring 500 μ in length and 250 μ in diameter (Figs. 3, 4). The walls of the cylinder are made of 27 tubules which are arranged into 9 evenly spaced groups of 3. The centriole does not have any accessory structures; however, several modifications occur when it acts as a basal body for the rudimentary cilium. One or 2 pyramidal basal feet project at right angles from the midregion of the cylinder and occasionally there is a rootlet extending from the proximal end deep into the cytoplasm. In addition there is a filament radiating from each triplet set near the basal body-cilium junction. This

Figure 3. An epithelial cell on the third day of stimulation. The diplosomal centrioles have migrated to the luminal surface, and one centriole has produced a rudimentary cilium. Glutaraldehyde-formaldehyde, 18,500X

Figure 4. A rudimentary cilium with a degenerating tubular system (hollow arrow). Procentrioles are being generated from the free centriole as well as the basal body (solid arrow). The presence of procentrioles indicates that this cilium is older than the one in figure 3. Glutaraldehyde, 18,500X



arrangement of 9 filaments may be analogous to the octagonal end structure (67) or the transitional fibers (25). The details of basal body structure will be described later.

An unusual number of aberrant centrioles and acting basal bodies are seen. The most frequently noted modification is a lengthening of the structure with a concomitant decrease in diameter, almost as if it had been stretched. Other modifications include degeneration of the tubule system and distortion of the basic cylindrical geometry. These latter changes are most often seen in basal bodies which are inducing procentrioles to form.

The rudimentary cilium is similar to the primary cilium described by Sorokin (64). Only one cilium per cell has been observed in secretory cells as well as in future ciliated cells. The rudimentary cilia appear on the third day of estrogen treatment which is 3 days before the main cilia are formed. Rudimentary cilia are never seen after the fifth day of estrogen stimulation, and therefore probably do not become a part of the main complement of cilia.

The cell membrane is always modified in the region where the cilium arises. Commonly the membrane is invaginated at the basal body site to form a cup from which the cilium emerges (Fig. 4). The cilia in these situations are short and wavy with an incomplete tubule system. In cross-section, the peripheral doublets are imperfect and a degenerate central pair is sometimes seen; the tips are often bulb-shaped. The irregular structure of these cilia seems to be the result of aberrant tubule organization. In another frequently encountered organizational pattern the cilium extends from a finger-like projection of the cell

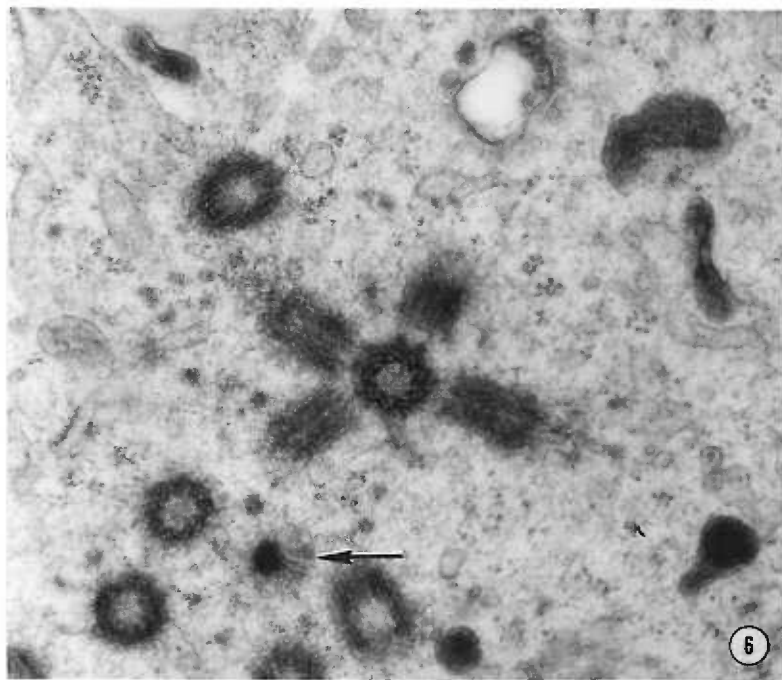
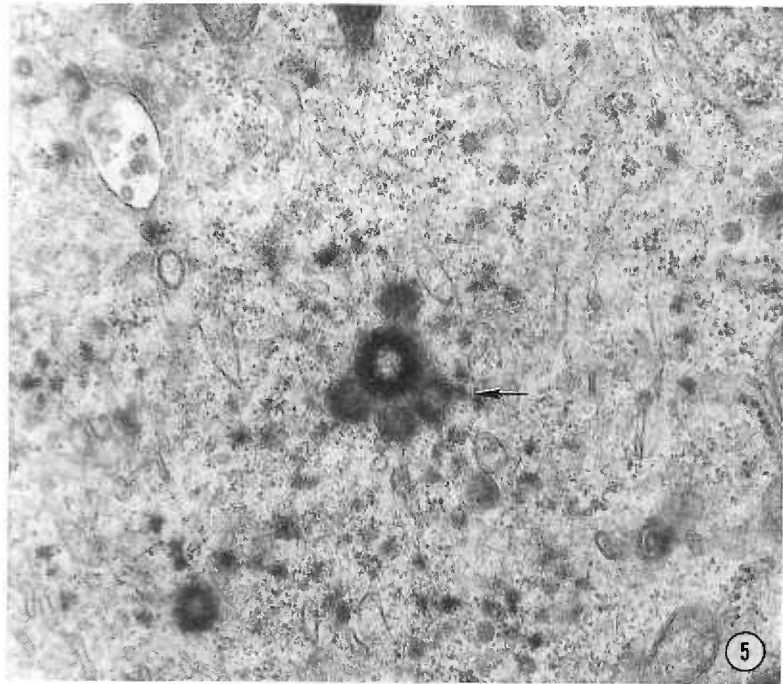
surface (Fig. 3). Here the cilium is tall and very straight, with a great deal more order than in the previous case. These cilia with their accompanying basal bodies are similar to those formed later, although their tips seem to be more sharply pointed. It is possible that these differences in structure reflect the age and therefore the state of maintenance of the cilium.

The centriole-cilium and centriole-centriole relationships persist into the fourth day of development. Late in the third day, procentrioles (probasal bodies) begin to form at right angles to the wall of the centrioles. Both centrioles, or the centriole and the basal body, produce procentrioles (Figs. 4, 5, 6). Fibrous granules appear near the centrioles either shortly before or concurrent with the appearance of the procentrioles (Figs. 4, 5). The number of procentrioles seen associated with each centriole varies from 1 to 15, and they all seem to be in the same stage of development. This indicates that the differences in the number of procentrioles per parent is not the result of variation in the time of procentriole initiation, but is due to the difference in capacity of each centriole to initiate procentriole formation.

A centriole engaged in procentriole production appears in cross-section to have a 40-50 μ thick coat of flocculent material around its outer wall (Fig. 5). This material varies from amorphous to filamentous and is not uniformly thick around the centriole. It sometimes resembles the cortex of the deuterosome (to be described later) and it may have a similar function. The base of the forming procentriole is enmeshed in the outer region of this corona so that 30-40 μ separate the parent

Figure 5. Diplosomal centriole generating four procentrioles. The procentrioles are enmeshed in a corona of flocculent material that encircles the parent. Fibrous granules are being deposited at the apical end of a procentriole (arrow). Glutaraldehyde-formaldehyde, 37,000X

Figure 6. Procentrioles which are maturing into basal bodies while associated with a diplosomal centriole. The presence of maturing basal bodies which are associated with deuterosomes (arrow) indicates that the acentriolar pathway is at the same stage of development. Glutaraldehyde-formaldehyde, 37,000X



from the daughter during the early stages of induction. One or 2 filaments extend into the base of the procentriole from the corona and they are aligned with the longitudinal axis of the daughter structure (Fig. 5). The significance of these relationships will be included in the description of acentriolar procentriole formation.

Generally the procentrioles form at right angles to the centriole but their longitudinal and radial arrangement varies, depending on the number of daughters and the state of the parent, i.e., whether or not it has accessory structures. The centriole has a capacity for induction from the midregion to the base. This is substantiated by the fact that serial sections show 1 set of 3 or 4 procentrioles encircling the midregion and another set around the basal region of the same centriole. Alternatively, the procentrioles spiral up the centriole from base to midregion. The presence of a basal foot or an anomaly in the centriole structure will cause a distortion of the perpendicular orientation of daughter-axis to parent-axis. Characteristically, these procentrioles point away from the cell surface which gives the impression that they have been pushed toward the basal end of the parent. In extreme cases, procentrioles project from the basal opening of the centriole lumen.

The variation in procentriole orientation and the differing capacities for procentriole production demonstrates that centrioles have a potential for procentriole induction that is not expressed by similar organelles in other cell systems (1, 11, 15, 23, 26, 32, 42, 53, 64, 67). It would seem that the centrioles, basal bodies, and kinetosomes in the various cell types must have mechanisms which not only regulate the number of procentrioles produced but the orientation

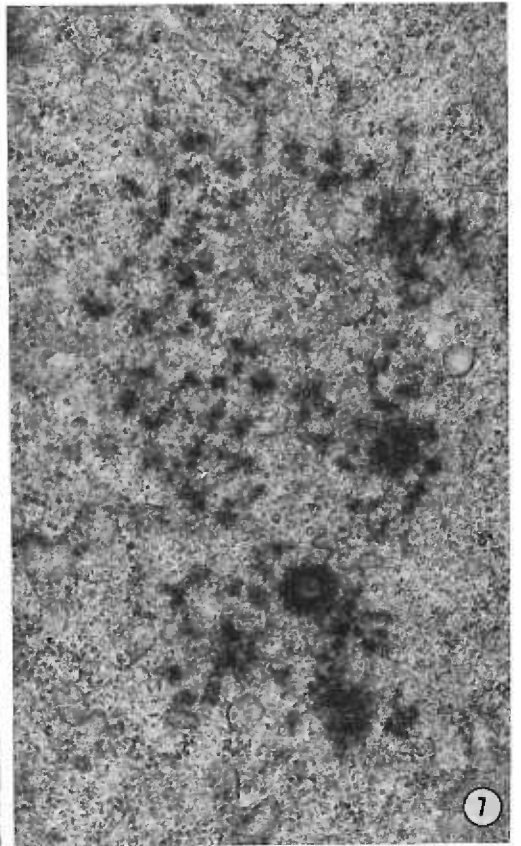
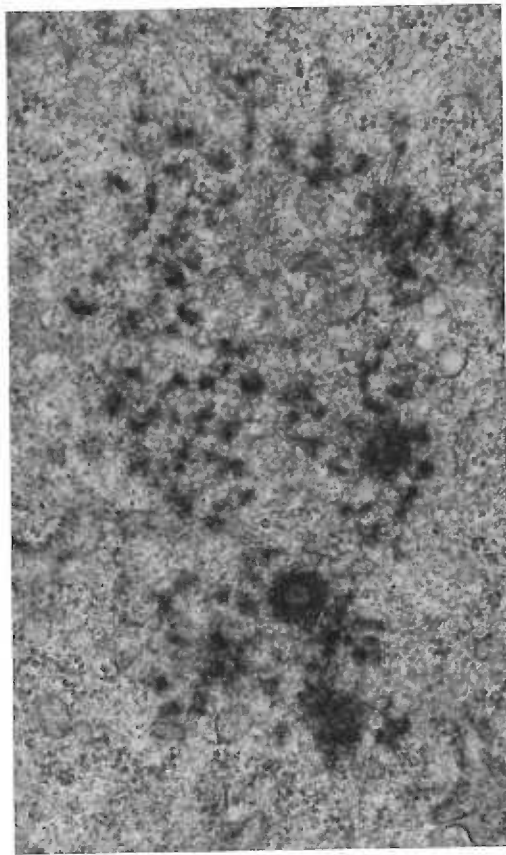
of their induction. For example, in diplosomal centriole replication (42, 53, 67), only one procentriole is formed at the basal end and in Paramecium (15) the prokinetosome always forms on the anterior side of the kinetosome. These controlling forces are not functioning in the oviduct. The data, e.g., the loss of right angle orientation under certain conditions of centriole structure, also indicates that the procentriole organizing capacity is not a function of its architecture, i.e., the centriole does not act as a template for procentriole formation (67). It is more likely that the parent possesses a molecular species which induces procentriole formation in the adjacent cytoplasm.

The procentrioles rapidly develop into mature basal bodies by a process of elongation and expansion. The characteristic daughter-to-parent orientation is maintained throughout this phase (Fig. 6). The mature basal bodies break away from the parent and join the population of basal bodies made via the major pathway. The persistence of the parent-to-daughter relationship until maturation of the daughter is completed does not occur in unicellular organisms (1, 15, 32).

Acentriolar Basal Body Formation: The Major Pathway

Late on the third day of the differentiation cycle, 40-60 μ granules appear in the apex of those cells which eventually will become ciliated. The granules are irregularly shaped and vary in their electron opacity. Stereomicroscopy reveals that the darker granules are composed of 40-75 Å fibers embedded in an amorphous material. Often these fibers radiate from the center of the granule with amorphous material adhering in diminishing amounts towards the periphery. The fibers thus appear to taper as they extend further from the granule center, giving the

Figure 7. A stereomicrograph of an aggregate of fibrous granules. Notice the fibrillar composition of the granules. Numerous fibers of different lengths and thicknesses are present in this aggregate. Glutaraldehyde-formaldehyde, 28,000X

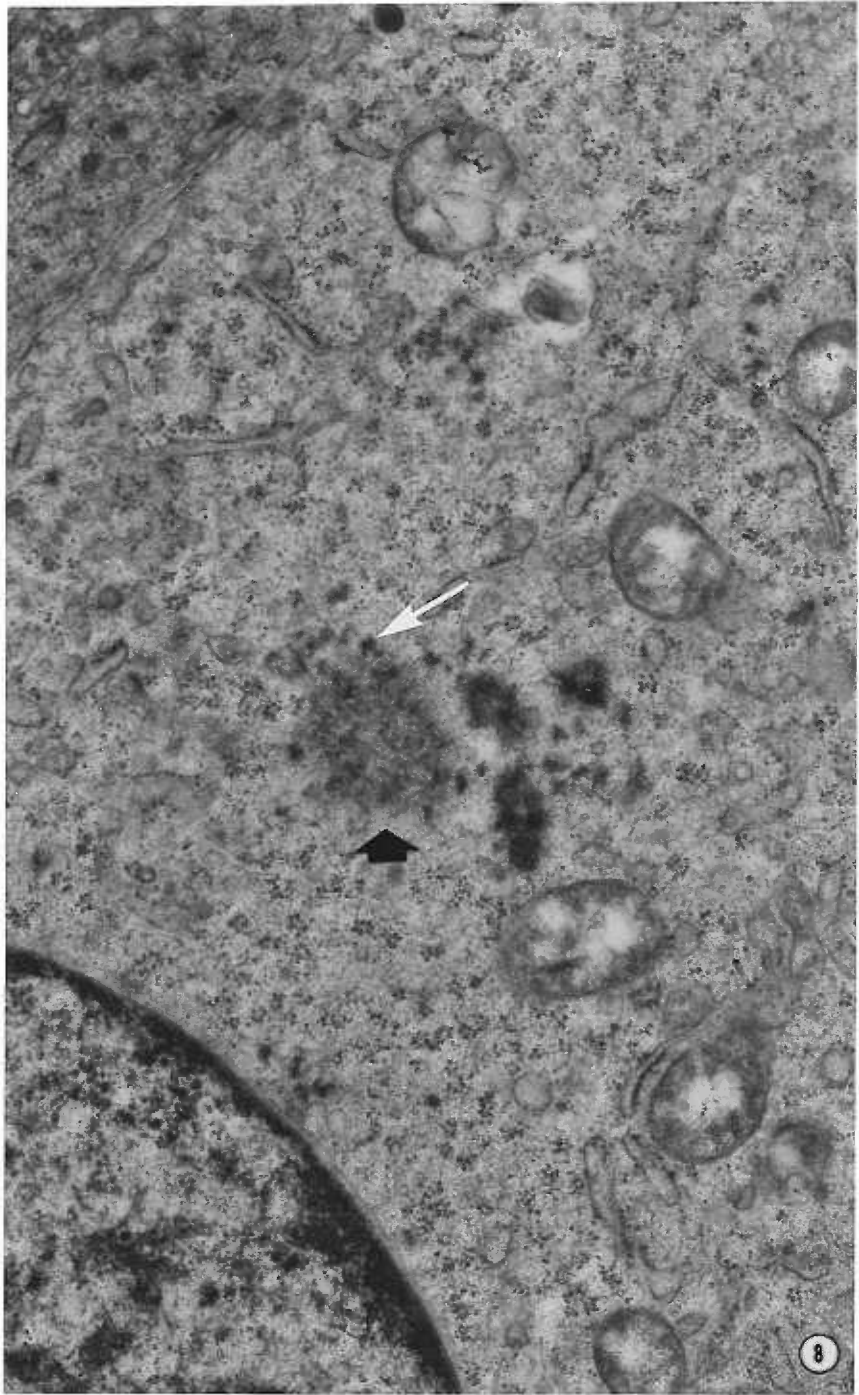


granule a stellate appearance. The less electron dense granules seem to be amorphous material without the fibers or with smaller diameter fibers (Fig. 7).

Like other organelles these fibrous granules are arranged and distributed in different ways within the cell. Although individual granules scattered throughout the apical cytoplasm are sometimes seen, usually the granules are aggregated into regions of the cell which are devoid of other organelles (ribosomes, mitochondria, etc.). Three-dimensionally, the regions appear as sheets, clouds, or spheres, and their boundary is delimited by an obvious difference in the state of the cytoplasm between the two phases. The ground plasm surrounding the granules contains numerous fibers of various lengths and thicknesses (40-80 Å thick). The fibers are similar to those in the granules, and appear to be composed of 40 Å subunits. Sometimes several fibers are grouped into bundles and occasionally microtubules are present, possibly arising from the fibers (Fig. 7). In Araldite-embedded material, the granules are generally scattered within these regions without much order; in glycol methacrylate-embedded material the granules are arranged in a more orderly pattern of strings and whorls (Fig. 56). The conditions of Araldite embedding may slightly perturb the normal orderly distribution of the granules.

The fibrous granules appear just prior to the formation of the procentrioles and then disappear after the basal bodies are completed. The basal bodies migrate to the surface of the cell and begin to form cilia, rootlets, and to complete basal foot maturation, at which time more fibrous granules appear. At these two stages of ciliogenesis, a

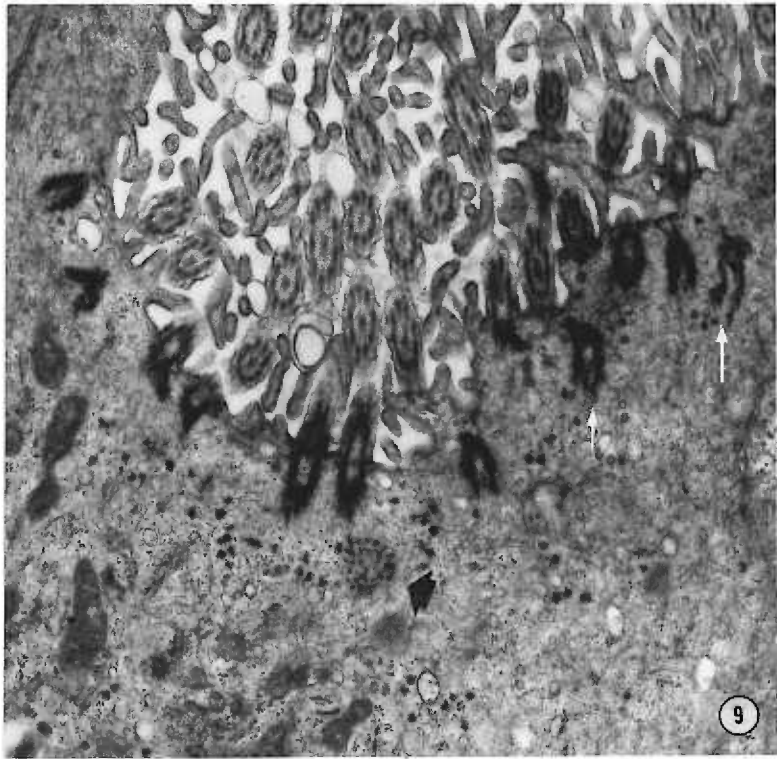
Figure 8. The nucleus is located in the lower left corner of this micrograph showing a fibrogranular sphere (black arrow). Fibrous granules are located at the periphery of this sphere (white arrow). Three procentrioles are at the right of the sphere. Glutaraldehyde, 37,000X



fibrogranular sphere measuring up to 600 μ (Figs. 8, 9) in diameter is sometimes seen. A similar structure, the fibrogranular aggregate, is a precursor to procentriole formation in rat trachea (64); the sphere is not seen frequently enough in the oviduct to know whether it is a precursor or just a fortuitous arrangement of fibrous granules. The structure is composed of numerous ill-defined densities which seem to have formed from a condensation of the surrounding matrix; it is difficult to measure them because of the subtle change between dense areas and light areas (Fig. 8). The denser areas, which are reminiscent of the fibrous granules, sometimes appear to be strung together into whorls within the sphere. Near the periphery of the sphere, the densities begin to look more like fibrous granules. Further from the boundary region the granules are more characteristic. The organization of the sphere, and the relationship of the granules gives one the impression that the granules are being thrown out or distributed by the fibrogranular sphere.

The kinetics of fibrous granule appearance and disappearance as well as the juxtaposition to developing procentrioles suggests that the granules are consumed during the synthesis of basal bodies. As will be seen, the procentrioles begin to develop within the aggregates of fibrous granules. Serial sections show that the granules become symmetrically arranged around the distal end of the procentriole, and then merge with the existing wall material (Figs. 5, 12, 14, 18). The material of the procentriole wall is indistinguishable from the material of the fibrous granules. The granules also surround the region of the developing basal foot and rootlet (Fig. 9). It appears in some

Figure 9. A fibrogranular sphere (black arrow) in a cell which is making cilia. Fibrous granules are being deposited at the base of the basal body (white arrows). Glutaraldehyde-formaldehyde, 18,500X



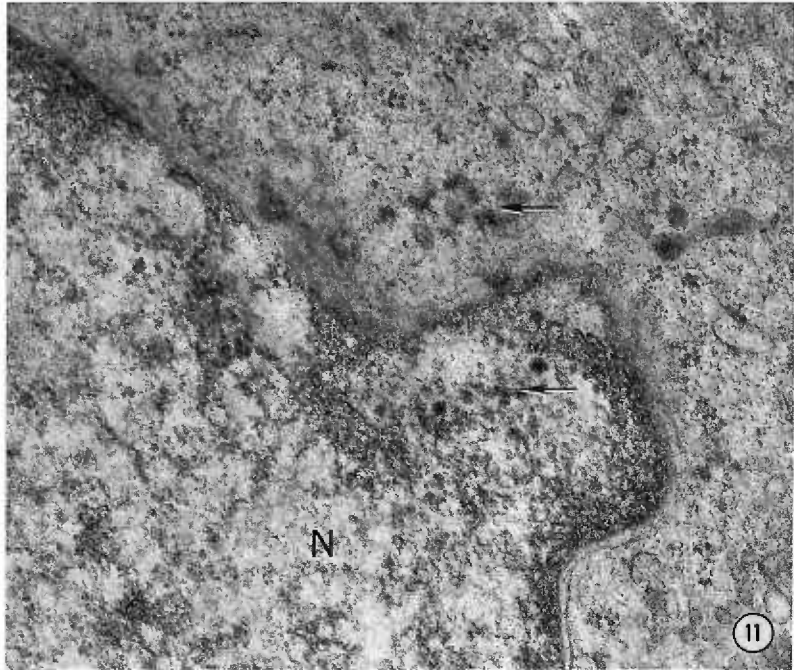
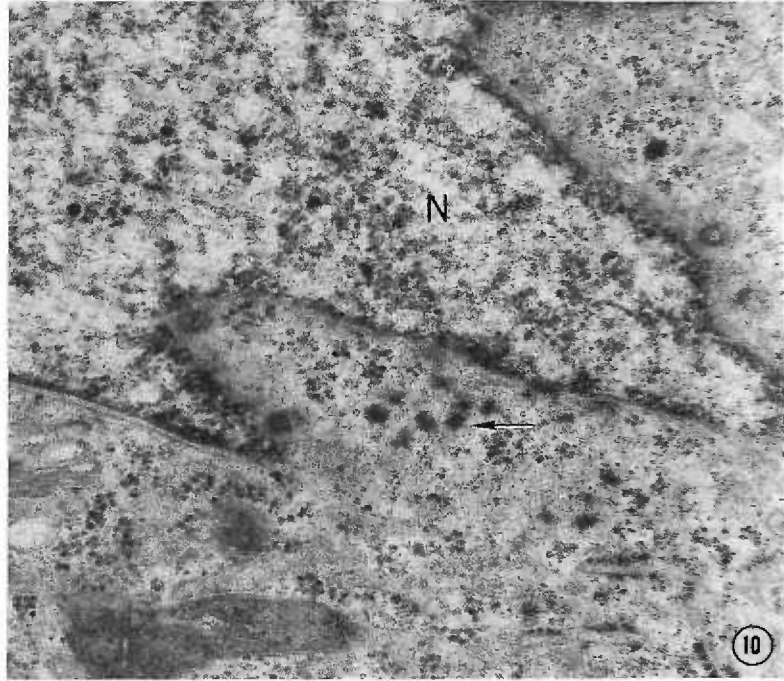
photographs as if the granules become attached to the wall or to the proximal end of the basal body during the synthesis of the accessory structures. The rootlet fibers are similar to those found in the fibrous granules.

It is difficult to determine the origin of the fibrous granules. They appear very rapidly, and there is little delay between their appearance and the beginning of procentriole formation. The granules are not conspicuously associated with other organelles; they are only seen associated with centrioles that are producing basal bodies. The granules have been seen within folds of the nuclear membrane. In these instances there were granules in the nucleoplasm in juxtaposition to those in the cytoplasm (Figs. 10, 11). Other times the granules appeared to be crossing the nuclear membrane. The relationship between the fibrogranular sphere and the fibrous granules also suggests a product-producer relationship. But like the association with the nucleus, this organizational situation is rarely seen.

The procentrioles begin to form shortly after or simultaneously with the appearance of fibrous granules. When a procentriole is recognized, it usually appears to be growing from an electron dense sphere (Figs. 12, 13). This sphere measures 80-90 μ at maturity. One or 2 procentrioles projecting from one sphere is the most common arrangement, but as many as 4 procentrioles to 1 sphere have been seen (Fig. 13). There are occasions when a newly developing procentriole is not associated with this secondary body at all. A similar structure appears in the rat trachea during ciliogenesis, and has been termed a deuterosome by Sorokin (64). The same terminology will be used in this

Figure 10. Fibrous granules (arrow) located within the fold of the nuclear envelope (N). Glutaraldehyde-formaldehyde, 46,500X

Figure 11. Fibrous granules (arrows) seem to be located on both sides of the nuclear envelope (N). In some regions, granules appear to be crossing the nuclear envelope. Glutaraldehyde-formaldehyde, 46,500X



report; other investigators have used the terms "condensation form" (17) and "procentriole organizer" (65) to denote the same organelle.

There is little variation in the structure of the deuterosome in the rhesus monkey oviduct. The organelle is usually spherical but occasionally appears either ovoid or kidney shaped. The sphere is composed of fibers which are organized differently in the center than at the periphery, producing a corticomedullary organization (Fig. 26). The medulla is the densest and therefore the most noticeable region, and it is composed of tightly interwoven fibers (50 Å) with a surrounding matrix. At the transition between the medulla and cortex the amorphous matrix becomes thinner, and the fibers become oriented perpendicular to the medulla. The matrix material diminishes toward the outer cortex, and the radially arranged fibers become less numerous. The deuterosome is always a solid structure, but the cortical region varies in prominence. This is in contrast to the hollow deuterosomes which sometimes appear in rat trachea (64). Usually the cortex is best developed in the later stages of basal body formation.

The deuterosome has the same spatial relationship to the procentriole as the diplosomal centriole does during centriolar basal body formation. This relationship has led some investigators to conclude that the deuterosomes (and diplosomal centrioles) somehow "generate" or organize the procentriole (17, 64, 65, 67). It is difficult to decide what link there might be between a spherical mass of fibers and any procentriole generative powers but in the monkey oviduct there is definite structural continuity between the cortex of the deuterosome and what will later be described as a "cartwheel" (25). The filaments of the cartwheel are

similar to the fibers of the deuterosome, and in a longitudinal section of a procentriole the central cylinder of the cartwheel appears to originate from the deuterosome (Fig. 20). In contrast to this structural relationship is the observation that some procentrioles can be initiated and presumably develop independently of either a deuterosome or a centriole.

The deuterosome is generally not distinguishable from a fibrous granule until it is seen associated with a procentriole, and the structure remains attached to at least one of its daughter basal bodies until cilia formation is initiated. In the early stages of procentriole development the deuterosome is 5-10 μ smaller in diameter than when mature. It is much more irregularly shaped at this stage and somewhat resembles an enlarged fibrous granule (Fig. 12). Thus, the deuterosome not only originates within an aggregate of fibrous granules, but it is structurally similar to them in early procentriole formation. This suggests that the fibrous granules have a deuterosome precursor component as well as a procentriole precursor component. Other investigators have suggested a similar origin of deuterosomes (17, 64).

Procentriole Formation: Serial Section Analysis

A procentriole is first recognizable as an annulus of amorphous material which has an irregular outside diameter (100-195 μ), a very uniform internal diameter (85 μ), and an approximate length of 125 μ (Fig. 16). The variation in the outside diameter is created by the unequal distribution of material around a uniformly circular band which demarcates the circumference of the lumen. This wall material is either amorphous or fibrous and does not contain any microtubules or subfibers.

Figure 12. A tightly arranged group of procentrioles which have formed within an aggregate of fibrous granules. Notice that the deuterosome (white arrow) has a similar structure to the fibrous granule (arrow head) at this stage of development. Glutaraldehyde-formaldehyde, 28,500X

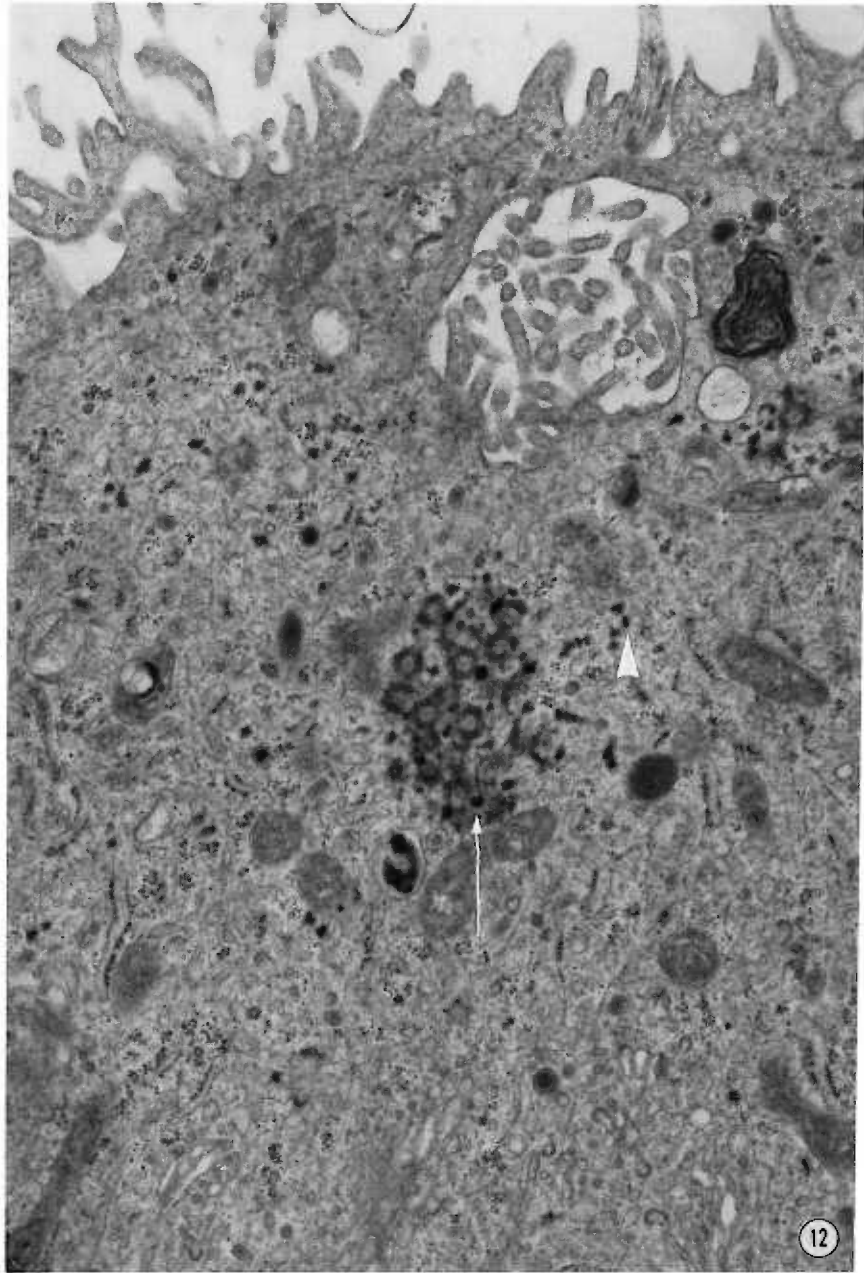
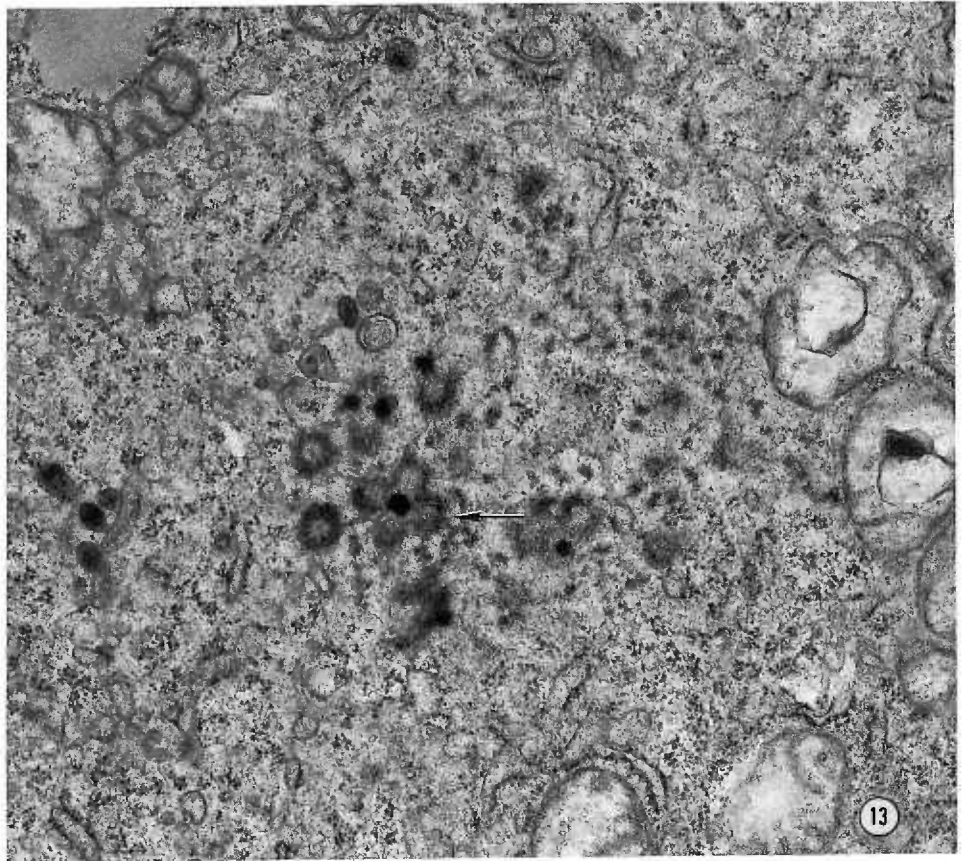


Figure 13. A deuterosome inducing four procentrioles to form. Fibrous granules apparently are being deposited at apex of one procentriole (arrow). Glutaraldehyde, 24,000X

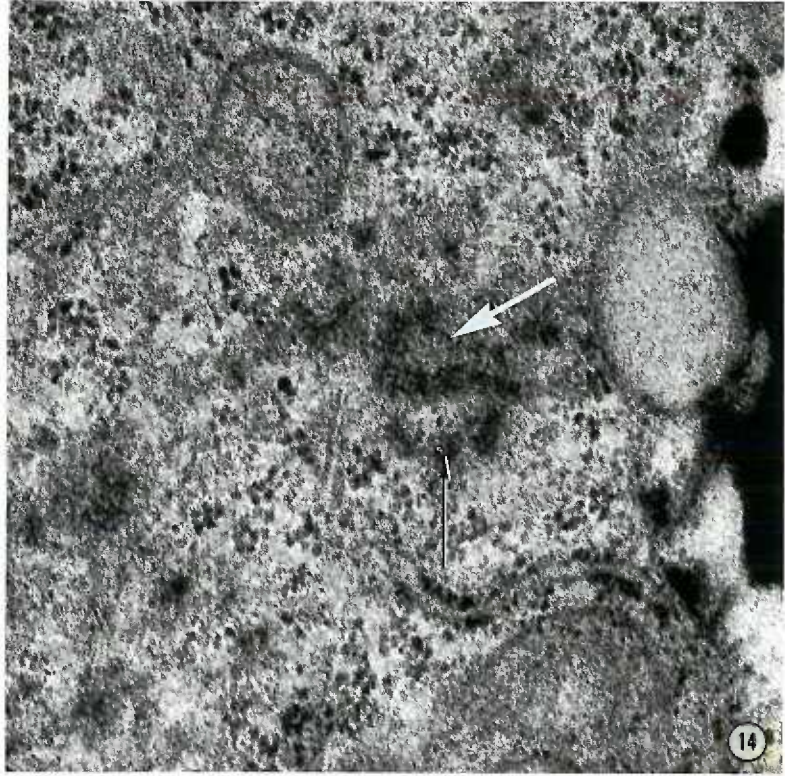


The annulus is formed within groups of fibrous granules almost immediately after the granules are synthesized. Because of this intimacy it is very difficult to interpret the initial phases of annulus formation. Several favorable sections indicate that the circumferential band is formed from fibers, or thin sheets of material, which are similar to those associated with the granules. Fibrous granule-like material simultaneously gathers around this band, and the individual granules are recognized as segmentations of the wall material (Fig. 14). The circularity of the lumen does not seem to be established immediately. A filament system which is analogous to the cartwheel (25) begins to form at this stage (Figs. 14, 15).

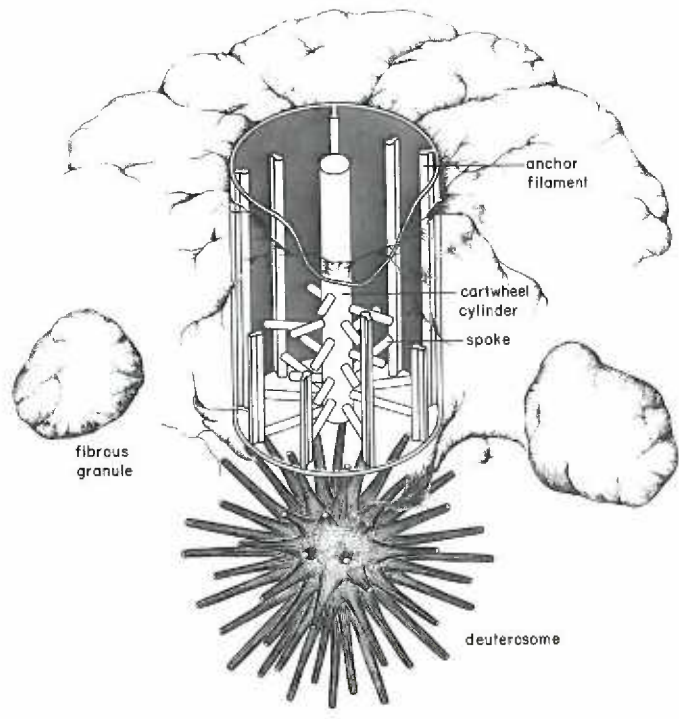
A high magnification micrograph of an early procentriole sectioned through its base shows a remarkable arrangement of filaments within the lumen. It is apparent in such a section that 9 filaments radiate symmetrically from a central filamentous ring to 9 equidistant points on the procentriole's luminal circumference (Figs. 16, 18, 22). The figure 9 is partly conjecture because not all of the filaments are clearly seen; however, other evidence indicates that the structure has nine-fold symmetry. A longitudinal section reveals that the centrally placed filament ring is really a very thin walled ($\sim 40 \text{ \AA}$) cylinder which extends from the base to the apex of the procentriole (Fig. 20). When a deuterosome is present this cylinder seems to merge with the cortex material. The addition of the third dimension to the interpretation of this filament system establishes that elements which extend from the central cylinder to the circumference are rod-shaped filaments rather than sheets. They originate at right angles to the cylinder,

Figure 14. A transverse section of a forming annulus. Fibrous granules (black arrow) are being arranged to form the wall of the annulus. The luminal band (white arrow) is being formed, and a partially complete cartwheel is in the future lumen. Glutaraldehyde, 85,000X

Figure 15. A diagrammatic interpretation of the earliest stage of procentriole formation. At this stage, neither the annulus nor the cartwheel are completed.



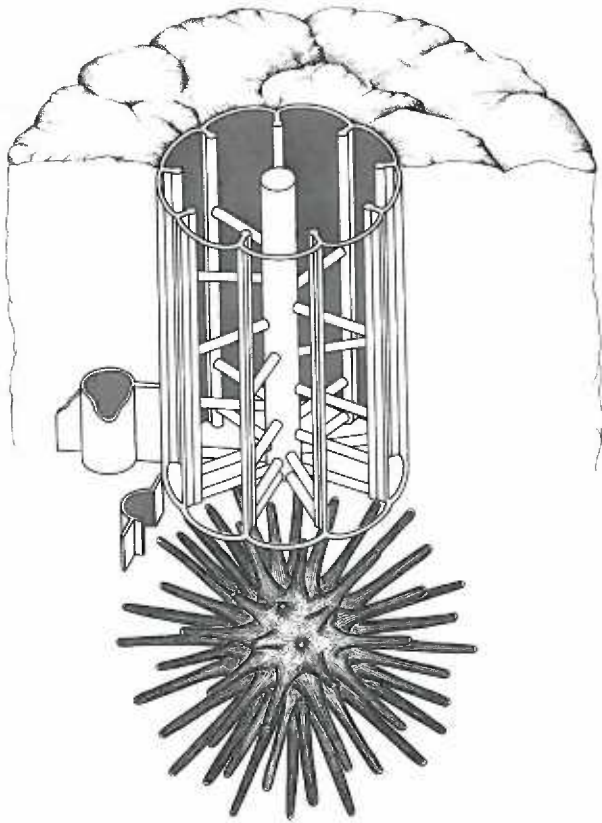
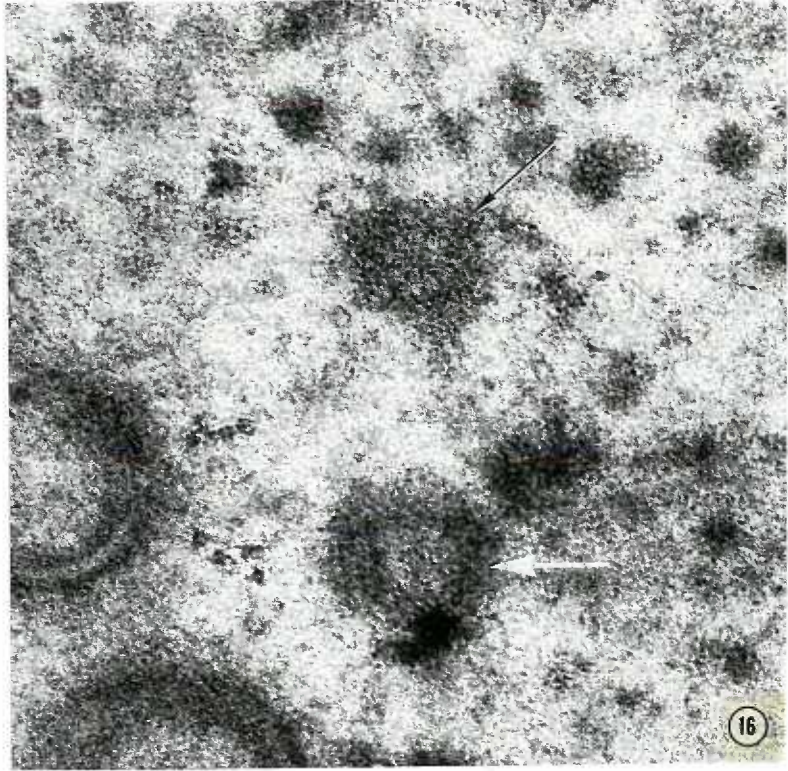
14



15

Figure 16. An annulus cut transversely (black arrow) and longitudinally (white arrow). Although the cartwheel is well developed, the A tubules have not begun to form. The black arrow points to a region where fibrous granules are being added to the wall material. This figure shows the diameter and length of the procentriole at this stage of development. Glutaraldehyde-formaldehyde, 77,000X

Figure 17. A diagram showing A tubule initiation. The cartwheel is complete, and the first A tubule is completely initiated with its inside and outside 100 Å sheets formed. Counterclockwise from the first tubule, a second A tubule is forming. It has not become attached to the luminal attachment site.



and they seem to be more numerous near the base of the procentriole.

More information about the radial arrangement of this structure can be obtained by studying photographs which have been processed to enhance the image detail (38). The negative image of a structure which appears to have radial symmetry, e.g., a transverse section of a procentriole, can be projected onto a rotatable platform. The center of the platform is aligned with the center of the image. After a piece of film is put into place, the platform is rotated and a photograph is taken every 40° of arc. The exposure period for each photograph is equal to $40/360^{\text{th}}$ ($1/9^{\text{th}}$) the time necessary for a normal print. Forty degree stops will reinforce a nine-fold symmetry, but one can test for other symmetries by choosing an appropriate arc spacing. In the case of the cartwheel structure, each of the 9 radial filaments seen in the final photograph represents the superposition of all 9 filaments, i.e., each filament is the average of 9 photographs of 9 different filaments. The result is that whereas 1 or 2 individual filaments may be incomplete or absent, the superposition of the other 8 will fill in the void. Although this reinforcement process can effectively increase the resolution one must conservatively interpret these photographs, e.g., a particularly electron dense structure could reinforce with any chosen symmetry. Thus, there may never be 9 filaments all within the same plane of section, but the ones that are present will reinforce only with nine-fold symmetry.

Figure 23 is a processed photograph of figure 16, a very early procentriole. The triplet tubules have not begun to form, but the basic pattern of the cartwheel structure has been established. The

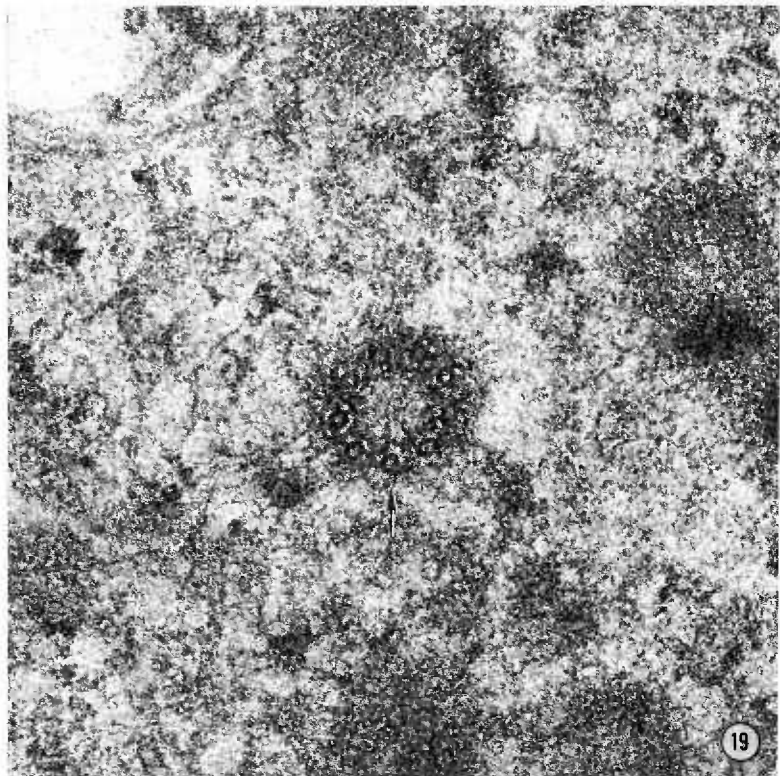
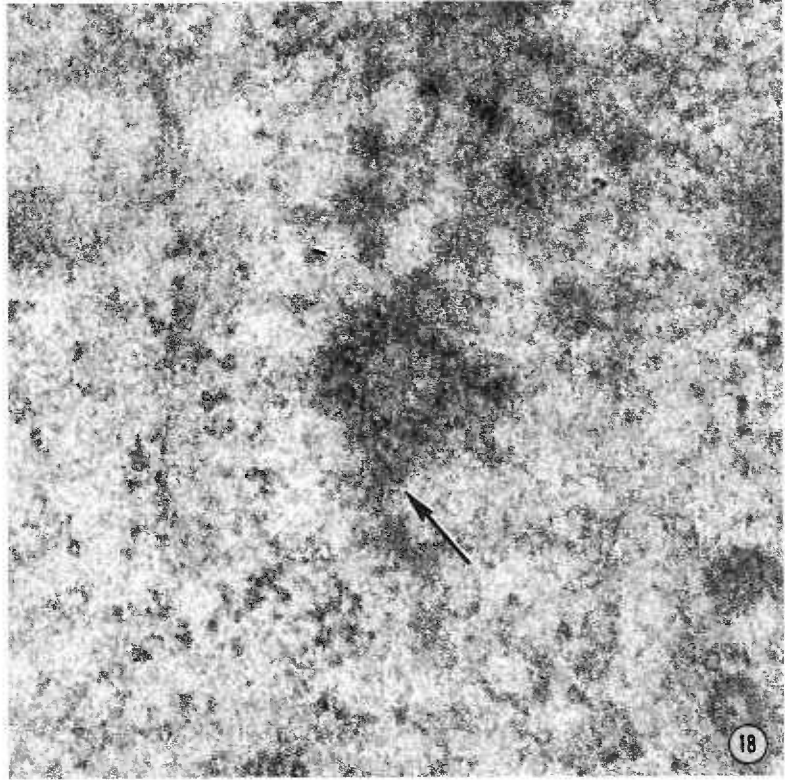
photograph shows that the system is more complex than the original micrograph had indicated. The band of material which delimits the lumen of the procentriole is segmented into 9 electron dense regions. Within the lumen in juxtaposition to each dense region there is a 100 Å long dense filament oriented parallel to the plane of the luminal circumference. Each of these 30 Å thick anchor filaments is spaced 85 Å from the dense region, and there is a suggestion that a connection exists between the two. The spokes of the cartwheel have two components. Arising at right angles to each anchor filament is a 30 Å thick filament which extends toward the center of the lumen for 165 Å (outer spoke component). There is a slight curvature to this filament. The second part of each spoke is a 40 Å thick filament which originates from the central cylinder and projects outwardly for 100 Å to terminate just clockwise to the endings of the 30 Å filaments (inner spoke component). The central cylinder is 135 Å in diameter. This three-part pattern of the cartwheel will be reinforced and strengthened but not modified as the procentriole develops. A three-dimensional description of the structure revealed by this photographic procedure will be given later.

Single Tube Formation

Very shortly after the annulus is formed, single 200 Å diameter tubules begin to appear within the wall material. These tubules appear first in the thicker regions of the wall (Fig. 18). A micrograph of a procentriole engaged in tubule formation shows that each tubule begins as a 40-50 Å thick fiber which is formed into a half circle. The open

Figure 18. A transverse section of a procentriole which is beginning A tubule initiation. Three A tubules are complete on the left side of the organelle. Notice that the wall material is thicker here, and that fibrous granules seem to be merging with the wall (arrow). Glutaraldehyde, 110,000X

Figure 19. A procentriole with all of the A tubules present. At the arrow, an A tubule, with its 100 Å sheets, which has not attached to the lumenal band. Glutaraldehyde, 93,000X



half of each incomplete tubule is randomly oriented with respect to the lumen of the procentriole (Fig. 17). Eventually more material is added to complete the tubule, but the tubule wall is not as thick in the recently completed region (Figs. 18, 19). The final tubule has a uniformly thick wall and two 100 Å long fibers project at right angles from the wall. The fibers are positioned 180° apart on the tubule, and one of them attaches to the circumferential band.

Serial sections of a procentriole at this stage do not contribute to the understanding of tubule development because the structure is only 125 μ long. However, tube formation does take place in three dimensions and figure 17 is an interpretation of this process. What was represented as a fiber in the photograph of a transversely sectioned procentriole is shown as a thin wall of material. Tubule formation, then, begins by the formation of a half cylinder. The completion of the cylinder probably begins at the base and proceeds apically. The 100 Å long fibers originating from the tubule wall are actually sheets of material which extend the length of the tubule. The circumferential band is also a thin walled cylinder, and one of the two 100 Å broad sheets of material continuously connects its tubule to this cylinder. This drawing illustrates that the clockwise orientation refers to rotating the structure on its base to the left.

The first tubule which forms is the A tubule (25) or the inner tubule of the eventual triplet set; similarly, this is the first tubule to form in Paramecium (15) and in chicken tracheal cells (33). Another similarity with these two cell types is that A tubule formation seems to occur in sequence around the annulus. In a section where the

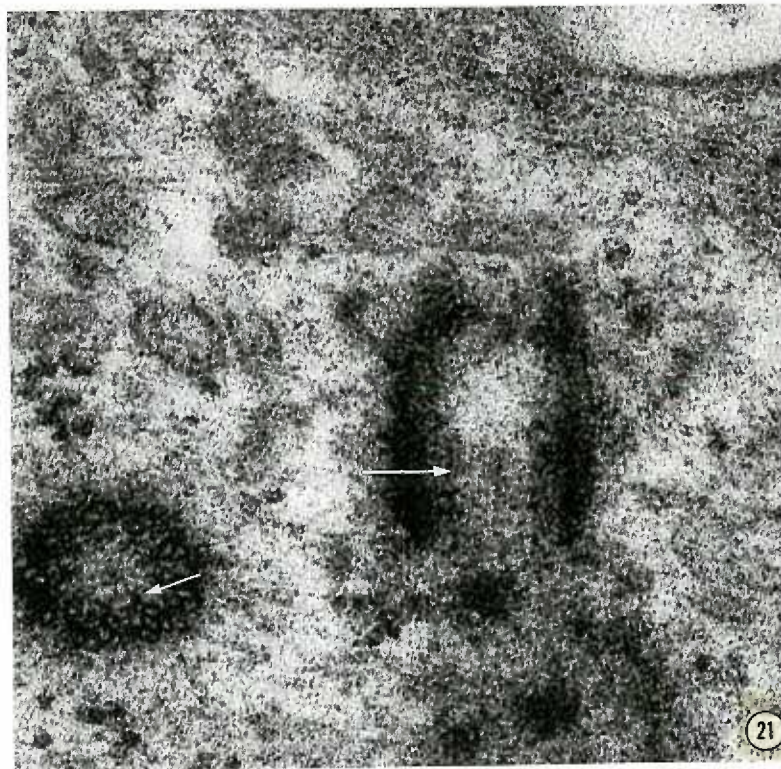
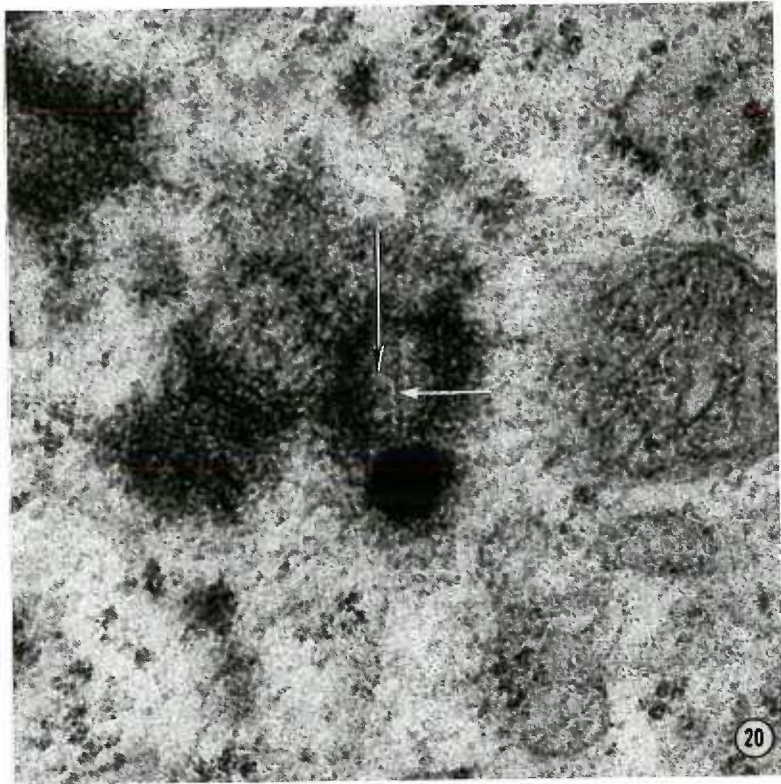
cartwheel structure is well developed the tubules that have formed are spaced 40° from each other around the annulus (Fig. 22). In sections where the cartwheel is incomplete (Fig. 26), there exists gaps in the sequential order of tubule formation, e.g., 80° may separate two well formed tubules. The cartwheel-containing sections are from the very basal region of the procentriole, and tubule formation represents the initial appearance of the tubules; initiation occurs in a sequential order, probably clockwise (looking from apex to base), around the annulus (Fig. 22). On the other hand, the sections with incomplete cartwheels are through the apex of the procentriole and the more disordered appearance of the tubules represents a less uniform growth process. This would result in tubules of various lengths randomly arranged around the procentriole; serial sectioning of more mature procentrioles substantiates these interpretations (Figs. 25, 26).

During the initiation phase, complete tubule formation is not a prerequisite for the initiation of the next tube in the sequence. Not enough early procentrioles have been seen to determine conclusively if the formation of all nine A tubules occurs before the beginning of B tubule initiation, but so far the evidence indicates that this is the case. Figure 19 shows 9 completed A tubules and the beginning of B tubule formation. Note that the final orientation of the 100 \AA broad sheets may occur after the tubule is formed and that there may be more than 2 such sheets per tubule during these early stages. All of these projecting sheets appear to have some function in orienting and maintaining the position of the tubule in the wall.

It is difficult to interpret molecular events in an electron

Figure 20. Longitudinal view of a nearly complete procentriole showing the cartwheel structure. The white arrow points to the central cylinder and the black arrow points to one of the spokes oriented perpendicular to the cylinder. The cylinder seems to merge with the cortex of the basally positioned deuterosome. Glutaraldehyde-formaldehyde, 93,000X

Figure 21. Longitudinal section of a nearly complete basal body. On the left is a transverse view of the basal region. The white arrows point to the anchor filament (both transverse and longitudinal views) which runs parallel to the central cylinder. Notice that the length of the cartwheel region has not increased from figure 20, while the walls of the procentriole have lengthened. Glutaraldehyde-formaldehyde, 93,000X



micrograph because of the vicissitudes of electron microscopic preparation procedures. A fortunate photograph of the developing tubule system is the basis for the following discussion on B and C tubule initiation because the procenteriole appears more orderly than in other micrographs - order being the criterion of favorable preparation conditions. Other photographs corroborate this evidence.

The illustrated interpretation of A tubule formation established the three dimensional nature of these events (Fig. 17). Keeping this in mind, the stereomicrographs of figure 22 show that the newly formed A tubule is aligned such that the 100 Å broad attachment sheet intersects the circumference of the lumen at a 90° angle. As the B tubule forms this angle changes to 65-75° because the A tubule has rotated on its axis in a counterclockwise direction. This simultaneously displaces the outer 100 Å sheet so that it now appears to be on the counterclockwise side of the A tubule. However, this sheet of material is no longer in the same plane as the attachment sheet. It is still in a plane which would intersect the circumference at a 90° angle. The B tubule begins by the perpendicular attachment of a new sheet to the outer 100 Å sheet. The newly added wall material projects clockwise from the 100 Å sheet. The right angle smooths out into a curve and more wall material is added at the open edge. Eventually the wall curves around through another 90° and attaches to the clockwise side of the A tubule. This completes the initial formation of the B tubule. The C tubule forms in a similar way; however, the counterpart to the outer 100 Å sheet in B tubule formation may begin on either the clockwise or counterclockwise side of the B tubule.

Figure 22. Stereomicrograph showing a transverse view of a procentriole which is engaged in B and C tubule initiation. The arrow points to a complete A tubule and the initiation of the B and C tubule is shown in progressive stages counterclockwise around the procentriole. The angle of the completed triplet indicates that we are looking down the procentriole from the apical opening. This micrograph establishes the clockwise sequence of tubule initiation. Glutaraldehyde, 140,000X

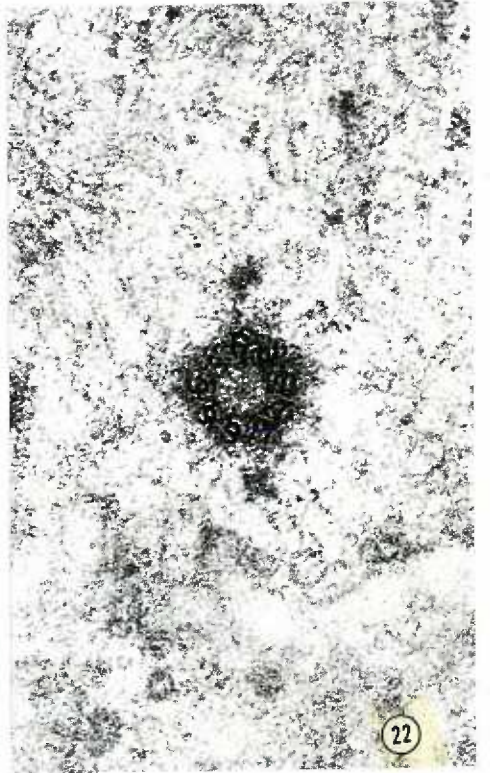
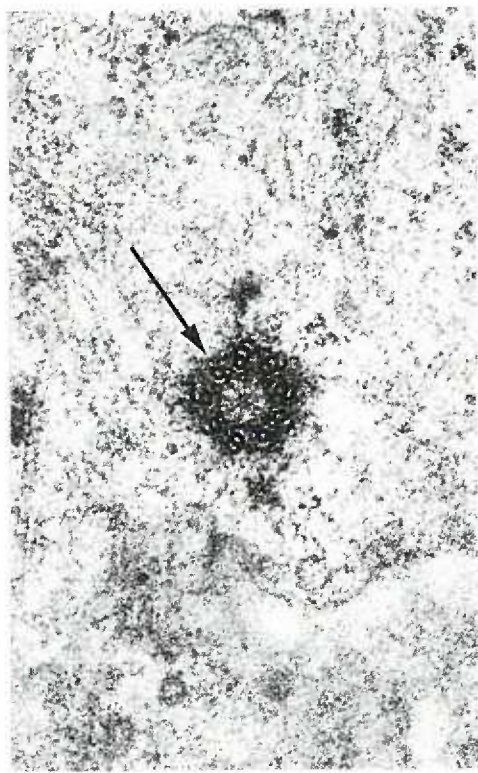


TABLE 2

	Procentriole with- out tubules	Procentriole with two sets of tubules	Procentriole with three sets of tubules	New Basal Body with cartwheel	Mature Basal Body
Internal Cartwheel Cylinder	130 A°	220 A°	210 A°	260 A°	—
Internal Spoke Component	130	70	100	100	—
External Spoke Component	140	130	150	160	—
Anchor Filament- luminal band Connector	85	100	100	100	—
Total Internal Diameter	850	850	930	1000	1500
Angle of Triplet to luminal Circumference	—	60-65°	60-65°	50°	40°
Total Outside Diameter	1700	1800	2100	2700	2500

Like A tubule formation, the initiation of the B and C tubule takes place in sequence around the procentriole. The C tubule begins to form before all of the B tubules are completed. When all three of the tubules are formed, a line drawn through their transverse axis intersects the lumen circumference at about 65° . The transverse axis of each triplet set is slightly curved in the clockwise direction of the 65° angle. This curvature has been created during the triplet formation by the slight clockwise displacement of each succeeding tubule.

The cartwheel structure has undergone some changes by the time B and C tubule initiation takes place. Figure 24 is a Markham processed photograph of figure 22. The same structures which were present in the immature procentriole are seen, but the detail is increased because of the maturation process. Although the diameter of the lumen is unchanged, some alterations in the dimensions of the three cartwheel components (the anchor filament, the spokes, and the central cylinder) have occurred. The central cylinder has expanded to 200 \AA in diameter while the inner filaments of the spoke have decreased to 65 \AA in length. The outer filament of the spoke and the anchor filament remain unchanged although there seems to have been an increase in curvature of the spoke filament (Table 2). It is now clear that connections exist between the anchor filament and the dense regions on the luminal circumference. In addition, this dense region has developed into the attachment site of the A tubule attachment sheet. At each attachment site the wall of the lumen has become indented to form a concavity. The A-B tubule complex sits within this concavity and the attachment sheet runs from the A

tubule to a point in the curvature which is in juxtaposition to the anchor filament. Each anchor filament and its corresponding A tubule are connected to the same location on the wall of the lumen.

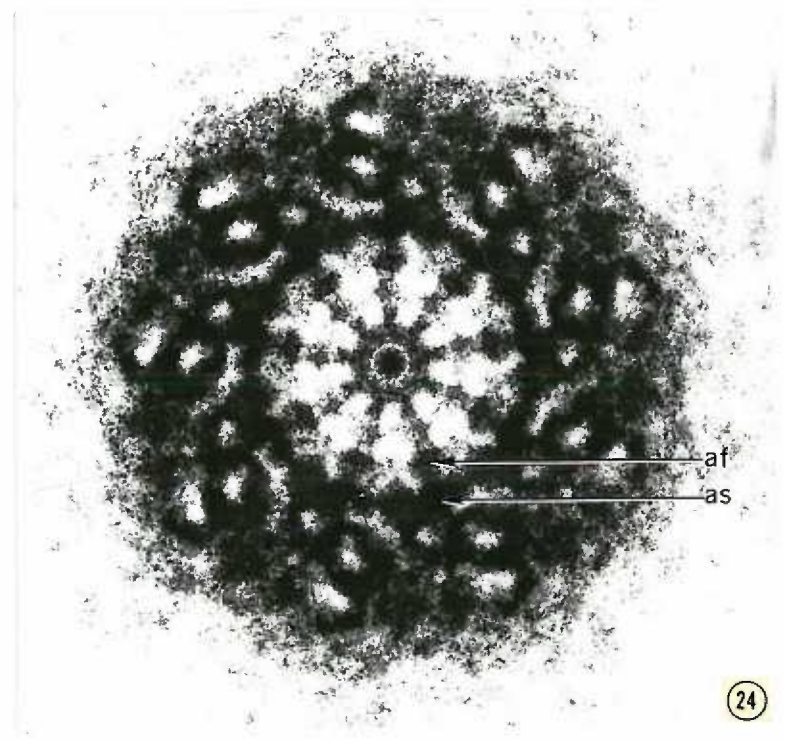
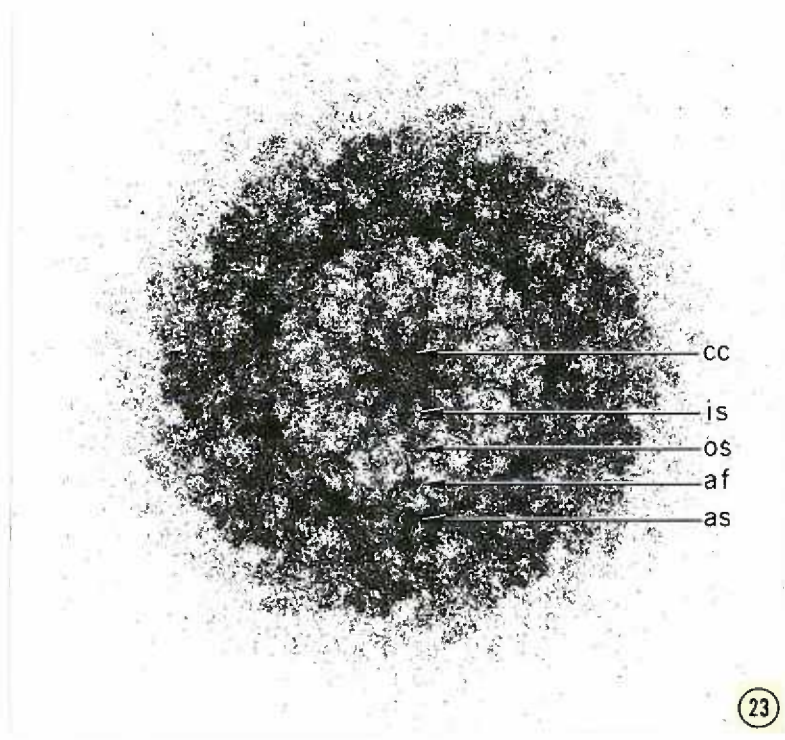
Longitudinal sections of procentrioles during these various stages of development show that the cartwheel structure does not grow as the procentriole lengthens (Figs. 20, 21). It remains a fairly consistent length, and transforms into a more robust network of filaments resembling a scaffolding for the establishment of procentriole morphology. Now the spokes are seen to connect the central cylinder with a filament that runs parallel to the lumen wall through the entire length of the cartwheel. This filament corresponds to the anchor filament seen in the image-enhanced photograph. Figure 17 is a three-dimensional drawing which incorporates the ideas presented in the description of the cartwheel structure.

It is not possible to determine the lengths of the newly initiated tubules because after they are initiated they immediately begin to grow. Thus, the A tubule is growing longer while the B and C tubules are still being initiated. At the completion of triplet initiation - i.e., when all the triplets are completed at the basal end of the procentriole - the outside diameter at the basal end measures about 200 μ . The diameter of the lumen is unchanged, and the length is about 200 μ .

The A tubule is the first to appear at the base and it is the first to complete its procentriole growth phase. The growth process seems to be a uniform deposition of material at the apical end of the tubule. It is as if the initial tubule was acting as a template for the laying down of new tubing. However, one side of the tube may grow

Figure 23. An image-enhanced photograph of figure 16. No tubules have formed, but the basic architecture of the cartwheel is established. Central cylinder, cc; inner spoke, is; outer spoke, os; anchor filament, af; attachment site, as. 350,000X

Figure 24. An image-enhanced photograph of figure 22. The cartwheel is more prominent, and there is a connection between the anchor filament (af) and the attachment site (as). The A and B tubules are nearly complete. 350,000X

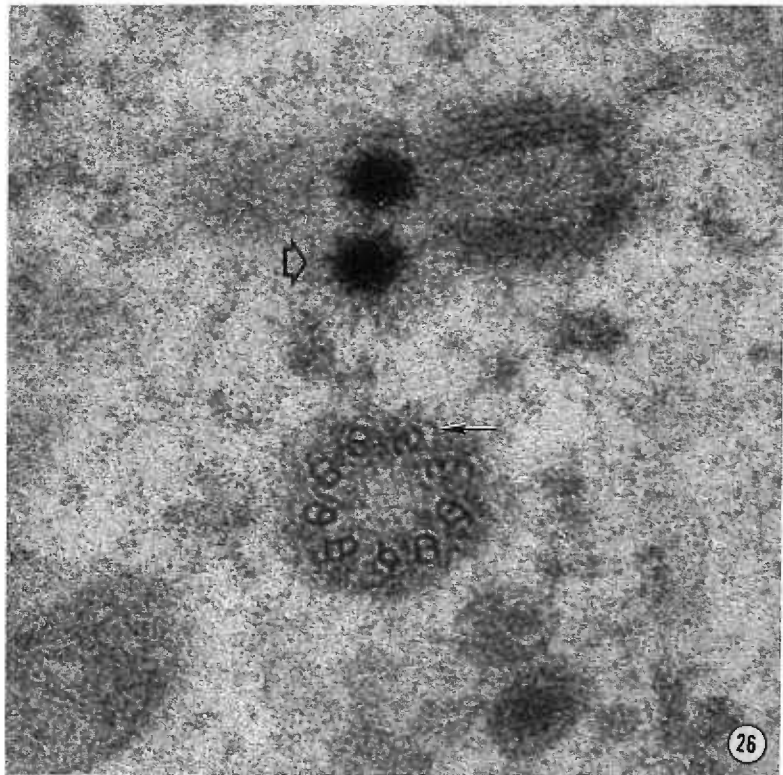
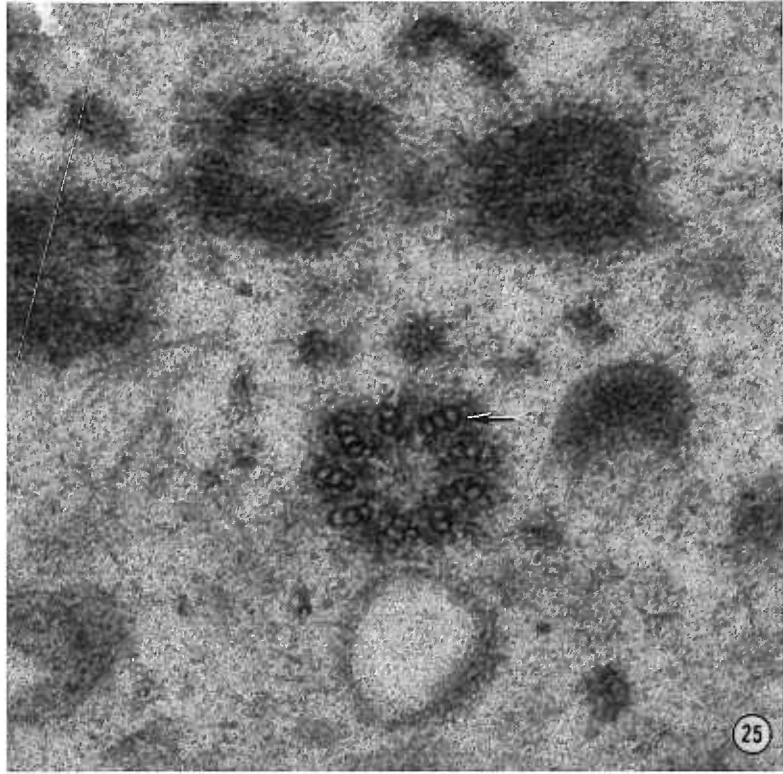


faster than another (Fig. 27) so that in one section the tube appears as a semi-circular band while in the serial section below, it appears as a complete circle.

The longitudinal growth of the C and B tubules is somewhat different. The tubule begins to lengthen as soon as the initial sheet (100 Å) is formed, i.e., this sheet grows while the broadening and shaping process is taking place at the base. A complete B or C tubule may exist in one transverse section through the procentriole while in the section above only the initial sheet is seen (Figs. 25, 26). This means that lengthening of the initial sheet occurs rapidly, and the lateral growth of the sheet with its formation into a tube progresses from base to apex. The long edge of the forming tubule wall spirals up the base tube because the broadening and shaping stages are continuously less complete from base to apex (Fig. 27). In some photographs it appears that the tubule had completely formed from base to apex before the final attachment to the base tubule. The attachment could have occurred simultaneously throughout the length of the new tubule. This latter mechanism for tubular growth is probably a variation of the first processes described.

The sequential clockwise ordering of tubule initiation is not maintained into the growth phase. The lack of synchrony in A tubule growth was discussed before. The initial sheets grow in length and breadth at different rates even within the same forming triplet. The result is that tubule growth is only ordered in the sense that A tubules form first, etc., within each triplet set. Usually the A tubule is completed at any one level of the procentriole before the next tubule begins to

Figures 25 and 26. Two serial sections through a partially completed procentriole. Figure 25 is through the basal region and figure 26 is the next section towards the apex. The triplet tubules are in the growth phase. The black arrows point to the same triplet set in each micrograph. Whereas the C tubule is complete in the more basal view (Fig. 25), this tubule is incomplete in the more apical section (Fig. 26). The triplet clockwise from the arrow in figure 26 has incomplete A, B and C tubules. The hollow arrow points to a mature deuterosome with its characteristic corticomedullary arrangement. Glutaraldehyde-formaldehyde, 110,000X

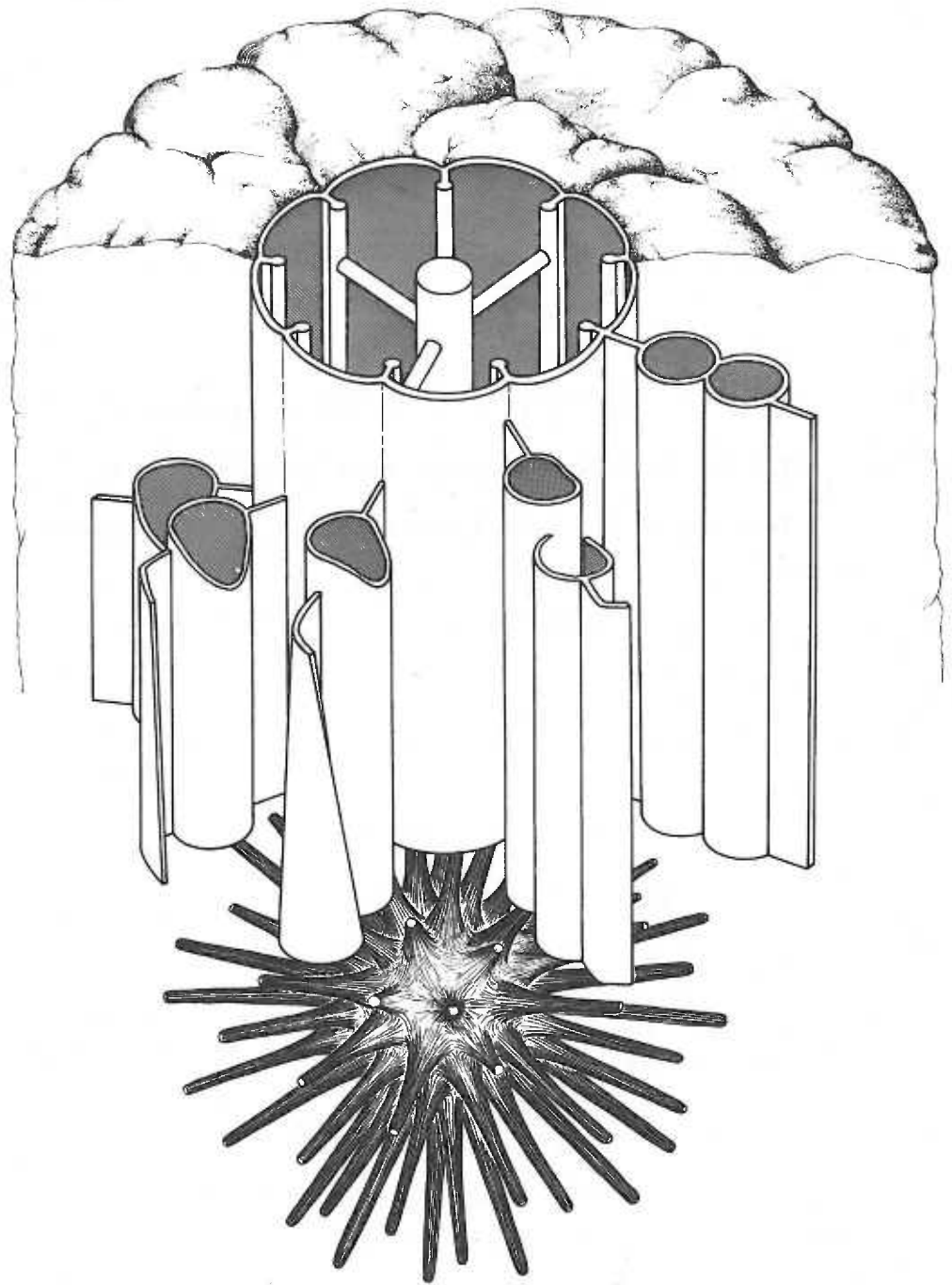


appear; however, incomplete A, B, and C tubules within one triplet set have been seen (Fig. 26).

The end of procentriole formation occurs when the structure reaches a length of 250 μ and has a basal diameter of 210 μ . These values are representative of the procentriole dimensions at a time when there seems to be a lag in the development phase; that is, many procentrioles are found with these dimensions which indicates that there is a time delay at this point. It is not possible to determine if the triplet sets must be complete throughout the 250 μ length before maturation occurs or whether once a tube begins to grow it continuously lengthens until the basal body is completed. The basic pattern of the cartwheel structure has not changed (Fig. 28) although there has been a slight increase in the lumen diameter with concomitant changes in the dimensions of the various parts of the filament system (Table 2). The angle of the triplet set to the lumen circumference is still 60-65°, and serial sections establish that this angle decreases from base to apex (Figs. 25, 26).

The mature basal body is formed by the lengthening of the procentriole and by the addition of several accessory structures. The apical extension of each triplet set is a very rapid and disordered event. The result is that the complete development of the triplets often does not occur until ciliogenesis is in progress. There is certainly not the radial sequence of development seen in tubule initiation. The angle of the triplet sets to the lumen circumference also changes from base to apex. This angle change seems to be introduced as the tubules grow. After the cylinder has almost reached its mature length, one or

Figure 27. A drawing that shows B and C tubule initiation and growth. This illustration is based on figures 22, 25 and 26. The B tubule is forming at the left and the C tubule at the right.



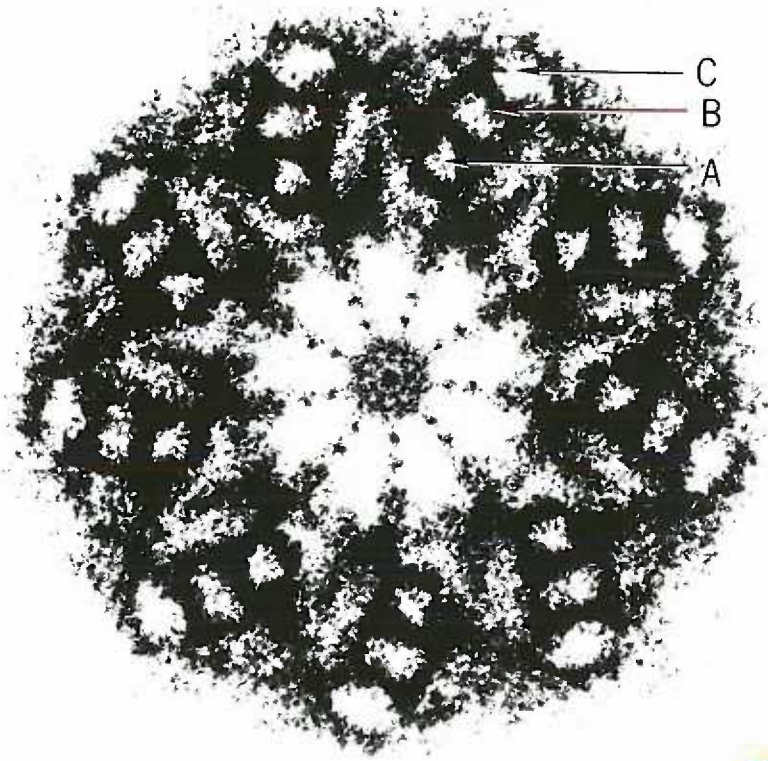
two basal feet begin to form at right angles to the wall in the mid-region. These pyramidal structures appear to be formed by the deposition of fibrous granule-like material onto the wall of the basal body. Other accessory structures, the so-called alar sheets (see "Basal Body Structure") also begin to form at this time. Each of the 9 sheets extends from the C tubule in the apical region, but they do not assume their normal arrangement until the basal body-cilium relationship is finally established.

The final form of the cartwheel is seen in the recently completed basal body (Fig. 29). All of the previously described structures are evident, but as Table 2 shows, the dimensions have changed from the mature procentriole stage. An increase in the diameter of the lumen to 1,000 Å has been accompanied by an increase in the diameter of the central cylinder. The angle of the triplet to the lumen has decreased to 50° and it will decrease even further as the basal body assumes its functional role in the cell. It is interesting that the basal angle of the triplets is more acute during the development of the tubules. In this regard, it is possible that the increase in lumen diameter occurs as a result of the reduction in the triplet angle if this change occurs by the centrifugal rotation of the triplet on the longitudinal axis of the C tubule.

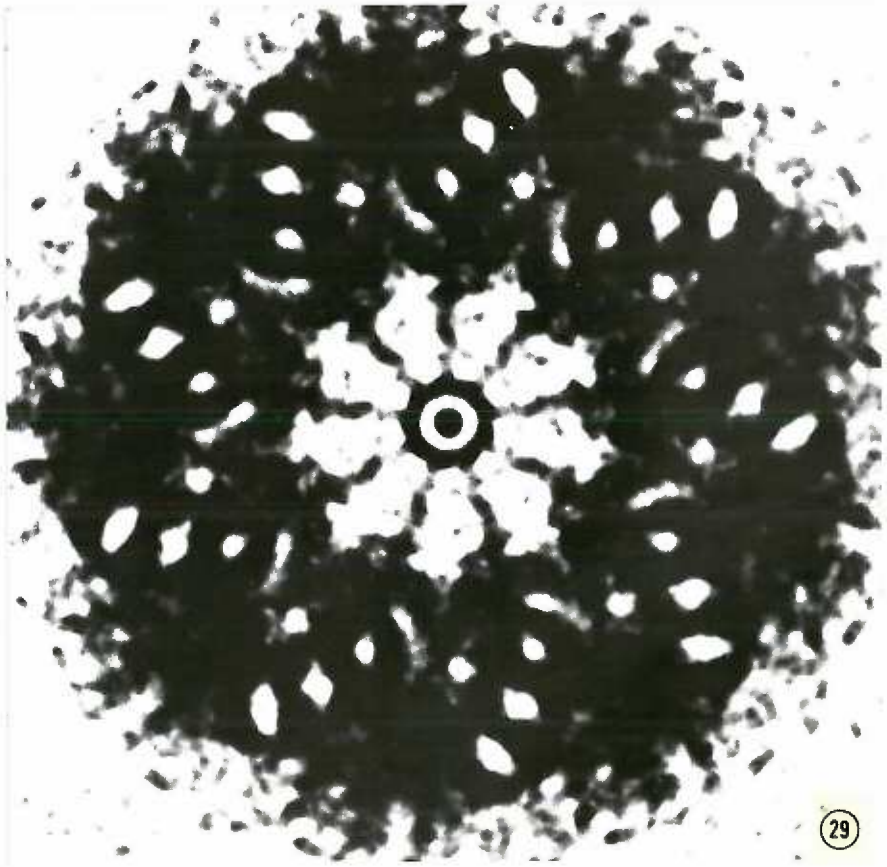
The completed basal body begins to migrate to the cell surface. During this time, or while cilium formation is taking place, the cartwheel structure breaks down. As the cartwheel regresses the central cylinder expands in diameter as it apparently resorbs the spoke system. When the cartwheel is gone, there remains a vesicle which represents

Figure 28. An image-enhanced photograph of a completed procentriole. The basic architecture of the cartwheel is unchanged. All of the triplets are complete. Notice the dense material which connects the C tubule of each triplet set with the A tubule of the triplet clockwise to it. These are the linker sheets which begin to form before the cartwheel breaks down. 400,000X

Figure 29. An image-enhanced photograph of a fully formed basal body just before the cartwheel disappears. The triplets have become surrounded by dense, amorphous material which obscures the details of the linker and A tubule attachment site. 350,000X



28



29

the expanded cylinder (Fig. 37). This vesicle is commonly seen within the lumen of centrioles and basal bodies in other cell systems (64, 67).

The completed basal bodies are now randomly arranged in groups within the apical cytoplasm of the cell. By some unknown process they migrate to the cell surface. Their previous random orientation is lost as the apex of each structure comes into contact with the cell surface and the formation of a cilium begins. At the same time, fibrous granules reappear and the rootlets start to form. Like the basal foot, the rootlets seem to form by the aggregation of fibrous granules onto the basal end of the basal body (Fig. 9).

Basal Body Structure: Introduction

Basal bodies occur in groups within the apex of a future ciliated cell at the end of their maturation phase. In such a cell the structures are arranged more or less randomly, and it is apparent that oblique or longitudinal views are the most common. A perfect transverse section is rare. In those organelles which are favorably sectioned, one can see the details of basal body structure and there is not much matrix material surrounding the tubular system. On the other hand, after the basal bodies have migrated to the surface of the cell and made their cilia, the matrix material in the wall becomes much denser. This completely obscures some of the structural details seen in the free basal bodies. In addition, the problem of finding a perfect transverse section is compounded several-fold. For these reasons, the descriptions of basal body structure are primarily based on studies of less mature structures.

It is possible to establish from a longitudinal section that the

basal body is about 500 μ long and 250 μ wide. There is the impression that the geometric form is cylindrical and that the walls of the cylinder are composed of tubules or fibrils. However, the structure does not always appear cylindrical; alternative interpretations are barrel-shaped or truncated-shaped (Figs. 33, 36). In a perfect longitudinal section through the whole length of the structure one can see that one end is dense and robust while the other end is thinner and less dense. The latter end is where the cilium forms when the structure lines up at the cell membrane, and it is referred to as the apical end of the organelle. It is also clear that there exist accessory structures, e.g., a pyramidal structure projecting at right angles from the wall (basal foot) or, in the case of fully mature basal bodies, a cone-shaped arrangement of filaments extending obliquely from the basal end of the structure (rootlet).

The only view of the structure which clearly shows the arrangement of the wall is a near-perfect cross-section, the rarest view. The longitudinal and oblique views are only useful after an understanding of the transverse sections is achieved. A reconstruction of the structure from transverse sections taken at different levels in the basal body followed by corroborative evidence from the longitudinal and oblique views is the best way to comprehend the three dimensional structure.

The following description begins with a consideration of the transverse sections through the base region, the midregion, the apical region, and the basal body-rootlet transition zone. A description of the transverse view will be accompanied by interpretations based on

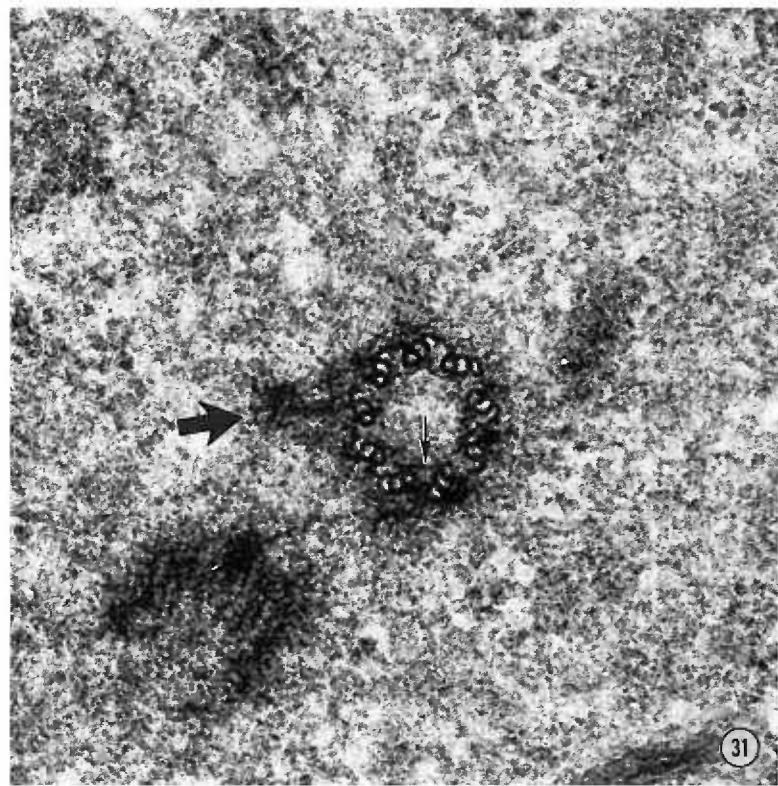
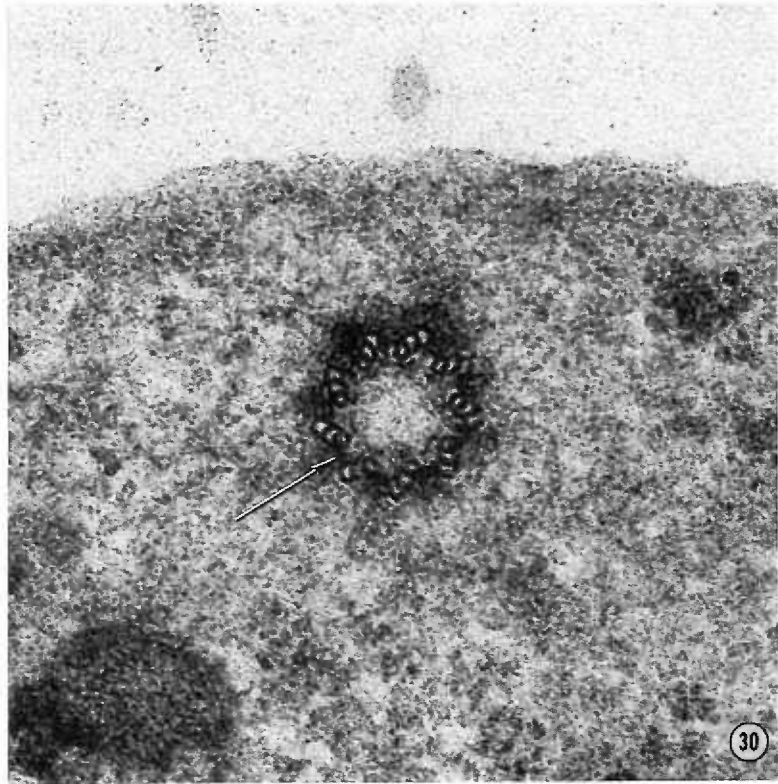
longitudinal sections. The experimental efforts to understand the structure will include stereomicroscopy, photographs of the same sections at different angles, and sectioning a model in order to compare the real with the imagined. Finally, a description will be presented of a scale model constructed from this data.

Basal Body Description

A transverse section through the base region establishes that the wall material is tubular (Fig. 30). In fact, there are nine sets of three tubules equally spaced around the cylinder wall. The tubules within each set seem to be attached in a row although a line connecting the centers of each tubule (the axial plane) would have a slight curvature to it. The peculiar thing is that each set does not consist of three tubules attached to one another in tandem, but rather it appears as if an oblong-shaped tubule has been partitioned at two regions to produce three compartments. That is, the inner and outer walls of the middle tubule, or the B tubule according to Gibbons and Grimstone (25), are also the outer and inner walls of the A (inner) and C (outer) tubules respectively. One can understand from the description of tubule development that actually the outer A wall is common to the B tubule and the outer B wall is common to the C tubule, thus establishing the crescent-shaped architecture of the B and C tubules. The diameter of each tubule is roughly 200 Å. The axial plane of each triplet set intersects a tangent to the lumen's circumference through the A tubule to form a 40° angle which is directed clockwise when the section is viewed from apex to base and counterclockwise when viewed in the opposite direction. The previously described curvature of the axial

Figure 30. A transverse section through the base of a mature basal body. We are looking from apex to base, and the transverse axis of the triplets intersects the luminal circumference at a 40° angle (see appendix). The arrow points to the linker sheet which connects adjacent triplet sets. Glutaraldehyde-formaldehyde, 110,000X

Figure 31. Transverse view of the midregion. The small black arrow points to part of the A tubule connection sheet which encircles the lumen when fully developed. The larger black arrow points to the basal foot. Glutaraldehyde-formaldehyde, 110,000X



plane is in the direction of the 40° angle; this emphasizes the pin-wheel effect of the inclined triplets. Although the 9 triplets are the most prominent structural features of the wall, there is a continuum of amorphous material surrounding all of the tubules. The amount of amorphous material and therefore its opacity increases with the maturation of the basal body. In a newly formed basal body there is a 40 \AA thick connection between the B or C tubule of each triplet and the A tubule of the triplet set clockwise to it (apex to base view) which is obscured by the increased amorphous material in later development. There is some variation in the orientation of this connecting material (Fig. 30). Sometimes it runs from B to A while other times it extends from C to A. Most often it extends from the junction of the B and C tubules to the A tubules. It does not seem as if this variation is due to a difference in the level of sectioning. A final important observation about the base region seen in transverse orientation is that the outside diameter (C tubule to C tubule) measures $250 \text{ m}\mu$ while the inside diameter (A tubule to A tubule) measures $150 \text{ m}\mu$.

The serial section above the most basal section does not reveal much change in the structure of the wall. The axial angle of the triplet sets seem to have decreased slightly although it is not possible to measure the change. The A tubule to B-C tubule connecting material is still present. This means that the linking material, which is similar to the A-C links in Trichonympha (25), is a sheet of material. Since the links are not seen in the next section above, this sheet of material is about $200 \text{ m}\mu$ long ($100 \text{ m}\mu$ thick sections). The amorphous wall material is of the same density and distribution as in the more

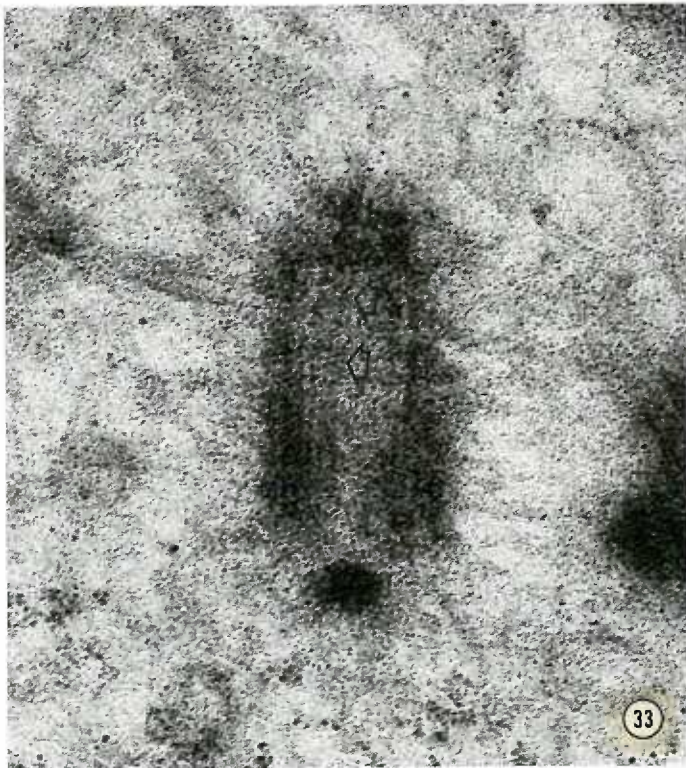
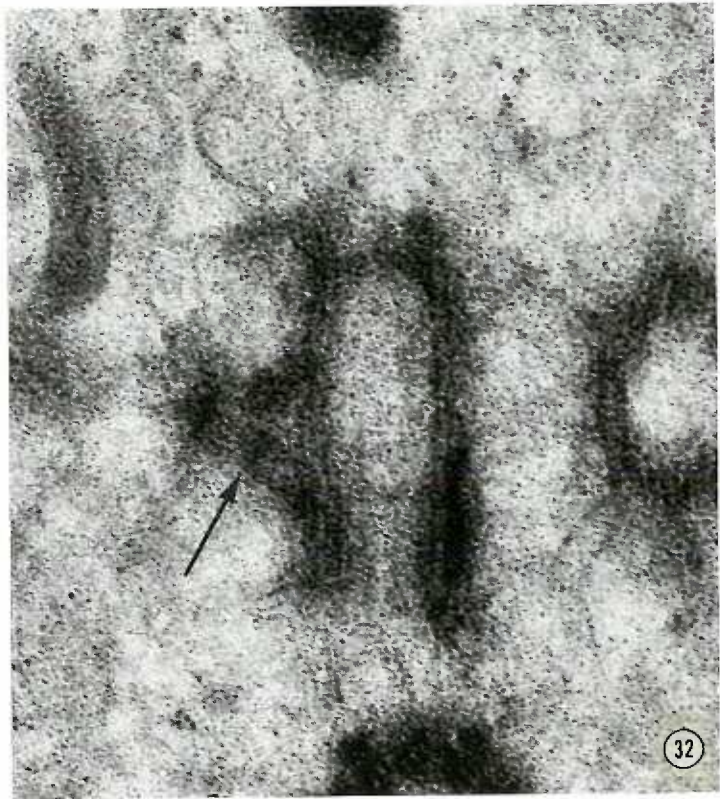
basal section.

The next section in the progression up the basal body brings us into the midregion (Fig. 31). Several structural changes occur in this region. The intertubular linking material is absent, and in its place is a continuous 50 Å thick band of material which encircles the lumen (Fig. 42). The band makes contact with each A tubule and thus appears to connect these tubules. Each triplet set appears to be unchanged from the previous description, although the axial angle of each triplet has decreased to 30°. It is hard to determine from the serial analysis if this angle change is a continuous process or whether there are different amounts of angle change depending on the region of the basal body. The inside diameter of the midregion measures 140 mμ while the outside diameter has decreased to 200 mμ (Table 3). The most notable change in the structure is the appearance of the basal foot. This triangular-shaped structure extends at right angles from the cylinder wall, and its base attaches to three of the triplet sets within the wall. Rods of fibrous material (tubules?) 140 Å in diameter extend at about a 60° angle from each of the outside triplets and sometimes a similar material extends from both sides of the middle triplet. All of these fibers are surrounded by an amorphous matrix. These rods of material merge like the struts of a teepee into a spherical mass about 125 mμ from the wall. Microtubules are often seen splaying out into the cytoplasm from this spherical structure.

The basal foot in a longitudinal view appears triangular, and it has about the same dimensions (150 mμ at base x 130 mμ high) (Fig. 32) as in the transverse view. This means that three-dimensionally the

Figure 32. Longitudinal view of a basal body showing the basal foot. Notice the tubules within the wall of the foot. The arrow points to a longitudinally arranged thickening in the basal foot wall material. This thickening gives the foot a striated appearance. Numerous microtubules extend from the apex of the foot. Glutaraldehyde-formaldehyde, 90,000X

Figure 33. Longitudinal view of a basal body which shows a triplet set in the back wall that is slanted with respect to the longitudinal axis of the basal body (arrows). Glutaraldehyde-formaldehyde, 90,000X



structure is shaped like a cone. Note the arrangement of the tubes or fibers within the wall. This view also reveals thickenings in the wall material which run from side to side of the foot oriented parallel to the long axis of the basal body; these may encircle the whole structure. The periodic placement of these longitudinal densities gives the foot a striated appearance.

In the next serial section, the diameter of the basal body lumen is unchanged and the circumferential band is still present. This establishes that the A tubule connecting material is really a sheet which encircles the lumen, as if one had put a cylinder within the lumen in the midregion. The presence of the sheet in two midregion sections establishes that it is about 200 μ long. In some transverse views of this region there seems to be an outside band of material which connects the C tubules of each triplet. Presumably this band is actually a sheet of material which encircles the outside circumference. It appears to merge with the base of the basal foot in some views.

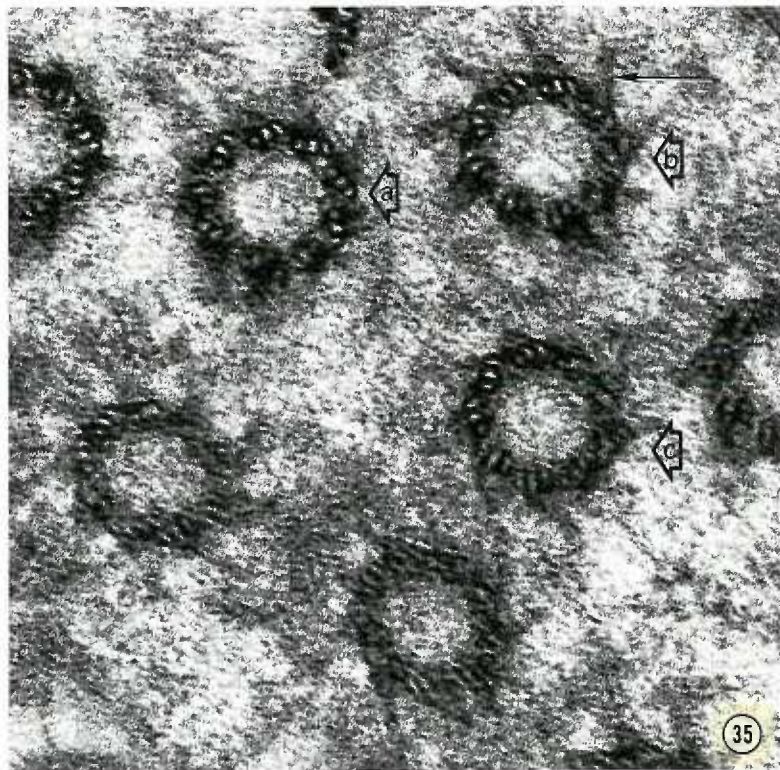
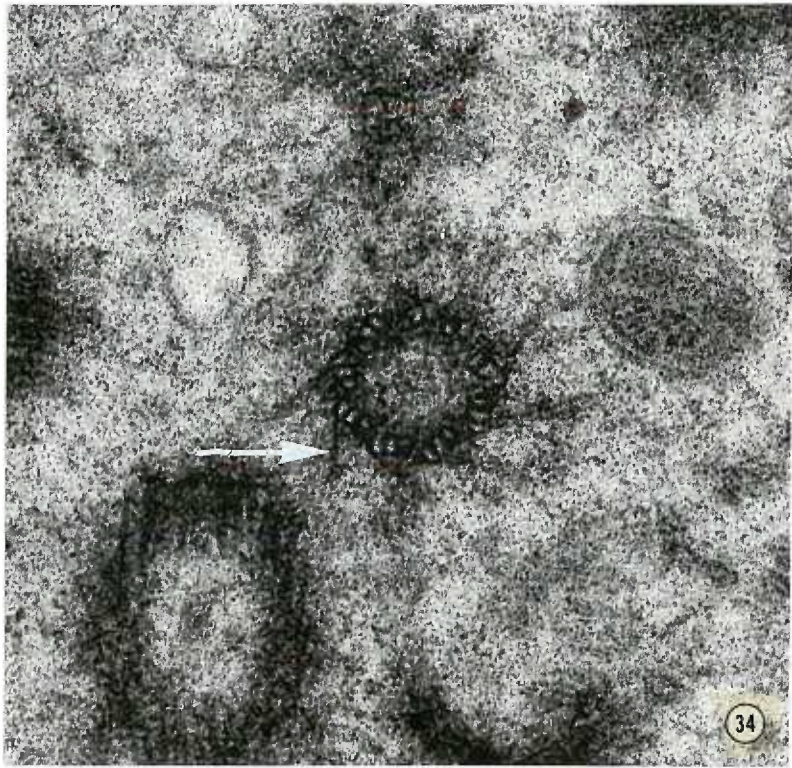
Several conclusions about the tubule organization can be made from the last section in the series (Fig. 34). The angle of each triplet set is now 15° , which has resulted in a decrease of the outside diameter to 165 μ . The diameter of the lumen has decreased to 130 μ . Considering a composite view of the serial sections, it is apparent that the axial angle of each triplet has changed from 40° at the base to 15° at the apex (Table 3). Accompanying this angle change has been a decrease in the outside diameter (C tubule to C tubule) from 250 μ to 165 μ . These dimensional changes establish that the angle change is the result of a centripetal rotation of each triplet on the longitudinal axis of

TABLE 3

	<u>Angle of Triplets</u>	<u>Luminal Diameter</u>	<u>Outside Diameter</u>
Base	40°	150m μ	250m μ
Midregion	30°	140	200
Apex	15°	130	165

Figure 34. Transverse section through the apex of the basal body (apex to base view). The axial angle of each triplet measures $\sim 10^\circ$. The arrow points to an alar sheet which extends from each C tubule at a 50° angle to the wall of the triplet. The counterclockwise side of the sheet is not as apparent as it is in figure 35. Glutaraldehyde-formaldehyde, 93,000X

Figure 35. An effective serial section of the basal body's apical region (apex to base view). The alphabetical markings represent the base (a), the midregion (b), and the apex (c) of the alar sheets. Notice that in b, the triangular appearance of the alar sheet is most apparent on those triplet sets which are the clearest (arrow). On the opposite side of this basal body, the alar sheets seem to be sectioned obliquely. Glutaraldehyde-formaldehyde, 93,000X



the A tubule. In addition, the decrease in lumenal diameter indicates that the whole triplet is positioned in the wall so that it slants towards the center of the lumen as it traverses from base to apex.

The inner and outer bands of material are absent in the apical region; however, a new accessory structure appears in this section (Figs. 34, 35, 38). Each triplet set has a triangular-shaped piece of material projecting from the C tubule. The clockwise edge (apex to base view) of this material is very sharply defined and it intersects the transverse axis of the triplet set at about 50° . The angle faces counterclockwise giving a pinwheel effect similar to that made by the triplet sets in the transverse view of the basal region. Another observation is that the size of the triangle varies with the clarity of the adjoining triplet set, i.e., it varies with the angle of the triplet to the plane of section (Fig. 35). When the triplet seems to be the most clear, the size of the triangle is reduced almost to a line. A very fuzzy appearing set of tubules does not appear to have this accessory structure at all. Only when the tubules are moderately sharp is the full extent of the triangle seen. In a stereo view of a transverse section through the apex region the structure appears to have a very sharp edge (40 \AA), as just described, which is at the top of the section, and a very fuzzy edge at the bottom of the plane of section. These observations are consistent with the idea that the triangular structure is really a sheet of material which runs up the C tubule at an angle to the triplet wall. In the stereo view, the sharp edge of the triangle represents a transverse section of the sheet while the rest of the triangle appears to be the side of the sheet going out of the plane of section. The fact that the sheet seems to be twisting out

Figure 36. A longitudinal view of the alar sheet. The arrow points to the region where the sheet folds on itself as it attaches to the counterclockwise side of the triplet set. One gets the impression that as the sheet unfolds apically it forms an incomplete cone with the wall of the triplet. Glutaraldehyde-formaldehyde, 93,000X

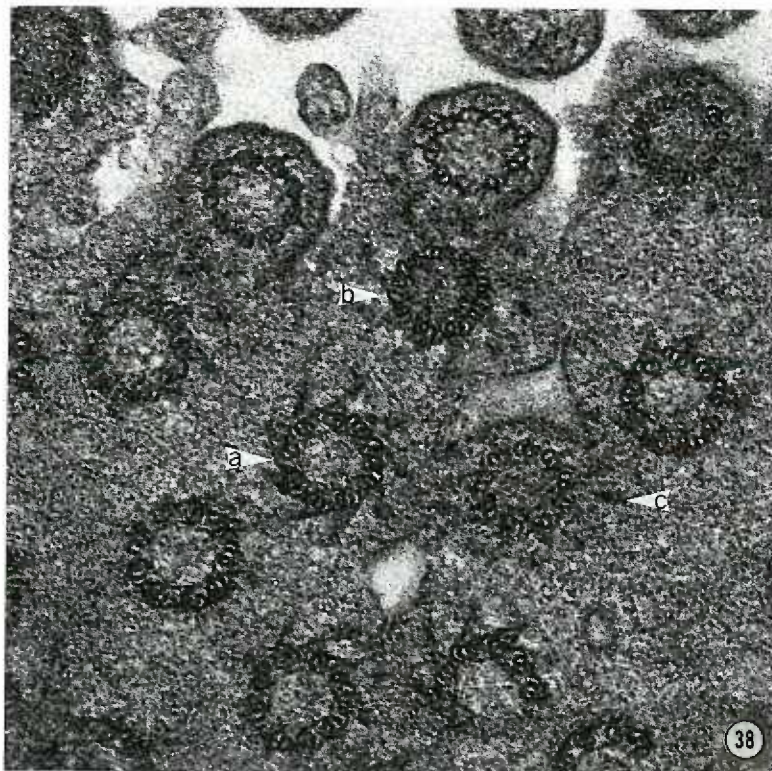
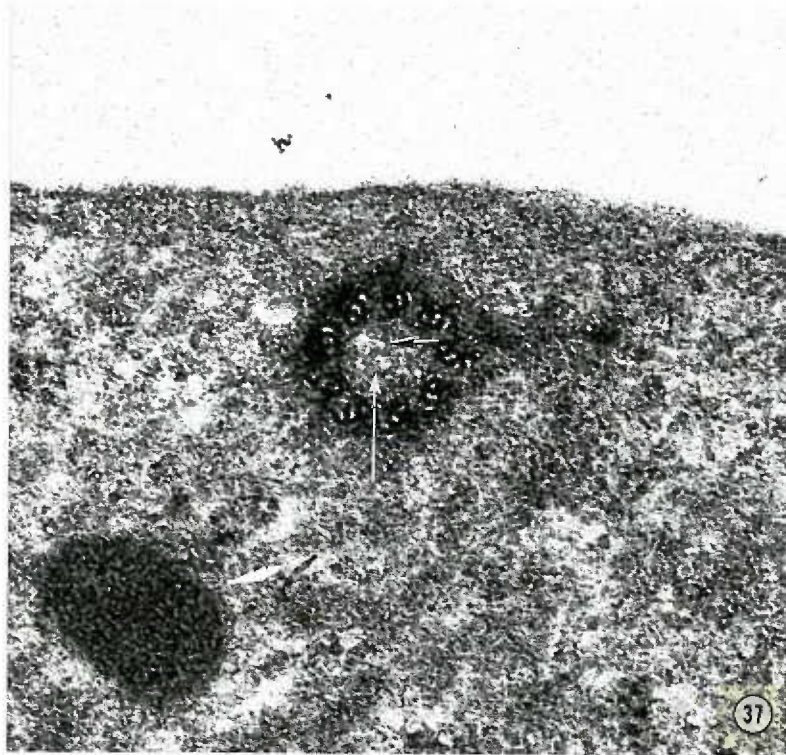


of the plane of section, together with the variation in the amount of the sheet that is seen, indicates that the material is oriented at an angle to the longitudinal axis of the basal body. If it is continuously attached to the C tubule through its entire length, then the C tubule and therefore the whole triplet is oriented at an angle to the basal body's longitudinal axis. The outer corner of each sheet merges with the base of the ciliary membrane at the basal body-cilium junction. Each attachment site on the cell membrane is a spherical electron-dense plaque (Fig. 38). In transverse section the triangular-shaped sheet with the attachment site at its apex gives the appearance that a golf club is attached to each C tubule. The various types of transverse views just described have been seen in other cell systems (18, 25, 50, 67), and the accessory structures have been called transitional fibers (25), or compositely an octagonal end structure (67). Since these structures are sheets, not fibers, the term alar (wing-like) sheets seems more appropriate.

The longitudinal view confirms the interpretation from the stereomicrographs (Fig. 36). The alar sheet begins just distal to the basal foot with its lower edge and clockwise (apex to base view) lateral edge attached to the triplet set. Since the other two edges are free, the sheet gradually unfolds toward the apical end, thus forming an incomplete cone with the wall of the triplet set. Notice in figure 36 the denser border on the outside of the ala created by the overlap of the sheet as it curves around to attach to the wall of the triplet set. We are looking through the curvature of the unclosed cone at this point. This photograph also shows that the sheet is broader at its

Figure 37. Transverse view of the midregion. The white arrow points to a vesicle in the lumen which seems to have formed from the breakdown of the cartwheel. The black arrow points to a remnant of the spoke system. Glutaraldehyde-formaldehyde, 110,000X

Figure 38. An effective serial section of the transition between basal body and cilium. The "a" basal body is sectioned through the middle of the alar sheets while the "b" and "c" basal bodies are at successively higher levels of the alar sheet region. In the "c" basal body, only the endings of the sheet are visible. These endings merge with the cell membrane. The "b" basal body shows the "golf club" shape of the sheets just before they merge with the cell membrane. Glutaraldehyde-formaldehyde, 115,000X



apex than at its base; trapezoid-shaped.

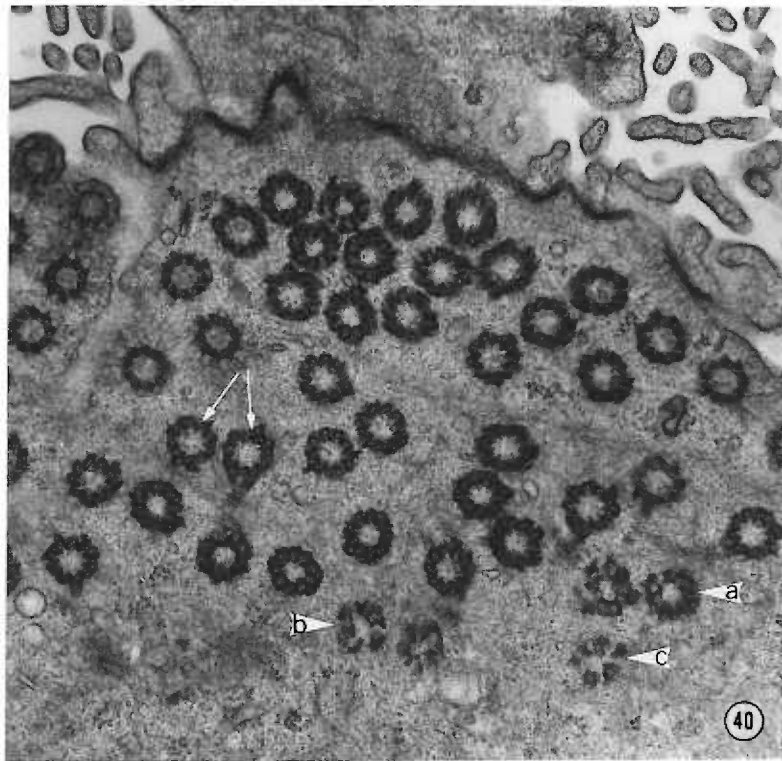
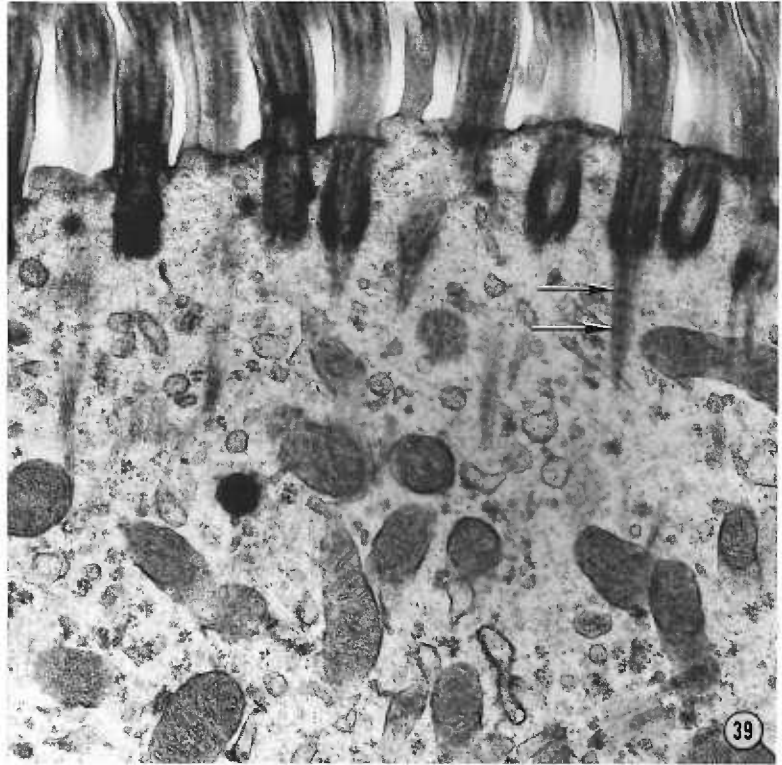
There is not a very sharp change in the transverse appearance of a basal body as one enters the rootlet. By the time the rootlet has formed, each triplet sheet has been encased in electron dense material. At the transition between the basal body and the rootlet, a transverse section shows the encasing material outlining where each triplet should be; however, the walls of the tubules have disappeared (Fig. 40). What remains are 9 spaces which are outlined by this dense material. At lower levels, these spaces collapse and the lumen of the rootlet becomes smaller. Eventually all of the material merges into one solid rod.

A study of the longitudinal section helps to clarify the nature of the rootlet (Fig. 39). The rootlet is a cone-shaped fibrillar structure which extends into the cytoplasm. Reconsidering the previous transverse views, it is concluded that each triplet set is attached to a strand of this fibrous material. The strands then form into a bundle several millimicrons away from the base region and this bundle gradually decreases in diameter as it extends into the cytoplasm. Every 110 μ on the rootlet there is a 50 Å thick fiber which runs from side to side of the bundle. Presumably these secondary fibers encircle the whole bundle, possibly acting as a binding to hold the fibers in place like barrel staves. The periodic presence of this secondary fiber gives the rootlet a striated appearance. It is not uncommon to see the rootlet running from the basal body at a fairly sharp angle.

The general features of the longitudinal view of a basal body have been described. The base to apex continuity of each triplet set was

Figure 39. Longitudinal view of the basal body rootlets. The arrows point to the bands of material which periodically encircle the conical arrangement of rootlet fibers. These bands are spaced every 140 m μ . Glutaraldehyde-formaldehyde, 17,000X

Figure 40. An effective serial section through the basal body-rootlet transition. The white arrows point to two views of the basal body which show the asymmetry of tubule clarity that indicates the triplets are helically disposed within the basal body wall. The alphabetic listing of transverse sections indicate successive sections through the rootlet region. Glutaraldehyde-formaldehyde, 25,000X

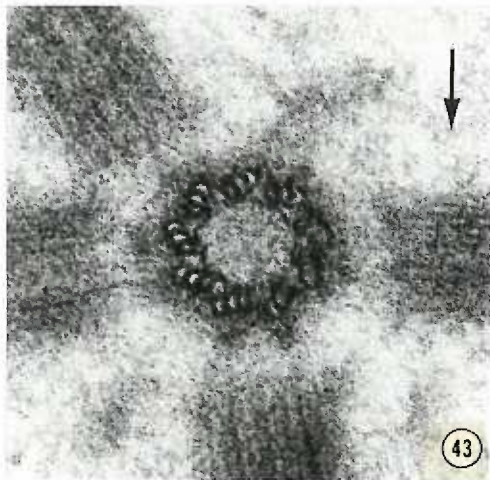
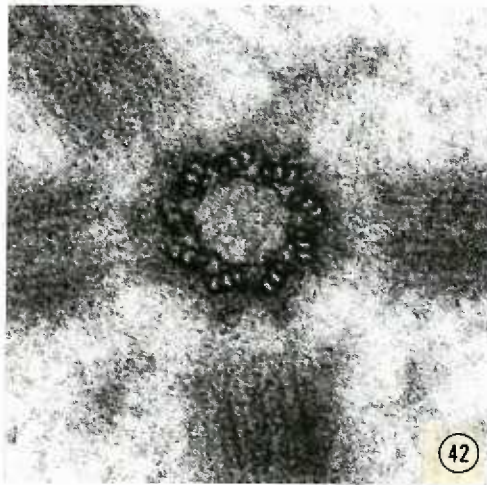
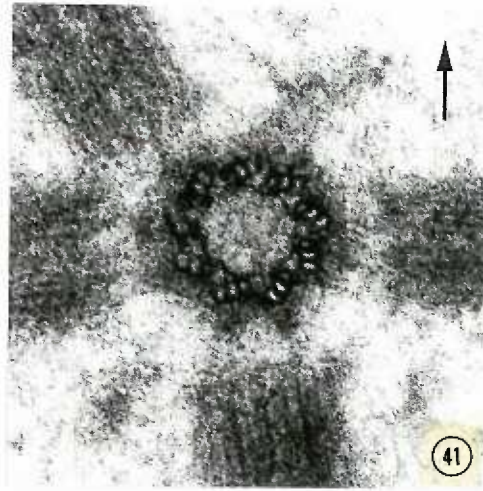


established in the serial transverse sections and likewise in a longitudinal view the tubules usually appear to be continuous. However, studying a good photograph will reveal that sometimes there are breaks in the continuity of the tubules. Sections which show these breaks are usually full-length longitudinal views. In the area of discontinuity, one can see the end of the tubules, and they appear to have been sectioned obliquely. Apparently these breaks represent the termination of a triplet sheet. One would not expect to see such an arrangement if the triplet sheets ran parallel to the longitudinal axis of the basal body through their entire length.

Several investigators have noted that a basal body or centriole in cross-section rarely has all 9 triplets sharply in focus (2, 19, 24, 46). This characteristic has been noted in transverse views of oviduct basal bodies, especially basal bodies which have a cilium. In fact, one can draw a line through the middle of a good transverse view such that on one side all the tubules are cut transversely and on the other side the tubules appear to be sectioned obliquely (Fig. 40). This has been interpreted to mean that the triplet sets do not run parallel to the longitudinal axis of the basal body but instead follow a helical path (2, 19, 46). An alternative interpretation is that those tubules which are clearly seen are oriented parallel to the longitudinal axis while the less distinct tubules are somewhat pitched (24).

Three pieces of evidence have been presented which indicate that at least some of the triplet sets are not oriented parallel to the longitudinal axis of the basal body. Suppose that each triplet is equally pitched in the same direction; then in a transverse view the

Figures 41, 42, and 43. The middle photograph (Fig. 42) is of a diplosomal centriole which is perpendicular to the axis of the electron beam. Almost all of the tubules are clearly seen. Tilting the stage of the microscope backwards 6° (Fig. 41) causes the tubules on the left to appear fuzzy while tilting the stage forward 6° (Fig. 43) causes the tubules on the right to appear fuzzy. The tubules on the opposite side in each case are sharper than in the level section (Fig. 42). The A tubule connecting sheet is clearly seen in the lumen of the centriole. Glutaraldehyde-formaldehyde, 74,500X



tubules on one side of the basal body would be coming out of the section in one direction while on the other side of the basal body they would be slanted in the opposite direction. If one tilted such a section, with respect to the electron beam, the tubules which are pitched in the direction of the tilt would become less sharp because the incident electron beam would no longer pass through the lumen of the triplet, but instead would pass through the walls of the tubules. That is, after the tilt we would be looking at the sides of the tubules. However, on the other side of the basal body in this tilted view, the tubules would become more aligned with the path of the electron beam and therefore seem to be sharper.

Figure 42 is a transverse section of a centriole engaged in basal body production. The section is through the midregion of the centriole, and almost all of the triplets are clearly seen. When the stage of the microscope is tilted backwards 6° in the direction of the arrow, the triplets on the left side of the centriole no longer appear sharp while the triplets on the opposite side are seen more clearly (Fig. 41). Tilting the stage in the reverse direction 6° makes the formerly sharp tubules appear fuzzy and the adjacent side sharper (Fig. 43). The tubules on each side of the tilting plane respond to the tilt as if they were pitched in opposite directions. This experiment establishes that each triplet is indeed pitched, and the response of the tubules to the direction of tilt indicates that the triplets are pitched to the left (clockwise in the apex to base view). This data agrees with the evidence for the direction of pitch obtained from the transverse sections of the alar sheets.

Figures 44, 45, and 46. Three views of a section of the scale model which demonstrates that the model responds to a backward tilt (arrow, Fig. 44) and a forward tilt (arrow, Fig. 46) in a similar way to the section of the real centriole (Figs. 41, 42, 43).

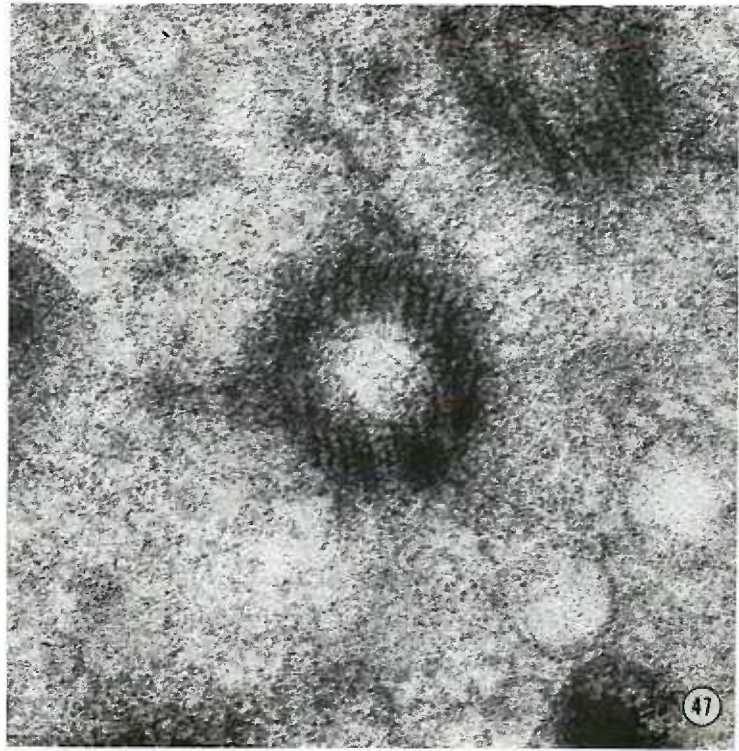


Other views of the basal body clarify the nature of the pitch. Oblique sections of basal bodies are important because enough of the tubules can be seen to establish their relationship to the longitudinal axis (Fig. 47). These sections usually show the tubules to be slanted in opposite directions on either side of the basal body. The angle between the axis of two opposite tubules is 30° ; therefore each tubule is pitched 15° . The pitch can also be detected in a stereo view of a transverse section, and measurements from these photographs give a pitch of 14° . Finally, there is a rare longitudinal section which grazes through either the front or back tubules but mostly contains side tubules (Fig. 33). Sometimes the back or front tubule is slanted to the long axis of the basal body at an angle of approximately 15° in this view.

Both the tilting experiment and the arrangement of the alar sheets support a clockwise pitch. However, serial section analysis thus far has either not detected a pitch or the pitch was in the counterclockwise direction. There are several technical difficulties to overcome with serial sectioning analysis, and maybe the results reflect an inability to solve these problems. What is more intriguing is that the serial sections analysis is accurate but that the pitch can change depending on the functional state of the organelle. For example, one of the basal bodies that was serially sectioned was in a cell that was resorbing its cilia. The analysis showed a counterclockwise pitch, and the alar sheets were not normally disposed. Possibly the resorption of the cilia had caused a change in the pitch of each triplet set. In another serial section analysis of a newly formed basal body, no pitch was detected;

Figure 47. An oblique section of a basal body. The triplet sets on the bottom side are pitched to the left while those on the top side are pitched to the right. The angle between the triplets on opposite sides of the section is 30° ; therefore, each triplet is pitched $\sim 15^{\circ}$.
Glutaraldehyde-formaldehyde, 93,000X

Figure 48. A section of the model photographed to show that the pitch of the triplets matches the triplet pitch seen in the oblique section (Fig. 47).



yet the typical asymmetry of tubule sharpness is often seen in a transverse section of these less mature basal bodies. Thus, the pitch may vary continuously as a part of basal body function.

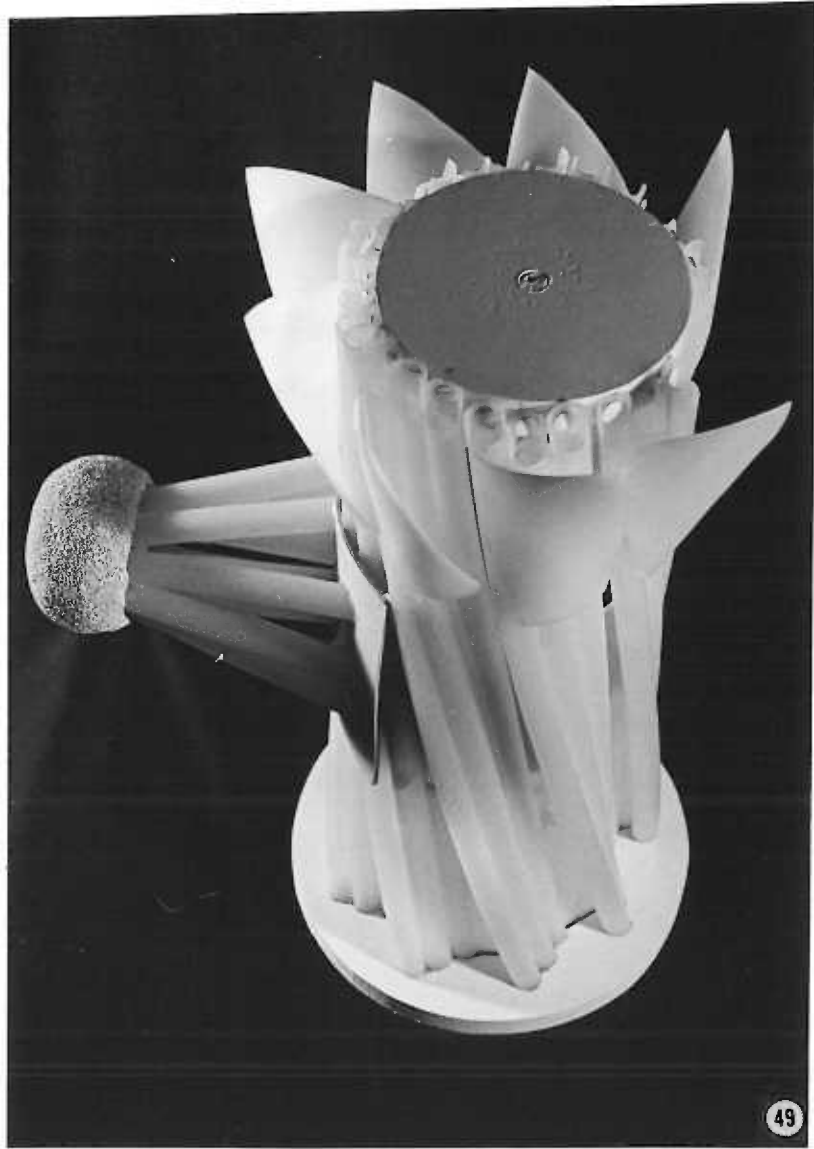
Basal Body Model

The aim of this study was to construct a three dimensional model of the basal body which accurately represented the real structure. The most controversial aspect of the basal body structure is the three-dimensional arrangement of the triplet sets. If the model is accurate, then one should be able to experimentally reproduce the tilting experiments performed in figures 41, 42, 43.

A scale ($330 \text{ \AA} = 1 \text{ inch}$) model of the tubule arrangement was constructed from polyethylene tubes so that each triplet was pitched to the left at 14° . The whole model was embedded in plastic and sectioned on a band saw. One of the three-inch thick sections (3 inches = 100 μ) was first photographed with the section oriented perpendicular to the camera (Fig. 45). Two other photographs were taken with the sections tilted backwards and forwards respectively (Figs. 44, 46). From this series of photographs, it is clear that the tilting of the model exactly reproduces what was seen when the centriole was tilted. In addition, a photograph of the section when it is acutely tilted produces a picture which strongly resembles an oblique section of the real basal body (Fig. 48).

A complete scale model of the basal body was constructed (Fig. 49). Those features built into the model include: clockwise pitch of the triplet sheet, continuous centripetal rotation of each triplet from base to apex, cone-shaped basal foot composed of 13 tubules, linker sheets

Figure 49. A full view of the complete model. The basal foot (left), the 14° left-handed pitch, the centripetal rotation of each triplet on the longitudinal axis of the A tubule and the alar sheets at the apex are clearly seen.



connecting the A and B tubules of adjacent triplets, middle band of material around the circumference of the lumen, and alar sheets on each triplet set. In order to test the accuracy of the model, various views of the replica can be compared with appropriate electron micrographs of the real structure (Figs. 50, 51, 52).

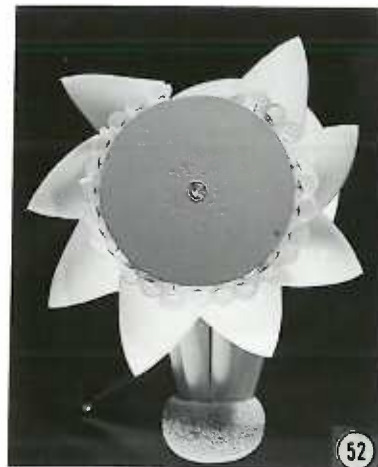
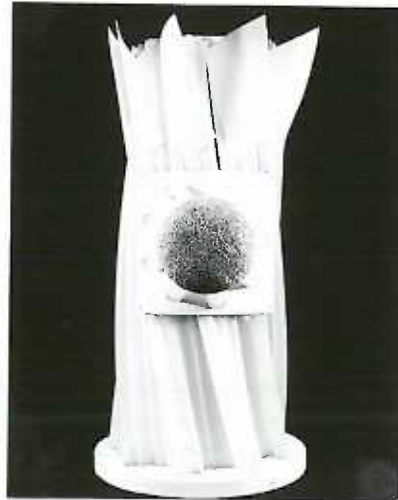
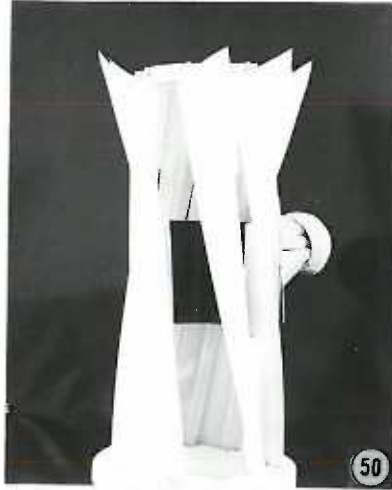
A longitudinal section of a basal body either shows the walls tapering from base to apex (Fig. 33) or they are slightly convex which makes the structure appear barrel-shaped (Fig. 36). Figure 50 and figure 51 are views of the model which show these two configurations of the basal body wall. It is apparent that the combination of the triplet pitch and the continuous base to apex centripetal rotation of each triplet creates the barrel-shaped geometry that is sometimes seen (Fig. 51). A view through the front wall of the model (Fig. 50) shows the slant of the tubules in the back wall. Removing one or two sets of the side tubules would reproduce the kind of tubule arrangement seen when a longitudinal section just grazes through the back tubules of an actual basal body (Fig. 33). This view of the real structure is rare because it is necessary to have several sets of side tubules to establish the longitudinal axis of the basal body; this acts as a reference point in detecting the pitch. Most sections of the front or back wall show all of the tubules running parallel to each other so that it is impossible to identify the true longitudinal axis.

The accuracy of the model's accessory structures and their arrangement can also be established. It is not difficult to visualize that transverse sections through the base and midregions will appear similar to actual sections, e.g., the A-B linkers or the luminal band. Likewise

Figure 50. A view of the model which shows the A tubule connecting sheet (inner black band) and the A-C tubule linker sheets at the base. Looking through the opening to the back side of the model, the triplet sets slant to the right as they did in figure 33 of the real basal body. Also, the overall longitudinal view gives the impression that the walls of the basal body taper towards the apex. (Compare with figure 32.)

Figure 51. A longitudinal view of the model in which the walls of the basal body appear barrel-shaped. Compare this view with figure 36.

Figure 52. An effective transverse view of the alar sheets. Notice the triangular appearance of the sheets in this view. Compare with figure 35.



the cone shape and tubular arrangement of the model's basal foot will give a triangular shaped structure both in longitudinal and transverse views. Possibly there are not as many tubules in the real foot and the diameter of the tubules is probably smaller than is depicted by the model. Viewing the model lengthwise (Figs. 49, 51), the overlapping appearance of each alar sheet created by the attachment of its bottom edge is exactly like that seen in the longitudinal section of the real sheet (Fig. 36). The curvature of the upper edge of each ala is an artifact caused by a bending of the material used for the model and is not apparent in either a transverse view or a longitudinal view of the basal body. A top view of the model (Fig. 52) reproduces the triangular shape of the ala seen in a transverse section through the apex although in the real structure the apical angle of this triangle is much smaller. This means that either the twist in the ala created by the attachment of its basal edge to the triplet wall is greater than is depicted by the model or the counterclockwise edge of the sheet is slanted backwards rather than running parallel to the long axis of the basal body. The depth of field in the photograph of the model makes the sheets appear to twist down the axis of the model. One gets the same effect in a stereo view of a transverse section through the apex of a basal body; such a twist would not be detectable if the triplet tubules were not pitched.

Enzyme Digestion Studies

Leduc has developed a method for embedding tissue in the water-miscible plastic glycol methacrylate (GMA) (35). This permits one to study tissue which has never been exposed to the damaging effects of

TABLE 4

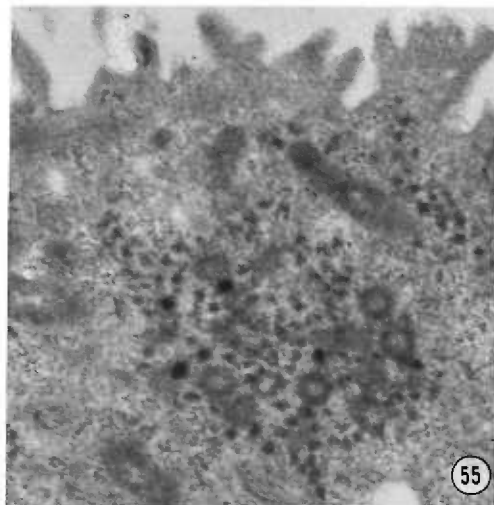
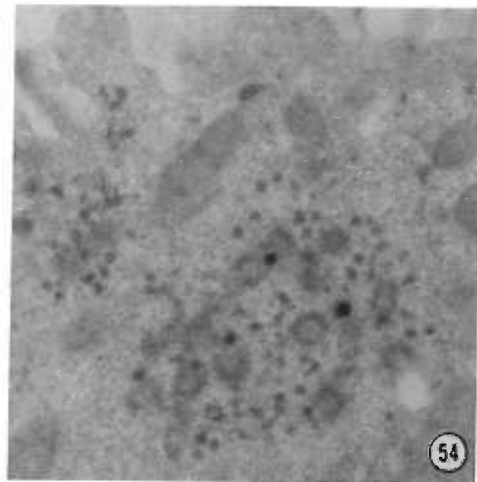
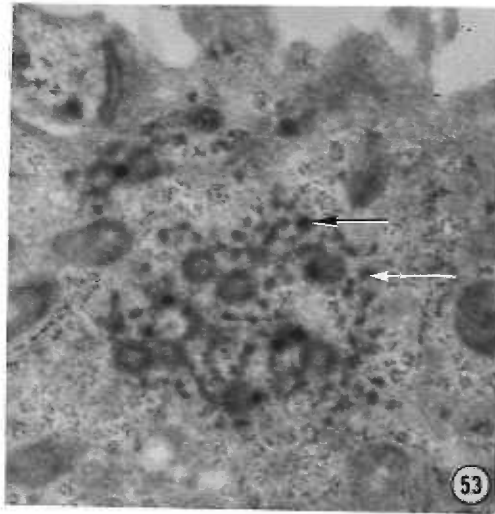
<u>Subject</u>	<u>Araldite</u>	<u>Glycol Methacrylate</u>
Fibrous Granules	50 - 75m μ	60 - 80m μ
Deuterosome	85	120
Procentriole Diameter	120	180
Procentriole Length	120	170
Basal Body Diameter	250	280
Basal Body Length	500	530

alcohol and propylene oxide. In addition, when thin sections from unosmicated blocks are exposed to hydrolytic enzymes the staining properties of various cell components are altered. The plastic allows the enzyme to penetrate the tissue and selectively remove sensitive components (36). Thus, organelles which contain RNA should be specifically affected by RNAse. These techniques are useful in studying the chemical composition of basal bodies and their precursors.

In GMA-embedded material most organelles appear larger than they do in equivalent Araldite-embedded preparations. Table 4 lists the measurements of basal bodies and precursor structures for both techniques. The smaller dimensions of organelles in Araldite-embedded tissue may be the result of either the osmium tetroxide postfixation or the alcohol dehydration procedure. It seems reasonable to assume that the minimum amount of trauma associated with the GMA embedding method preserves cell organelles in their natural dimensions.

Cell organization in the fimbriae is not altered by the GMA embedding procedure, but cells do look different than in the typical Araldite-embedded material. Generally, the membrane components do not stain well and thus appear translucent in contrast to the opaque ground plasm. This gives the membranes a negative-image appearance. The mitochondria appear normal except for the negative-staining criste (Fig. 58). Ribosomes stain very intensely, and the various organization patterns of the endoplasmic reticulum are similar to those seen in Araldite-embedded tissue (Fig. 53). The Golgi complex is not always visible. The cytoplasmic matrix often is filled with small vacuoles which are probably artifacts introduced during the embedding procedure.

Figures 53, 54, and 55. Three serial sections which have been treated with buffer (Fig. 53), RNAse (Fig. 54), and DNAse (Fig. 55). The white arrow points to a fibrous granule and the black arrow to a deuterosome. Glutaraldehyde-formaldehyde without post-osmication, glycol methacrylate-embedded, 18,500X



The nucleus is unchanged, and its border is sharply delineated by the unstained nuclear envelope. The heterochromatin stains intensely and its arrangement around the periphery of the nucleus is normal. The nucleolus is recognized by its staining intensity, its location within the nucleoplasm and its fibrillar structure.

Like the other cell organelles, the procentrioles and basal bodies are easily recognized (Fig. 53). The walls of the procentrioles stain homogeneously both in transverse and longitudinal views. The basic geometry of these structures appears unchanged; however, the details of tubule organization cannot be seen because of the reduced resolution that accompanies GMA embedding. Basal body geometry is also recognizable, but the walls do not stain homogeneously. Although the tubules are not distinguishable in a transverse view, their location in the wall is marked by an increase in stain intensity. Thus, 9 symmetrically placed electron dense regions are seen. The walls of a longitudinally sectioned basal body display a similar heterogeneity of stain uptake (Fig. 58). The base region and basal foot areas of the wall stain more intensely and sometimes the whole wall is segmented into light and dark staining areas.

The overall organization and order of the epithelial cell in the fimbriae is unchanged by the GMA embedding procedure; in fact, the arrangement of the organelles may be more ordered. This is particularly true of the distribution of fibrous granules within the granule aggregates. In contrast to the more or less random arrangement of granules seen in Araldite-embedded material, the fibrous granules appear to be connected together to form strings and sheets (Fig. 56).

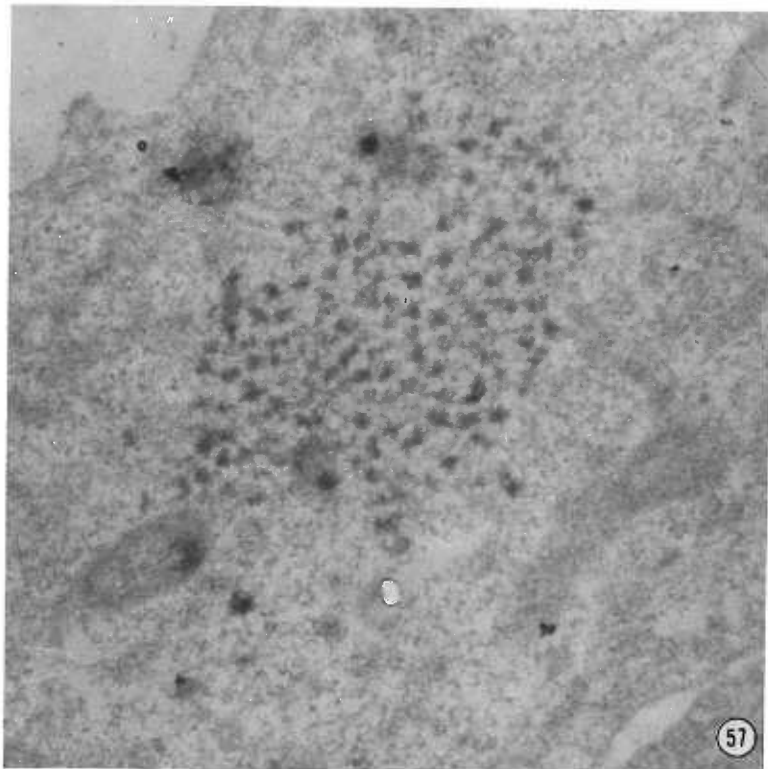
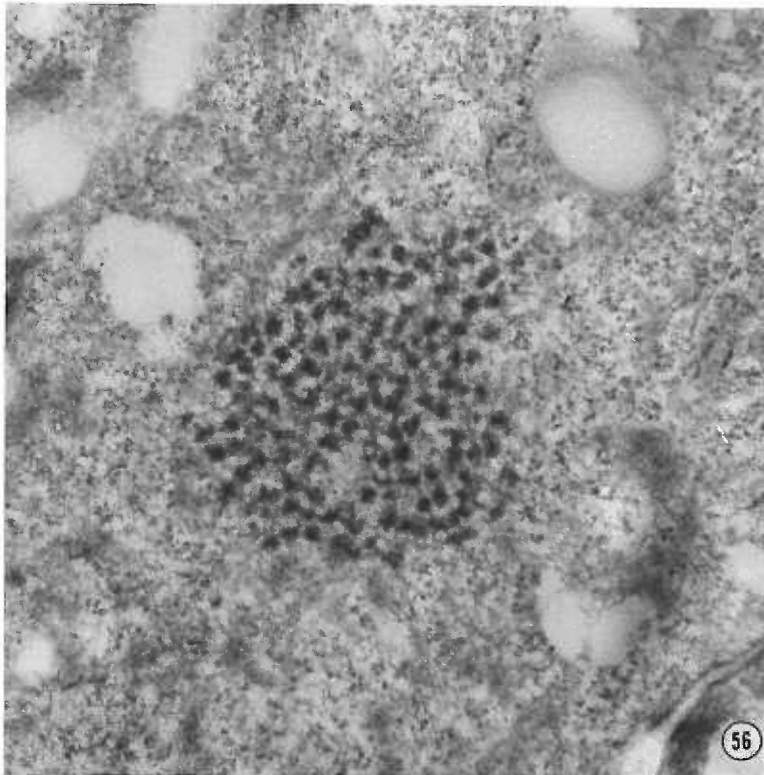
In addition each granule seems to be surrounded by a less dense cortical matrix. The cortical material of adjacent granules merges to form the strings of fibrous granules (Fig. 53). As in Araldite-embedded material, the granules vary in electron opacity. This may be due to the way the section passes through each granule, i.e., the lighter appearing granules may actually be fibrous granules sectioned through their less dense cortex. Other organelles such as ribosomes, mitochondria, etc., are rarely found within these tightly arranged aggregates of fibrous granules.

Deuterosomes are easily distinguished from fibrous granules because they stain much more intensely - even in their immature stages (Fig. 53). The corticomedullary organization is not as apparent due to the reduced resolution. However, the GMA embedding procedure does not alter the deuterosome-procentriole relationship.

The morphological juxtaposition and similar staining properties of the fibrous granules and procentrioles emphasizes the possible product-precursor relationship described earlier. It is not possible to distinguish either the fibers in the granules or the tubules in the walls of the procentrioles with this embedding procedure (Fig. 53). Therefore, the fibrous granules appear exactly like the procentriole wall material. In fact, it is often difficult to differentiate a procentriole from a short string of fibrous granules.

The digestion of GMA thin sections with nucleases had the same effect on cell structure as described by Leduc (36). Twelve hours of digestion with RNAse completely removed the ribosomes and caused the ground-plasm to stain less intensely (Fig. 54). Bound and unbound

Figures 56 and 57. Two serial sections of a fibrous granule aggregate. The first section (Fig. 56) was treated with buffer while the second section (Fig. 57) was treated with RNAse. Glutaraldehyde-formaldehyde without post-osmication, glycol methacrylate-embedded, 23,000X

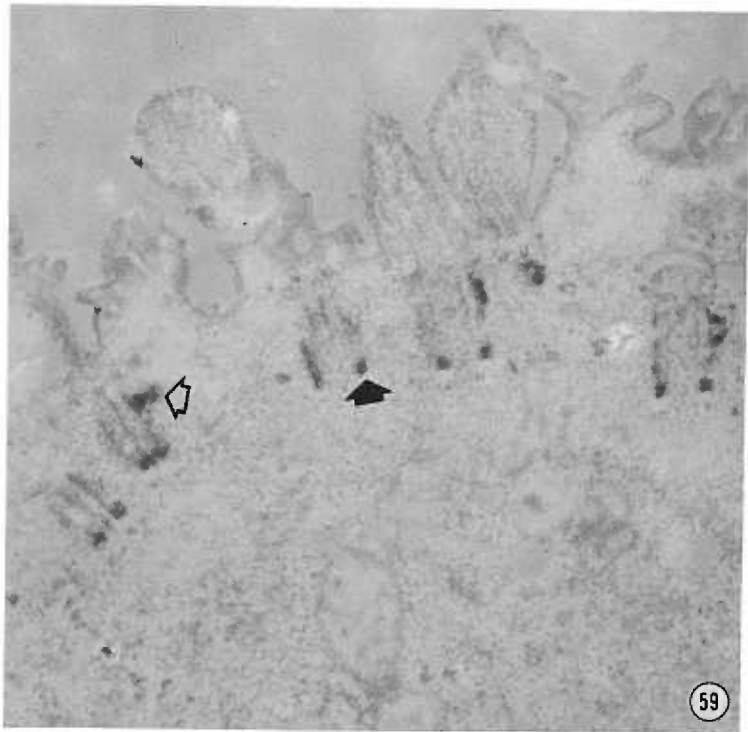
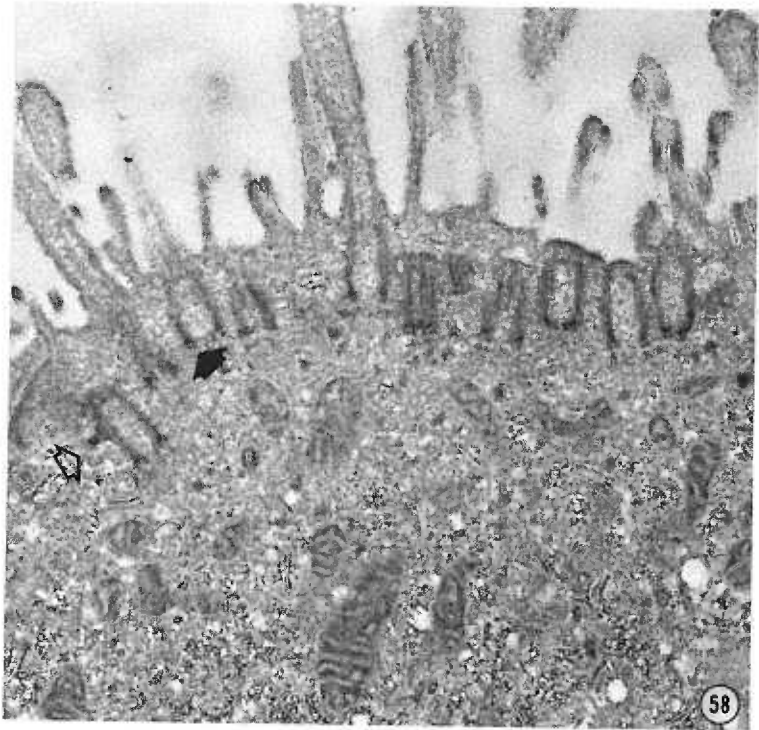


ribosomes were equally sensitive; however, the removal of the ribosomes did not leave holes in the plastic as reported by Leduc (36). The DNase had little effect on mitochondria or other cytoplasmic organelles but it did reduce the density of nuclear heterochromatin. Probably the reduced staining in the nucleus is due to a reorganization of the bound protein rather than to a removal of DNA because DNase does not remove much DNA from glutaraldehyde-formaldehyde fixed material (57). Both Pronase and Trypsin affected the staining properties of the ribosomes and ground plasm, but they had little effect on the nucleus. There is no doubt that the various enzymes tested do affect the staining of selected cell components and that nucleases in particular will alter nucleic acid containing structures.

In the initial digestion trials, the deuterosome, procentriole and basal body were completely unchanged after 12 hours exposure to .01% DNase or .01% RNase; however, there were some subtle changes in the fibrous granule aggregates after RNase treatment. The granules seemed to stain more intensely after treatment, and there was the impression that the aggregates contained fewer granules. The number of fibrous granules in an aggregate varies from cell to cell, and it is also difficult to quantitate the granule's stain intensity between enzyme treatments. For these reasons, the effects of the nucleases were analyzed by successively treating serial sections.

Figures 53, 54, and 55 are three serial photographs of the same cell after treatments with DNase, RNase and buffer respectively. The DNase and buffer treatments had no effect on the various cytoplasmic organelles, including the fibrous granules, the deuterosome and the

Figures 58 and 59. Two views of the basal body region in tissue that was embedded in glycol methacrylate. The section in figure 58 was untreated while the section in figure 59 was treated with pronase for a 1/2 hour. The hollow arrows point to a basal foot in each picture and the solid arrows point to the basal region of a basal body. Glutaraldehyde-formaldehyde without post-osmication, 18,500X



procentriole. The middle section in the series, treated with RNAse, no longer has any ribosomes. Comparing the three sections emphasizes the effect of RNAse on the fibrous granules. There seems to be fewer fibrous granules within the aggregates and each granule appears to be more separated from its neighbor. The granules are not really stained more intensely; however, the removal of some component within the aggregate has increased the contrast between the granule and its surrounding matrix. Figures 56 and 57 are two adjacent sections - one treated with buffer and the other with RNAse. Notice how the RNAse treatment has reduced the staining intensity of the granule connections so that the whole aggregate does not seem to be as tightly arranged. Although the changes associated with RNAse treatment are subtle, it does appear that some component of the fibrous granule aggregate has been removed. These observations suggest that the cortical material of each fibrous granule contains RNA, and that the RNAse removes this material. This data does not support Biava's observation that fibrous granules form from polyribosomes (6).

The effects of proteases on organelle integrity can only give qualitative data on the molecular composition of these structures. Pronase completely removes ribosomes while it only slightly reduces the stain intensity of fibrous granules and deuterosomes. This enzyme does affect the staining of basal bodies by accentuating the heterogeneous staining properties of the wall material (Fig. 59). The less opaque sites of the wall material in untreated preparations appear translucent after Pronase treatment whereas the electron-dense sites are unaffected. Because of the contrast created by this effect, the

base regions and basal foot regions are very prominent. These results indicate that the basal body must either be composed of several macromolecular species or of proteins which differ in their susceptibilities to Pronase.

Radioautography

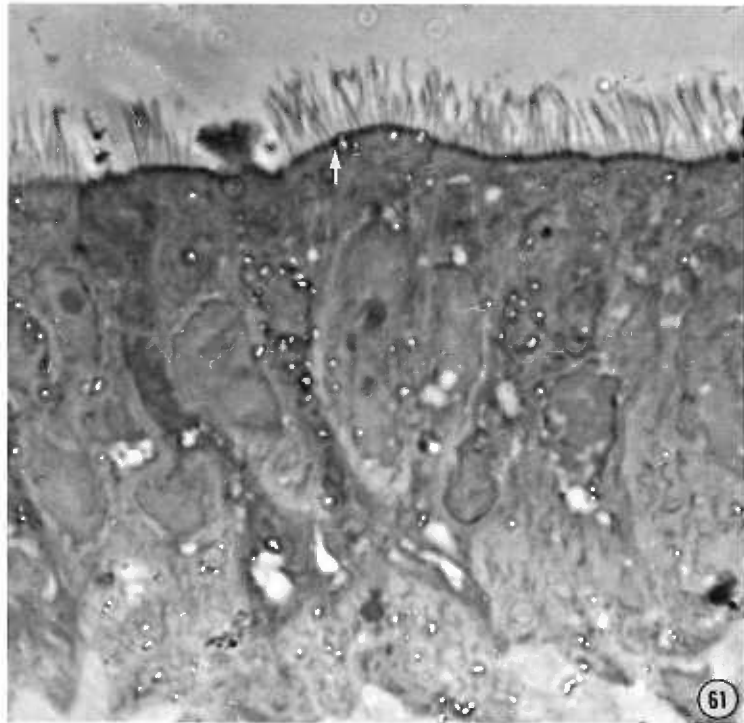
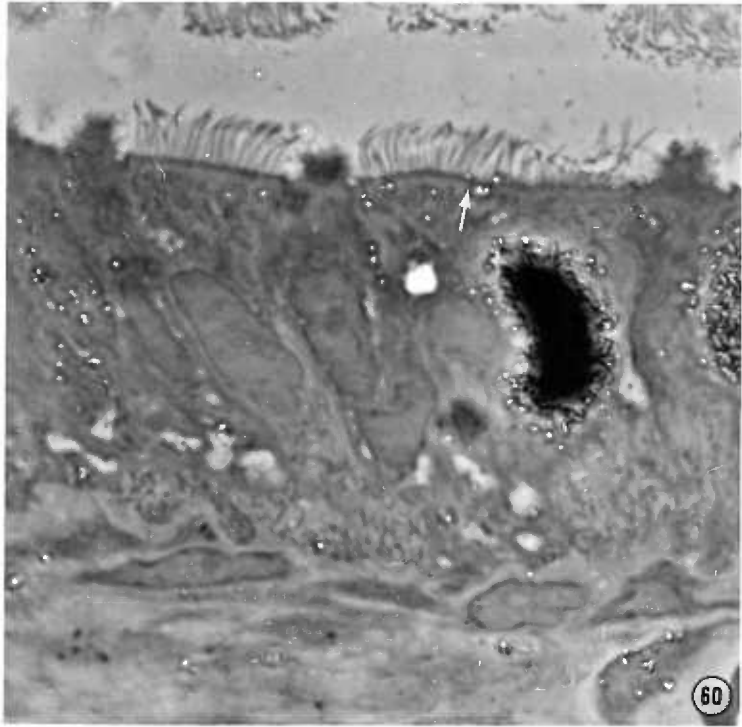
Radioautographic techniques were employed in an effort to determine if the basal body or any of its precursor structures contain nucleic acid. The cells were exposed to a radioactive nucleotide specific for RNA or DNA at a time when basal body genesis was taking place. The tissues were either fixed immediately after exposure to detect sites of synthesis or they were allowed to complete their differentiation before being fixed. The evidence from both light and electron microscopic radioautograph preparations of these tissues is incomplete.

Light radioautograms of fimbriae which were soaked in H^3 -thymidine in vivo for 3 hours on the fourth and fifth days of estrogen stimulation showed a significant number of grains in the basal body region after 8 weeks exposure (Figs. 60, 61). The basal body region is easily distinguished from other parts of the cell, and grain counts were tabulated according to the number of grains in this region per cell. A nonradioactive section on the same slide was similarly analyzed to get an average background measurement. Table 5 shows that the grain counts for both radioactive and control approximate a Poisson distribution. The hypothesis that the mean grain number in the control is equal to that of the radioactive was rejected at the 95% level of significance ($Z = 4$).

Attempts to remove the radioactivity with specific nucleases were

Figures 60 and 61. Two light radioautograms which show silver grains (arrow) in the basal body region of the cell. The tissue sample was taken on the tenth day of stimulation. Five days earlier, the fimbriae were exposed to tritiated thymidine. These are phase microscope photographs so the silver grains appear white.

Glutaraldehyde-formaldehyde, 8 weeks exposure, 2,000X



unsuccessful. In the trial just described, sections from DNase, RNase and buffer treated blocks of glutaraldehyde-formaldehyde fixed tissue were compared. Although an analysis of variance did show a difference between the RNase and DNase total grain counts, there was not a significant difference between DNase and buffer treated tissues. This latter data is consistent with the lack of effect of DNase on the nuclear labeling.

The resistance of glutaraldehyde-formaldehyde fixed tissue to DNase has been well documented in other laboratories (57). Recently I have found that fixation with Carnoy's fixative (absolute alcohol: acetic acid 7:3) renders the DNA susceptible to this enzyme. For example, light radioautograms show that 8 hours of treatment with DNase at 37°C will completely remove H³-thymidine labeled DNA from nuclei. The discovery of the Carnoy's fixative effects is recent, and I am now testing the sensitivity of the basal body H³-thymidine label to DNase in Carnoy's fixed blocks.

Table 5 shows that the number of basal bodies that incorporate H³-thymidine is not very high. This problem has continually thwarted efforts to statistically test thymidine incorporation in basal bodies with electron microscopic radioautography. Figure 62 shows an electron microscopic radioautogram of the same tissue described in the light study. Exposure was for 5 months and there are grains over several basal bodies. Although this amount of labeling is seldom seen, it does indicate that basal bodies can incorporate H³-thymidine. It is hoped that larger numbers of basal bodies can be labeled in the future so that a more detailed analysis can be performed.

TABLE 5

No. Grains / Cell	Unlabeled	Labeled
0	246	208
1	51	75
2	3	12
3	0	3
4	0	0
<hr/>		
no. grains / 300 cells	.19	.36

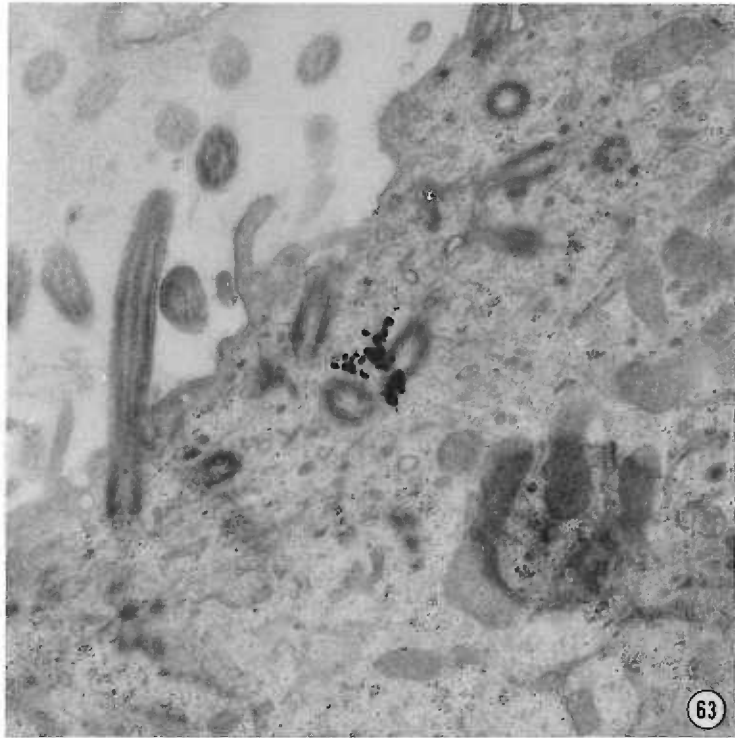
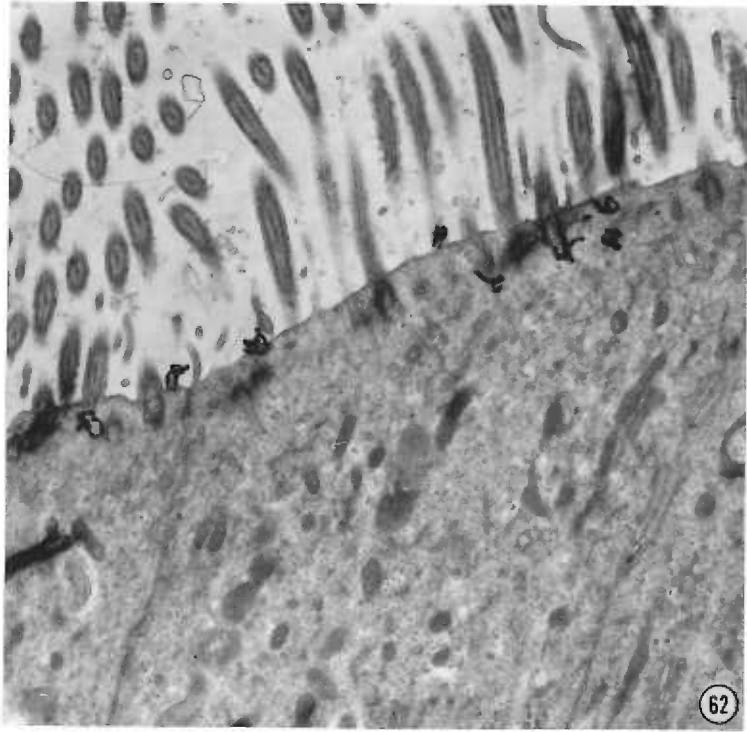
 $Z=4^{**}$

These various technical problems have made it difficult to decide when and where the thymidine is incorporated into basal bodies. Radioautograms of tissues labeled on day 4 and day 5 show occasional grains over forming basal bodies (Fig. 63); however, one cannot be sure that this is not due to background. In contrast, mitochondria are frequently labeled. The light radioautograms which showed incorporation indicated that most of the cells with basal body grains lacked nuclear grains. This suggests that the incorporation of thymidine into the basal body takes place just after the synthesis of the nuclear DNA. This would mean that the basal body molecule which utilizes H^3 -thymidine is synthesized at late interphase; about the time the diplosomal centrioles are replicating.

Electron microscopic radioautograms of fimbriae which were pulse labeled on the fourth day of estrogen treatment with H^3 -uridine show no silver grains in the fibrous granule aggregates. This indicates that any RNA present in the fibrous granules is synthesized before the aggregates appear. More extensive radioautographic studies on H^3 -uridine incorporation are in progress.

Figure 62. An electron microscopic radioautogram showing several basal bodies with grains over them. This tissue was taken on the tenth day of stimulation, 5 days after the final exposure to tritiated thymidine. Glutaraldehyde-formaldehyde, 6 months exposure, 14,000X

Figure 63. An electron microscopic radioautogram of tissue that was fixed immediately after exposure to tritiated thymidine (fifth day of stimulation). Notice the grains are located over the walls of developing basal bodies. Glutaraldehyde-formaldehyde, 6 months exposure, 23,000X



DISCUSSION

Introduction

The results of the present study show that basal body genesis in the oviduct is remarkably similar to centriole replication in the rat and mouse trachea (6, 17, 22, 64, 66), the chicken trachea (33), the embryo of Xenopus laevis (65), and the rat choroid plexus (39). In addition, the centriolar pathway for basal body production resembles kinetosome formation in unicellular ciliates (1, 15, 26, 32, 49), centriole replication during spermatogenesis (23) and diplosomal centriole replication (42, 53, 67). Likewise, the architecture of the basal body does not differ significantly from the description given by other investigators (2, 5, 11, 18, 19, 24, 25, 46, 50, 67). The purpose of the discussion that follows is to use all the available data to construct a coherent picture of how procentrioles form, the origin of their precursors and the structure-function relationship of the basal body.

Basal Body Formation

A recurrent theme presented in the various studies on basal body formation is that the fibrous granules are synthesized in the cytoplasm (17, 33, 64, 65), and that the diplosomal centriole is the major site of synthesis for this precursor material. The best evidence for this hypothesis was established by Kalnins and Porter (33) in their study of ciliogenesis in chicken trachea. The fibrous granule-like material always surrounds the diplosomal centriole during procentriole formation in this epithelial cell system. In rat trachea and in Xenopus embryos (17, 64, 65) there is, however, only an occasional association of fibrous

granules with the parent centriole. The juxtaposition of pericentriolar satellites (4, 11) and other fibrous granule-like material (42, 53, 67) to forming procentrioles during diplosomal centriole replication could be interpreted as support for the "centriole origin" hypothesis. Another possibility, proposed by Sorokin (64), is that the Golgi provides a component of the procentriole precursor material. He suggests that both the diplosomal centriole and the Golgi are involved in fibrous granule formation.

The fibrous granules in oviduct cells have been seen in morphological patterns which are similar to those just described. However, there are other explanations for these relationships. The granules usually appear in the apical cytoplasm but there is not any particular region or organelle with which they associate. Endoplasmic reticulum, Golgi and mitochondria are frequently found in the same cell region; however, it is impossible to decide whether the proximity of these organelles to fibrous granules is significant or fortuitous. When fibrous granules are associated with the diplosomal centriole - a frequent occurrence - procentriole induction is usually in progress. Possibly two or three examples of quiescent centrioles associated with fibrous granules have been seen, but in light of the probable function of the granules it seems more likely that they are near the centriole because of their future involvement in centriolar basal body formation rather than because they are being produced by the parent for use elsewhere in the cell. This could be the case in rat trachea too (64), since Sorokin has described centriolar procentriole formation in this cell system. Likewise, the data from diplosomal centriole replication

also supports this hypothesis (4, 11, 42, 53, 67). Dirksen's proposal that newly formed basal bodies produce fibrous granules for another wave of procentriole formation does not seem valid (17), because of the synchrony of procentriole formation (33) and also because of the numerous reports that fibrous granules are involved in rootlet formation (33, 64, 65).

As an alternative hypothesis, I would like to suggest that fibrous granules originate in the cell nucleus. Several examples of fibrous granules within pockets of the nuclear envelope have been seen. The granules are somewhat atypical for fibrous granules since the fibers are not readily distinguishable (Figs. 10, 11), but no other cytoplasmic structure, including polyribosomes (6), resembles these organelles. Not only are the granules in close proximity to the nucleus but the nucleoplasm contains similar granules in juxtaposition to those in the cytoplasm. One even gets the impression that the granules are being transported across the nuclear membrane. These relationships have not been seen very often. Several reasons could account for this: the overall investigation was not oriented towards the study of this phenomenon and therefore other examples may have been overlooked; the transport process could occur very rapidly, which would reduce the chances of seeing this relationship; granule transport may be dispersed throughout the nucleus so that a concentration of granules is not normally seen.

Support for the concept of a nuclear origin of fibrous granules is found in a recent study by Monneron and Bernhard on the organization of the interphase nucleus (41). These investigators have morphologically

and histochemically defined a new component of the nucleus: coiled bodies. A coiled body is a .3 - .5 μ spherical aggregate of coiled threads (granules?). Each thread is 40-60 $\mu\mu$ thick and contains bundles of 50 \AA fibrils. No more than one coiled body per section has been detected, which indicates that this structure is not a large component of the nucleus. The morphology of the bodies is not significantly affected by GMA embedding procedures, and nuclease digestion shows that they are slightly sensitive to RNAse but not to DNAse. Pronase treatment reduces the contrast but does not eliminate the bodies. Their morphology closely matches that of fibrous granules, and the two structures respond identically to enzyme treatments and to GMA embedding. These various points of similarity between the coiled bodies and aggregates of fibrous granules strongly suggest that they are the same elements.

The hypothesis that fibrous granules originate in the nucleus fits into the scheme of centriole replication in many cell systems. Prior to the division cycle in each cell, these granules could be transported to the cytoplasm to participate in diplosomal centriole replication. In a cell which is producing basal bodies, the transport could be preceded by or concur with a synthesis phase which produces the required number of granules. Possibly the fibrogranular sphere seen in the oviduct cells is evidence for such a synthesis phase. The concept that precursor material comes from the nucleus would also explain why in Allomyces (51) the new centrioles always arise and develop next to the nuclear membrane. Likewise, in the drone honey bee annulated lamelle as well as "nuclear pore like" material surrounds the developing

basal body during spermatogenesis (28). Most unicellular ciliates are able to generate new kinetosomes when their nucleus has been removed; therefore, the kinetosomes must not receive a component from the nucleus (63). On the other hand, a few unicellular organisms are able to convert from an amoeboid form without any centriole to a flagellated form with two basal bodies (14, 43, 58). Nuclear material may be required in this last case. The amoeba-to-flagellate transition that occurs during the life cycle of Naegleria gruberi (14, 58) may represent an evolutionary intermediate between a completely autonomous kinetosome replication system and a centriole replicating process that is partially dependent on the nuclear genome.

The ubiquitous occurrence of fibrous granule-like material when procentrioles are forming has strongly implicated this organelle as either a source of precursor material or as a direct precursor to the centriole. Except for the cells in the rat choroid plexus (39), every study on ciliated epithelium has revealed a fibrous granule component nearby forming procentrioles (6, 17, 22, 33, 64, 65, 66). In addition, most of the studies on diplosomal centriole replication reveal that a similar organelle surrounds the parent centriole during procentriole induction (4, 11, 42, 53, 67). There are only two cases where fibrous granules appear in cells that are not engaged in centriole production (21, 37); however, basal bodies are present in these two cell systems.

Several investigators have proposed that fibrous granules are arranged to form the procentriole wall. Bernhard (11) termed the granules associated with centriole replication "pericentriolar bodies", and he suggests that they could be transformed into the procentrioles.

Stockinger and Cireli suggest that in rat ciliated cells 9 granules are formed into a ring with each granule representing a future triplet (66). Studies on other ciliated epithelial cells indicate that these granules are consumed during the production of the basal bodies (33, 65).

In rhesus monkey oviduct the spatial and temporal relationships of fibrous granules to developing procentrioles also strongly suggest a precursor-product relationship. Early annulus formation and apical growth of the procentriole indicate that the granules are incorporated into the wall material. The various bands and tubules formed during procentriole development seem to be made of material contained within the granules. Possibly the fibers in each granule polymerize to form the structural components of the basal body.

The function of fibrous granules is not limited to the formation of procentriole wall material. Dirkson and Crocker (17) and Sorokin (64) suggest that the deuterosome (or condensation form) is a product of granule condensation. In monkey oviduct, the similarity in size and shape of early deuterosomes to fibrous granules and the fact that the deuterosome usually is first recognized when it is within an aggregate of granules strongly suggest their origin from fibrous granules. The granules have also been implicated in rootlet formation in other cell systems (22, 33, 64), although Steinman suggests they may provide a precursor for developing cilia (65). My studies show that shortly after the basal body reaches its mature length, fibrous granules seem to be deposited on the wall in conjunction with basal foot formation. In addition, during cilium formation the basal body rootlet is generated, and a new wave of fibrous granules appear, many of which are in close

proximity to the basal end of the basal body. Either the granules act as initiators which stimulate rootlet and basal foot development, or the granules themselves are transformed into the structural form that distinguishes these appendages.

Despite the importance of fibrous granules in centriole development, they are not endowed with the capacity to initiate procentriole formation and they probably do not dictate the eventual form of the centriole. This proposal is developed from observations on the appearance and disappearance of fibrous granules in relation to procentriole formation. In some cases, granules aggregate together and numerous procentrioles form within this cell region; the granules seem to be consumed during this process. Another relationship is characterized by the appearance of several procentrioles with only a few fibrous granules nearby. Rarely, one or two isolated procentrioles are seen without any granules in close proximity. This spectrum in the number of granules associated with procentriole initiation could be explained if we assume that the fibrous granules are formed into procentrioles by some type of organizer substance. If this organizer is present in a particular region of the cell when the fibrous granules appear, then immediate procentriole formation will take place possibly using up all of the granules in the process. Such a spatio-temporal organization would explain why two investigators (17, 64) have not reported the secondary aggregate of fibrous granules during the formation of procentrioles. On the other hand, a delay in the appearance of the organizer would allow the granules to aggregate. The morphological relationship between the procentriole and the deuterosome suggests that the latter structure

may contain the organizer substance.

All of the studies on centriole formation have noted that the procentriole first appears as a bud or protuberance from some other organelle. During diplosomal centriole replication, the procentriole forms at right angles to the parent (42, 53, 67) while in ciliogenic cells electron dense spheres (65), hollow spheres (17, 64), trellis-shaped membranes (39), and cylinders (33) function in a similar capacity. The diversity in morphological form of these organizational elements argues against the idea that the structure of the inducer somehow determines the structure of the procentriole (67). It is more likely that some molecular species which is common to all of these structures is responsible for the initiation and form of the procentriole. Three observations in the oviduct cells support this hypothesis. In centriolar procentriole development, the daughter is initiated at different regions as well as at different angles to the parent's wall. Serial sectioning has disclosed that not all procentrioles formed in the acentriolar pathway have a deuterosome associated with their formation. Finally, the deuterosome is not fully formed until after the procentriole is fairly well established. It would seem in this last case that some molecule first organizes some fibrous granules into a deuterosome and secondarily induces the procentriole to form (Fig. 64). Presumably the molecule is incorporated into the structure of deuterosome before becoming part of the procentriole.

Several observations suggest that the organizer molecule originates in the diplosomal centriole. It has been noted several times that the cell's centriole possesses organizational properties and that some

investigators have proposed a centriolar origin for procentriole precursor material. These relationships are understandable if the organizer originates from the centriole. If this is true, then one would expect two types of association patterns during acentriolar procentriole development depending on the temporal order of organizer synthesis. A system which manufactures its organizer before the fibrous granules appear would probably have procentrioles randomly forming throughout the cell. However, if the fibrous granule formation preceded organizer synthesis, procentriole formation may only take place in the region of organizer synthesis. Precisely these two kinds of patterns are seen in ciliogenic cells. The monkey oviduct, rat trachea (17, 64) and Xenopus embryo (65) are examples of the first system. The chicken trachea represents the second system (33). In this latter example, the organizer, a cylinder which resembles a procentriole, is intimately associated with the parent centriole. In some instances, this procentriole inducer appears as an appendage to the parent centriole.

The mechanism which forms the basis for organizer activity is a complete mystery. The only clue is the apparent continuity between the cortex of the deuterosome and the cartwheel. Although it is not entirely understood what role the cartwheel plays in procentriole formation, it is possible that the organizer forms this structure from the cortical elements of the deuterosome. Also, the deuterosome probably establishes a microenvironment which is necessary for the organizer molecule to function.

The cartwheel is as ubiquitous a structure in procentriole development as the organizer organelle. There is only one positive example

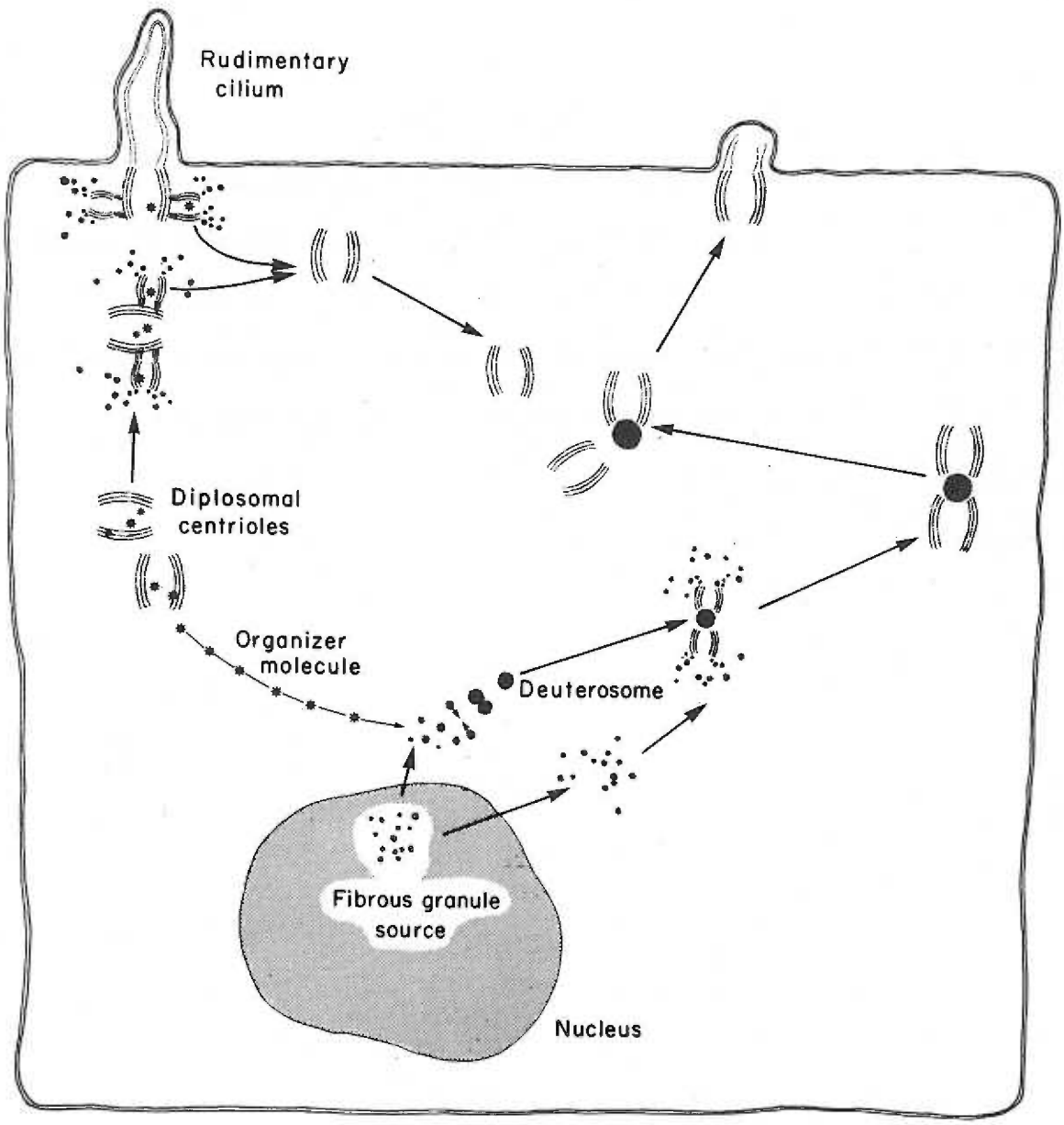
where this structure is absent during development, and this centriole has more than 9 sets of microtubules (45). In mammalian cells, this structure disappears shortly after the basal body or centriole is formed and during its brief existence in the newly formed organelle it is located in what was formerly the procentriole lumen. These observations indicate that this structure only functions during the procentriole formation phase. Those organisms in which the cartwheel is an integral part of the mature basal body (1, 15, 25, 32, 49) may be examples of a system that is unable to eliminate an unnecessary accessory. Most investigators only casually mention the presence of this structure during procentriole formation (23, 28, 33, 40, 51, 64, 65, 67). However, Dipple (15) has determined that in Paramecium this structure first appears between the formation of the A and the C tubules. She suggests that it does not function in establishing the symmetry of tubule arrangement.

The present study has revealed that the cartwheel is first detected before the annulus of amorphous material is formed. Image-enhanced photographs of a fully formed annulus show that the basic architecture of the cartwheel is established, although weakly established, before any tubules are present in the wall material. The cartwheel could be functional at this stage even if it is not well established. The spokes seem to be more numerous in the basal region - the site of tubule initiation - and after the A tubules form they become attached to the circumference of the lumen at the site of attachment for the cartwheel's anchor filaments. These observations suggest that the cartwheel functions to hold the tubules in place during future development phases. Several

other observations support this concept. As the procentriole develops the cartwheel becomes more prominent - as if reinforced - although the substructure remains the same; during procentriole maturation the centrifugal growth of the cartwheel and the increase in luminal diameter occur simultaneously with a reduction in the axial angle of each triplet to the lumen's circumference. It was discovered during the construction of the basal body model that a certain amount of force is required to maintain the triplet angle. Therefore, as the basal body develops there is probably a need for some force to stabilize this angle while the triplets lengthen, and it is conceivable that the cartwheel provides this support. The triplet linker sheets could maintain the angle after the basal body is formed.

The construction of each triplet begins with the initiation of A tubule formation. The first tubule appears in juxtaposition to a spoke of the cartwheel and new A tubules are synthesized sequentially every 40° around the annulus in a clockwise direction. Except for the presence of the cartwheel, this is the same as tubule formation in Paramecium (15). Obviously the nine-fold symmetry is established before the tubules begin to appear and it would seem that this initial symmetry dictates the placement of the A tubules. However, the A tubules do not become attached to the anchor filament attachment site until after the initial formation of each tubule is completed. It is possible that the equal spacing of the A tubules is independent of their final attachment to the cartwheel and that this latter component only functions secondarily to hold the tubules in place for the subsequent formation of the B and C tubules.

Figure 64. A hypothetical scheme for acentriolar and centriolar basal body formation. This shows the fibrous granules originating in the nucleus and the organizer molecule (stars) originating in the diplosomal centriole. Some of the granules are arranged into the deuterosome by the organizer molecules while the rest of the fibrous granules form the walls of the procentrioles. The procentrioles either form at the walls of the diplosomal centrioles or the cortex of the deuterosome.



After all of the A tubules are initially formed, the B and C tubules begin to appear. Unlike prokinetosome formation in Paramecium (15), the B and C tubules are sequentially initiated clockwise around the procentriole. The initiation of the C tubules begins before all of the B tubules are formed.

The recognition that the cartwheel is most prominent in the base of the procentriole together with serial sectioning analysis have established that the growth phase is very irregular compared to tubule initiation. For example, the A tubule begins to lengthen as soon as it is initially formed but there is not any sequential order to this growth. This could explain why Dipple suggests that B and C tubule formation does not occur sequentially (15), i.e., her interpretations are based on sections through the apex rather than the base of the procentriole.

Procentriole formation is a necessary and sufficient process for basal body formation. Once the procentriole is formed, the individual triplets elongate rapidly resulting in the completion of the basal body's tubular wall. As in procentriole maturation, this process is an unordered event, and frequently the apical aspect of the triplets are not well established by the time the basal body has migrated to the cell surface. Some investigators have implied that centrioles are formed by the attachment and arrangement of already formed microtubules into the 9 sets of triplets (67). This study as well as similar research endeavors (15, 32, 33) establish that not only is this concept incorrect but the 3 tubules of each triplet are not typical microtubules.

From the knowledge of basal body architecture it is possible to

deduce that several structural modifications must be made either while the basal body is forming or after the tubular system is complete. The angle of each triplet to the lumen must gradually change from 40° at the base to 15° at the apex. Serial sectioning shows that a slight decrease in angle is present from base to apex of the procentriole. However, measurements of the basal triplet angle in procentrioles and basal bodies during various stages of maturation indicate that the proper shift is not established until after the cartwheel breaks down (Table 2). These observations can be explained by supposing that each triplet develops a tendency to twist centripetally as it lengthens, and first the cartwheel and then the triplet linkers maintain the proper angle at the base. It is also clear that the helical pitch which each triplet follows from base to apex must be introduced some time during the development phase. There is no clue to how this occurs. Finally, sites on the wall of the basal body must be present to correctly position the formation of the basal foot, the alar sheets, and the rootlet.

The observations in this study would support the conclusion that two separate pathways exist in the oviduct for the generation of basal bodies. A similar situation has been described in the rat trachea (64) except that in this system centriolar procentriole genesis begins before the acentriolar pathway is initiated rather than occurring simultaneously as in the oviduct. Ciliated unicellular organisms use a mechanism which is similar to the centriolar pathway to produce their basal bodies (15). Since the ciliates have been in existence for a considerably longer time than mammals, one would expect that their mechanisms for basal body production could meet the requirements of any cell type. In fact, it

is the system used to replicate the diplosomal centriole every time a cell divides. Why, then, have the cells in the rat trachea and the monkey oviduct converted to a new system of producing basal bodies when it is obvious that the more primitive mechanism is functional? Two explanations are possible: it is impossible for the diplosomal centriole to produce 200-300 basal bodies in the required time; the centriolar pathway has changed during the evolution of multicellular organisms and it no longer functions as it does in unicellular ciliates.

There is not any apriori reason to suggest that a new synthetic pathway is necessary for the production of oviduct or rat trachea basal bodies if we assume that there are no differences between the centriolar mechanism in unicellular ciliates and in ciliogenic epithelial cells. Paramecium can manufacture a basal body (kinetosome) in 30 minutes to an hour (15), and the newly formed organelle is capable of producing a daughter. The studies on the oviduct indicate that it takes about a day for the epithelial cell to generate all of its basal bodies; therefore, there is adequate time for the centriolar pathway to produce 200-300 organelles. Simple calculations show that if each new basal body replicated itself it would take 7 generations to produce 250 basal bodies: this can be done in 7 hours. Therefore, Sorokin tacitly assumes that diplosomal centriole replication is different from kinetosome replication when he proposes that the former pathway is not capable of producing the required number of basal bodies (64). Yet, even if there are gross functional differences between the two systems, it does not explain why two mechanisms which can accomplish the same task are both functioning in the same cell. The only structural difference

between a centriole and a basal body is the presence or absence of accessory structures.

There is an explanation for the existence of these two pathways in the same cell which is based on the hypothesis already presented on the origin and function of the fibrous granules and the deuterosomes. I have concluded from my study of the oviduct that the only difference between the two generative mechanisms is the morphology of the organizer organelle. The fibrous granules are necessary to procentriole production in both pathways, and the formation stages as well as the end product are indistinguishable between the two mechanisms. Suppose that the estrogen stimulation induces the diplosomal centrioles to produce an organizer molecule just prior to the appearance of the fibrous granules. This molecule would diffuse away from the centriole, become randomly distributed in the cytoplasm, and induce deuterosomes to form - therefore, acentriolar procentriole formation - when it comes in contact with the fibrous granules. If some of the molecules remain with the parent or if organizer synthesis continues after the granules appear, then it is going to organize these fibrous elements into a procentriole at the site of the diplosomal centriole. Presumably, the environment around a centriole is favorable for the expression of the organizer. The number of procentrioles originating from a diplosomal centriole is a function of the number of organizer molecules associated with the parent at the time it comes into contact with the fibrous granules. By assuming differences in the temporal relationship between the organizer and the fibrous granules, one can account for the observations on other ciliogenic epithelial cell systems (17, 33, 64, 65).

Basal Body Structure

Despite the differences in structural details of the kinetosome, centriole and basal body, the cylindrical geometry and tubular walls seem to be features which are common to all of these organelles. Except for the giant centriole in Sciara (45), the tubular wall of these organelles is composed of 9 sets of three 200 Å tubules. Although the dimensions of these organelles vary in diameter (150-250 mμ) and length (300-500 mμ) (19), their structural homologies establish their common evolution.

The oviduct basal body is similar to other "centrioles" in another respect: it contains both radial and longitudinal polarity. The radial asymmetry is established by the placement of each triplet in the wall. The axial angle of the triplet to the lumen's circumference always faces the same direction, thus permitting one to identify the longitudinal orientation of the organelle in a photograph. Gibbons and Grimstone were the first to note this organizational pattern, and no one has described a centriole that violates this rule (24, 25). The differences in the triplet angle between the base and the apex establishes the longitudinal polarity. Accessory structures such as the rootlet, the transitional fibers or alar sheets and the cartwheel are always positioned at the same point along the longitudinal axis of the organelle.

The constant location of the accessory structures emphasizes that the structural polarity corresponds to a functional polarity. The apical end of the basal body always gives rise to the cilium, and the alar sheets located in this region seem to attach the organelle to the cell membrane. The rootlet which extends into the cytoplasm of the cell

and seemingly acts as an anchoring device emphasizes the functional polarity of the basal end. Gibbons has noted that the basal foot is always positioned in the direction of ciliary beat (24). This indicates that the basal body has a lateral functional polarity too.

Centriole replication offers another view of functional polarity. Numerous investigators have observed that forming procentrioles always appear at the same end of the parent (1, 11, 15, 23, 32, 42, 64, 67), and the present study shows that the centriole possesses organizing capacity from its midregion to its base. The procentriole always forms with its base in juxtaposition to the organizing region, and the procentriole itself ultimately becomes the basal half of the mature centriole. Therefore, the structural polarity of the organelle is established during the construction phase, and the organizing region (the basal half) originally is the first part organized (the procentriole). These observations suggest that the organizer molecule should be located in the basal half of the organelle.

Various studies including this one have presented evidence that the axial angle of each triplet to the lumen's circumference is greater at the base than at the apex (15, 24, 25, 50, 67). Assuming that the decrease in angle is continuous, there are three possible ways it can change: 1) centrifugal rotation on the longitudinal axis of the C tubule causing an increase in the luminal diameter; 2) rotation on the B tubule resulting in a slight decrease in outside diameter and a corresponding increase in the lumen's diameter; 3) centripetal rotation on the A tubule causing a decrease in outside diameter with no change in luminal diameter. Although some investigators have measured changes

in the outside diameter (24, 25), Stubblefield is the only one who has compared inside diameter changes with outside diameter changes (67). His measurements suggest that the angle change in the fibroblast centriole is the result of a rotation on the C tubule. However, my data on oviduct basal bodies suggest that the rotation occurs on the longitudinal axis of the A tubule.

For example, my measurements show that the triplet angle changes from $\sim 40^\circ$ at the base to $\sim 10^\circ$ at the apex - a $\Delta \angle = 30^\circ$. If in a transverse section each triplet is 600 \AA long (three 200 \AA tubules in a row) then under optimal measuring conditions one should detect a change in either the outside diameter or the inside diameter of 560 \AA (see appendix). When allowance is made for the slight reduction in internal diameter, the measurements on the oviduct basal body show a 650 \AA reduction in the outside diameter. Measurements on the fibroblast centriole, however, show only a 350 \AA reduction in the inside diameter with a 47° angle change. In addition, the photograph from which Stubblefield makes his measurements of the centriole's basal region appears to be of a pro-centriole because the overall dimensions are less than those given for the same organelle in other photographs, and there is a cartwheel present in the lumen. Pro-centrioles always have a smaller inner and outer diameter than the mature organelle, and as I have shown, the triplet angle is greater in the immature structure. If we discard this measurement, then Stubblefield's data shows a $\Delta \angle = 24^\circ$ with a 150 \AA reduction in the inside diameter. These measurements do not agree with those values calculated from trigonometric considerations (appendix). I suggest that the measurements on the fibroblast centriole are not

typical of all centrioles and that distortion due to sectioning as well as a lack of enough samples probably accounts for the data presented. My measurements on oviduct basal bodies were made from complete serial sections and from the numerous effective serial sections one obtains in tangential sections of the tips of fully ciliated cells. They are probably representative of all mammalian centrioles and basal bodies.

This study conclusively establishes that the triplets are helically arranged in the wall of the basal body. The frequency with which other investigators have noted the asymmetry of tubule clarity in transverse sections of centrioles indicates that this is a common feature of vertebrate centrioles (2, 19, 46). The maximum pitch measured is 15° ; however, there are conditions under which this value is reduced. It is not clear whether each centriole or basal body is constructed with a certain pitch or whether the pitch can change as the organelle functions. The basal body model offers a clue.

Two models of the basal body were initially constructed. One model was constructed with the triplets pitched to the left at 14° , while in the other model the tubules were arranged parallel to the longitudinal axis of the structure. It was discovered that more force was required to maintain the first configuration. It is difficult to know what mechanical similarities exist between the model and the real basal body, but the observation on the maintenance of the model's pitch raises the possibility that the pitched configuration of the basal body is more constrained than the unpitched form. Such a situation dictates that the basal body would have a tendency to return to the unpitched state. This type of structural relationship could introduce a variable pitch;

however, there would have to be some mechanism for returning the structure to the pitched state.

There are several ways that a variable pitch could function. Rather than be a passive anchor structure for the cilium, the basal body may be involved in initiating ciliary beat. Gibbons was the first to propose this possibility (24), and according to his study the beat would be initiated in the region of the basal foot, spread around the basal body and up the ciliary shaft. The variable pitch may be the underlying mechanism for initiating ciliary beat. If the triplets which are held by the basal foot remain pitched while the other 6 sets relax to the unpitched configuration, the asymmetry of movement could cause the cilia to beat. Such a relaxation of the triplet pitch would cause a rotation of the cilia on the axis of its central doublet; according to Satir, such a configuration change takes place during the cilia beat (56). The difficulty with this concept is that some flagella do not need a basal body to function (46), and isolated cilia are able to beat without a basal body attached (61). My studies could also be interpreted in favor of a passive role for the basal body during ciliary beat. The pitch might act as a sort of spring mechanism which adds resiliency to the ciliary beat. This concept would be compatible with the literature if we assume that such cells as spermatids (46) do not need this added flexibility to function. One final problem with both these concepts is that the centriole also has pitched triplet sets. Therefore, it is proposed that the variable pitch may also function to propel the organelle through the cytoplasm during the period when the cell is preparing for cell division. This may be the only way it functions in

the basal body since these organelles must be able to migrate to the cell surface after their formation.

The centriole and the basal body possess accessory structures which must be important to the function of the organelle. The triplet-linking material in the base and midregions and the alar sheets are common to both organelles (67). The basal foot and the rootlet are only found in the basal body.

The accessory structure previously called the transitional fiber (25) or octagonal end structure (67) is seen in this study to be a 170 μ sheet which extends from the midregion to the apex. The wing-like organization of these structures has suggested a new name: alar sheets. It is not possible to know whether these sheets are common to all basal bodies and centrioles because previous investigators have not shown longitudinal sections of this structure. However, Reese (50) has serial sectioned the apical region of the olfactory basal body and the so-called "transitional fibers" extend through two sections. It is probable that alar sheets are a constant feature of basal bodies.

The conformation and position of the alar sheets suggest two possible functions. In the mature basal body the apical tips of each sheet merge with the cell membrane at the basal body - cilium junction. The structure appears to hold the basal body perpendicular to the cell membrane. This may be a fortuitous arrangement because the cilium and rootlet should perform the same function; also, the alar sheets are present in centrioles. When the pitch is absent, in a transverse section the alar sheets do not appear triangular. This means that the sheets twist and untwist with the variation of the pitch. Since the sheets present a large surface

area to the cytoplasm, it is conceivable that their movement creates a paddle-like effect. This would support the concept that a variation in pitch functions as a propulsion mechanism.

The A tubule connecting sheets and the A - C tubule linkage sheets appear to function to maintain the structure of the organelle. The model indicated that these structures could easily hold the triplets together, and the A - C linker probably maintains the 40° angle of each triplet. There is no clue as to whether these reinforcement structures control the pitch.

The basal foot and the rootlet are ubiquitous accessories to the basal body (17, 18, 20, 25, 28, 37, 50, 64, 65). Their form and arrangement suggest that they anchor the basal body in place. The rootlet is probably responsible for the vertical positioning while the basal foot maintains the lateral orientation. As in mussel gills (24), the basal foot always faces the same direction although it is not known whether the foot faces the direction of cilia beat. Often there are numerous microtubules which radiate from the end of the basal foot, and filaments extend from the rootlet striations. These structures probably help to immobilize the basal body.

There are several investigators who have described accessory structures in the lumen of the kinetosome and basal body. These accessories include the cartwheel (1, 15, 24, 32, 49), filamentous material (54) and electron opaque granules (10, 15). The oviduct basal body does not contain any of these structures; however, occasionally a small vacuole is present which is formed during the breakdown of the cartwheel. Therefore, the presence or absence of luminal accessory

structures must not be important to centriole function. More than likely, these structures only function during procentriole formation.

Basal Body Chemistry

The major part of this study supports the concept that the centriole is a self-replicating structure. Certain precursor materials such as fibrous granules may be synthesized by the nuclear genome but they are worthless organelles without the organizational capacity of the centriole. If we assign the organizational properties to a molecular species then the self-replication of the centriole depends on an intracentriolar synthesis of this molecule. In addition, it is necessary that the molecule either be self-replicating or be synthesized by a molecule with these properties to account for the autonomy of these organelles. The nucleic acids are the only molecules which possess these capabilities. Therefore, there is a logical precedent for the idea that centrioles and basal bodies contain either DNA, RNA, or both.

The enzyme digestion and radioautographic data in this study support the observation of other investigators that basal bodies contain a DNA and an RNA component (3, 15, 27, 29, 30, 48, 59, 60, 62, 63). Although the basal body labeling in fimbriae treated with tritiated thymidine could be due to secondary labeling of the protein fraction (12), it seems unlikely that a protein would remain in a basal body for 4 to 5 days without being replaced by normal metabolic turnover. Preliminary work that I have done using electron microscope radioautography indicates that H^3 -Actinomycin D will bind to basal bodies and that this binding is DNase but not RNase sensitive. The RNase digestion of ultrathin sections does not conclusively demonstrate RNA in fibrous granules but the enzyme's effect does concur with the results from other investigators (15, 41).

The present dogma on nucleic acid function dictates that these molecules are involved in protein synthesis. Thus, the role of DNA and RNA in mitochondrial function has been placed within the framework of providing structural and enzymatic proteins necessary for the maintenance and division of this "cell-like" organelle. There are several reasons why this scheme cannot be applied to centrioles. To begin with, the centriole is not a membrane-bound organelle. If the organelle's nucleic acids function as they do in other cellular compartments, then it is imperative that the same cell machinery exist, i.e., without a limiting membrane there is no way to compartmentalize the nucleic acid. Another reason for the dichotomy is that the replication of the centriole is an induction process, not a division process. Finally, other investigators have calculated that each basal body contains 2×10^{-16} gr. of DNA (48), and this is not enough DNA to code for all the proteins which seem to be necessary for centriole replication.

One can only speculate as to how the nucleic acids function in centriole replication. It is possible that the DNA is responsible for the synthesis of an organizer protein which, in the case of acentriolar centriole formation, migrates into the fibrous granule fraction and induces procentrioles to form. The self-replicating capacity of kinetosomes and diplosomal centrioles dictates that this DNA also must be packaged into the forming procentriole; therefore, it would seem to be simpler for the DNA to act as the organizer. Its introduction into the structure would be a consequence of its organizer function. Electron microscopic radioautography does indicate that the DNA is located in the wall of the basal body. The concept that DNA functions

as an organizer has been proposed by other investigators (62), and the fact that some viral nucleic acids are implicated in the morphogenesis of viral structure establishes a precedent (34). Conceivably the DNA interacts with an RNA component present in the fibrous granules to organize the annulus that is first seen. The triplet tubules then may form by the polymerization of some protein component in the wall material.

There are a considerable number of gaps in our understanding of centriole formation and function; especially in regards to the nature and function of the organizer substance. What sets centriole formation apart from the replication of other organelles is the apparent multipotentiality of the precursor material. It is conceivable that all of the tubules, connectors, and accessory structures are formed from a basic protein type and that its organization into distinguishable structures is due to the influence of one or more organizer molecules. In addition, the difference in synthesis time for a basal body in Paramecium (15) compared to the same structure in oviduct indicates that various enzymes are involved in the assembly of this organelle. The synthesis of the basal body appears to be the result of a precise temporal and spatial interaction of various precursor materials with an organizer substance rather than due to a spontaneous organization of molecules which depends only on their concentration and tertiary or quaternary structure.

SUMMARY

Morphological, radioautographic and cytochemical methods have been used to study basal body replication and structure during estrogen-driven ciliogenesis in rhesus monkey oviduct. Two pathways for basal body formation are described: acentriolar basal body formation (major pathway) and centriolar basal body formation (minor pathway). Procentrioles are generated either in association with the diplosomal centriole (centriolar pathway) or with a deuterosome (acentriolar pathway). The initial step in procentriole formation is the arrangement of a fibrous granule precursor into an annulus. This event is probably controlled by an organizer molecule present in the deuterosome or the parent centriole. The A tubule of each triplet set initially forms within the wall material of the annulus in juxtaposition to a spoke of the cartwheel. After all nine A tubules are initiated, B and C tubules begin to form. Simultaneously, the tubules lengthen and the procentriole is complete when it is approximately 200 μ m long. The procentriole rapidly reaches the mature basal body dimensions, and the addition of a basal foot, 9 alar sheets, and a rootlet completes the maturation process. Fibrous granules are also closely associated with the formation of these basal body accessory structures. Each triplet set follows a helical course from base to apex and is pitched 14° to the left. Basal bodies can incorporate tritiated thymidine, but it has not been established whether this label is DNase sensitive. Enzyme digestions indicate that the fibrous granules contain an RNA component, and that the basal body is probably composed of a heterogeneous population of macromolecules.

BIBLIOGRAPHY

1. Allen, R. D. The morphogenesis of basal bodies and accessory structures of the cortex of the ciliated protozoan Tetrahymena pyriformis. 1969 J. Cell Biol. 40, 716-733.
2. André, J. & W. Bernhard The centriole and the centriolar region. Excerpta Medica Intern. Congr. Series 1964 77, 9 (Abstract).
3. Argentsinger, J. The isolation of ciliary basal bodies (kinetosomes) from Tetrahymena pyriformis. 1965 J. Cell Biol. 24, 154-157.
4. Bessis, M. & J. Breton-Gorius Sur une structure inframicroscopique pericentriolaire. Etude au microscope électronique sur des leucocytes de mammifères. 1958 C. R. Acad. Sci. [D] (Paris) 246, 1289-1291.
5. Bessis, M., J. Breton-Gorius & J. P. Thiery Centriol, corps de golgi et astre des leucocytes. Etude au microscope électronique. 1958 Rev. Hematol. 13, 363-386.
6. Biava, C. G. & S. Matsuura Morphogenesis of cilia from polyribosomes in differentiating tracheal epithelium of rats. 1967 J. Cell Biol. 35, 13A (Abstract).
7. Brenner, R. M. The biology of oviduct cilia. In E. S. E. Hafez and R. J. Blandau (Eds.) The mammalian oviduct. Chicago: University of Chicago Press, 1969. pp. 203-229.
8. Brenner, R. M. Renewal of oviduct cilia during the menstrual cycle of the rhesus monkey. 1969 Fertil. Steril. 20, 599-611.

9. Brenner, R. M. Hormonal control of cilia renewal in the primate oviduct: ultrastructural studies. In S. H. Sturgis and M. L. Taymor (Eds.) Progress in gynecology. Vol. 5 New York: Grune and Stratton Inc., 1970. pp. 77-97.
10. Bradbury, P. & D. R. Pitelka Observations on kinetosome formation in an apostome ciliate. 1965 J. Microsc. 4, 805-810.
11. Bernhard, W. & E. De Harven L'ultrastructure du centriole et d'autres éléments de l'appareil achromatique. 1960 Proc. Int. Conf. Electron. Microsc. 2, 217-227.
12. Bryant, B. J. The incorporation of tritium from thymidine into proteins of the mouse. 1966 J. Cell Biol. 29, 29-36.
13. Dales, S. & L. Siminovitch The development of vaccinia virus in Earle's L strain cells as examined by electron microscope. 1961 J. Biophys. Biochem. Cytol. 10, 475-503.
14. Dingle, A. D. & C. Fulton Development of the flagellar apparatus of Naegleria. 1966 J. Cell Biol. 31, 43-54.
15. Dipple, R. V. The development of basal bodies in Paramecium. 1968 Proc. Nat. Acad. Sci. 61, 461-468.
16. Dirksen, E. R. The presence of centrioles in artificially activated sea urchin eggs. 1961 J. Biophys. Biochem. Cytol. 11, 244-247.
17. Dirksen, E. R. & T. T. Crocker Centriole replication in differentiating ciliated cells of mammalian respiratory epithelium. An electron microscope study. 1966 J. Microsc. 5, 629-644.

18. Doolin, P. F. & W. J. Birge Ultrastructural organization of cilia and basal bodies of the epithelium of the choroid plexus in the chick embryo. 1966 J. Cell Biol. 29, 333-345.
19. Fawcett, D. The cell Philadelphia: W. B. Saunders Co., 1966. (pp. 49-62).
20. Flöck, A. & A. J. Duvall The ultrastructure of the kinocilium of the sensory cells in the inner ear and lateral line organs. 1965 J. Cell Biol. 25, 1-8.
21. Frasca, J. M., O. Aurebach, V. R. Parks, & W. Stoeckenius Electron microscopic observations of bronchial epithelium. II Filosomes. Exp. Molec. Path. 1967 7, 92-104.
22. Frisch, D. Fine structure of the early differentiation of ciliary basal bodies. 1967 Anat. Rec. 157, 245 (Abstract).
23. Gall, J. G. Centriole replication. A study of spermatogenesis in the snail Viviparus. 1961 J. Biophys. Biochem. Cytol. 10, 163-193.
24. Gibbons, I. R. The relationship between the fine structure and direction of beat in gill cilia of a lamellibranch mollusc. 1961 J. Biophys. Biochem. Cytol. 11, 179-205.
25. Gibbons, I. R. & A. V. Grimstone On flagellar structure in certain flagellates. 1960 J. Biophys. Biochem. Cytol. 7, 697-715.
26. Grassé, P. P. La reproduction par induction du blépharoplaste et du flagella de Trypanosoma equiperdum (Flagellé protomonadine). 1961 C. R. Acad. Sci. [B] (Paris) 252, 3917-3921.
27. Hoffman, E. J. The nucleic acids of basal bodies isolated from Tetrahymena pyriformis. 1965 J. Cell Biol. 25, 217-228.

28. Hoage, T. R. & R. G. Kessel An electron microscope study of the process of differentiation during spermatogenesis in the drone honey bee (Apis mellifera L.) with special reference to centriole replication and elimination. 1968 J. Ultrastruct. Res. 24, 6-32.
29. Hufnagel, L. A. Structural and chemical observations on pellicles isolated from Paramecium. 1966 J. Cell Biol. 27, 46A (Abstract).
30. Hufnagel, L. A. Observations on cortical organelles of Tetrahymena and Paramecia isolated in the presence of ethanol. 1968 J. Cell Biol. 39, 63A (Abstract).
31. Hufnagel, L. A. Properties of DNA associated with raffinose-isolated pellicles of Paramecium aurelia. 1969 J. Cell Sci. 5, 561-573.
32. Johnson, U. G. & K. R. Porter Fine structure of cell division in Chlamydomonas reinhardtii. Basal bodies and microtubules. 1968 J. Cell Biol. 38, 403-425.
33. Kalnins, V. I. & K. R. Porter Centriole replication during ciliogenesis in the chick tracheal epithelium. 1969 Z. Mikr. Anat. Forsch. 100, 1-30.
34. Kushner, D. J. Self-assembly of biological structures. 1969 Bact. Rev. 33, 302-345.
35. Leduc, E. H. & W. Bernhard Recent modifications of the glycol methacrylate embedding procedure. 1967 J. Ultrastruct. Res. 19, 196-199.

36. Leduc, E. H. & W. Bernhard Water soluble embedding media for ultrastructural cytochemistry. Digestion with nucleases and proteinases. In R. J. C. Harris (Ed.) The interpretation of ultrastructure. New York: Academic Press, 1962. pp. 21-46.
37. Lin, H. & I. L. Chen Development of the ciliary complex and microtubules in the cells of rat subcommissural organ. 1969 *Z. Mikr. Anat. Forsch.* 96, 186-205.
38. Markham, R., S. Frey & G. J. Hills Methods for the enhancement of image detail and accentuation of structure in electron microscopy. 1963 *Virology* 20, 88-102.
39. Martínez-Martínez, P. & W. T. Daems Les phases précoces de la formation des cils et le problème de l'origine du corpuscule basal. 1968 *Z. Mikr. Anat. Forsch.* 87, 46-68.
40. Mizukami, I. & J. Gall Centriole replication. II. Sperm formation in the fern, Marsilea and the cycad, Zamia. 1966 *J. Cell Biol.* 29, 97-111.
41. Monneron, A. & W. Bernhard Fine structural organization of the interphase nucleus in some mammalian cells. 1969 *J. Ultrastruct. Res.* 27, 266-288.
42. Murray, R. G., A. S. Murray & A. Pizzo The fine structure of mitosis in rat thymic lymphocytes. 1965 *J. Cell Biol.* 26, 601-619.
43. Outka, D. E. & B. C. Kluss The ameba-to-flagellate transformation in Tetramitus rostratus. II. Microtubular morphogenesis. 1967 *J. Cell Biol.* 35, 323-346.
44. Phillips, D. M. Observations on spermiogenesis in the fungus gnat Sciara corophila. 1966 *J. Cell Biol.* 30, 477-517.

45. Phillips, D. M. Giant centriole formation in Sciara. 1967 J. Cell Biol. 33, 73-92.
46. Phillips, D. M. Insect sperm: their structure and morphogenesis. 1970 J. Cell Biol. 44, 243-277.
47. Pyne, C. K. Sur l'absence d'incorporation de la thymidine tritiée dans les cinétosomes de Tetrahymena pyriformis. 1968 C. R. Acad. Sci. [D] (Paris) 267, 755-756.
48. Randall, J. & C. Disbrey Evidence for the presence of DNA at basal body sites in Tetrahymena pyriformis. 1965 Proc. Roy. Soc. (Biol.) 162, 473-491.
49. Randall, J., T. Cavalier-Smith, A. McVitte, J. R. Warr & J. M. Hopkins Developmental and control processes in the basal bodies and flagella of Chlamydomonas reinhardtii. In M. Locke (Ed.) Control mechanisms in developmental processes. New York: Academic Press, 1967. pp. 43-83.
50. Reese, T. S. Olfactory cilia in the frog. 1965 J. Cell Biol. 25, 209-230.
51. Renaud, F. L. & H. Swift The development of basal bodies and flagella in Allomyces arbusculus. 1964 J. Cell Biol. 23, 339-354.
52. Ritchie, A. E. & H. C. Ellinghausen Bacteriophage-like entities associated with leptospire. 1969 Proc. Elect. Microscopic Soc. 27, 228-229 (Abstract).
53. Robbins, E., G. Jentzsch & A. Micali The centriole cycle in synchronized HeLa cells. 1968 J. Cell Biol. 36, 329-339.

54. Roth, L. E. Aspects of ciliary fine structure in Euplotes patella. 1956 J. Biophys. Biochem. Cytol. 2 Suppl., 235-242.
55. Salpeter, M. M. & L. Bachman Autoradiography with the electron microscope, a procedure for improving resolution, sensitivity and contrast. 1964 J. Cell Biol. 22, 469-477.
56. Satir, P. Structure and function in cilia and flagella. 1965 Protoplasmatologia Band III, 1-52.
57. Schultze, B. Autoradiography at the cellular level. In A. W. Pollister (Ed.) Physical techniques in biological research. Vol. 3b. New York: Academic Press, 1969. (pp. 27-28).
58. Schuster, F. L. An electron microscopy study of the amoeba-flagellate, Naegleria gruberi: I. The amoeboid and flagellate stages. 1963 J. Protozool. 10, 297-313.
59. Seaman, G. R. Large scale isolation of kinetosomes from the ciliated protozoan Tetrahymena pyriformis. 1960 Exp. Cell Res. 21, 292-302.
60. Seaman, G. R. Protein synthesis by kinetosomes isolated from the protozoan Tetrahymena. 1962 Biochim. Biophys. Acta 55, 889-899.
61. Sleight, M. A. The biology of cilia and flagella. New York: Macmillan Co., 1962. (pp. 150-151).
62. Smith-Sonneborn, J. & W. Plaut Evidence for the presence of DNA in the pellicle of Paramecium. 1967 J. Cell Sci. 2, 225-234.
63. Smith-Sonneborn, J. & W. Plaut Studies on the autonomy of pellicular DNA in Paramecium. 1969 J. Cell Sci. 5, 365-372.
64. Sorokin, S. P. Reconstructions of centriole formation and cilio-genesis in mammalian lungs. 1968 J. Cell Sci. 3, 207-230.

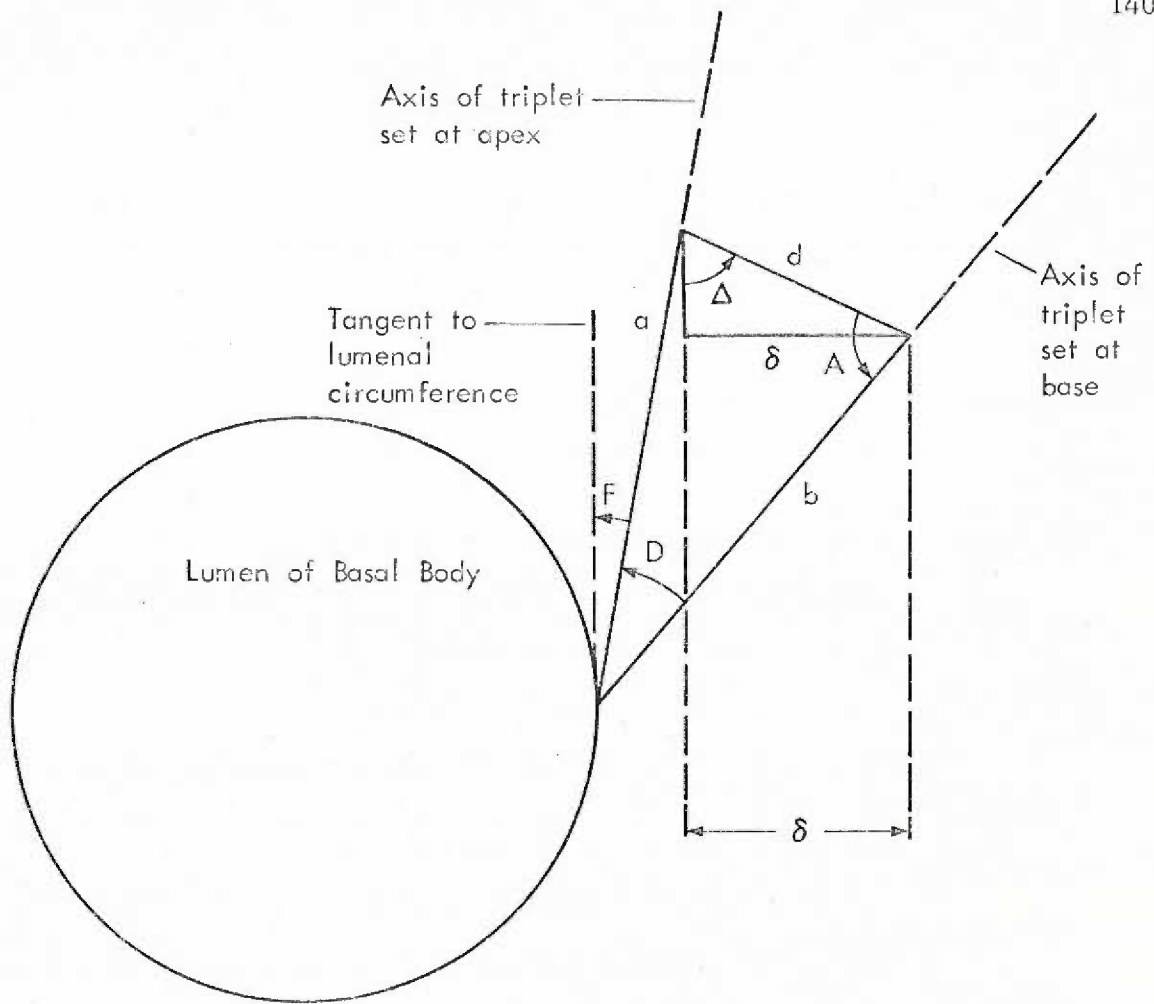
65. Steinman, R. An electron microscopic study of ciliogenesis in developing epidermis and trachea in Xenopus laevis. 1968 Amer. J. Anat. 122, 19-56.
66. Stockinger, L. & E. Cireli Eine bisher unberkannte art der zentriolenvermehrung. 1965 Z. Mikr. Anat. Forsch. 68, 733-740.
67. Stubblefield, E. & B. R. Brinkley Architecture and function of the mammalian centriole. In K. B. Warren (Ed.) Formation and fate of cell organelles New York: Academic Press, 1967. pp. 175-218.

APPENDIX

The distance between the C tubules of 2 triplet sets which are located on opposite sides of the basal body equals the outside diameter of this organelle. A reduction in the outside diameter occurs when the distance between these C tubules decreases as a result of a decrease in the axial angle of each triplet set. The diagram on the next page schematically shows the superposition of a triplet set (b) at the base (angle = 40° , approximate length 600 \AA) onto the same triplet set (a) at the apex (angle = 10°) of a basal body. Since the angle of the triplet has decreased from 40° to 10° between base and apex, the angle between a and b is 30° . The change in the position of the C tubule which resulted from the angle change is represented by δ . The value of δ represents 1/2 the total outside diameter change; therefore, the total diameter change equals 2δ .

δ is calculated using two trigonometric functions. The value of d (310 \AA), which is necessary for the calculation of δ , is obtained using the law of sines; 600 \AA is the approximate transverse length of the triplet set. Using these two values, δ equals 280 \AA . Therefore, the theoretical diameter change between base and apex is 560 \AA for an angle change of 30° . This value should apply regardless of whether the angle changes by a centrifugal rotation on the C tubule or a centripetal rotation on the A tubule.

Note: Triangle abd is an isosceles triangle, therefore the value of $\angle A$ is calculated to be 75° . The value of $\angle \delta$ was also calculated from the drawing.

Known values

$$\begin{aligned}
 a &= 600 \text{ A}^\circ \\
 b &= 600 \text{ A}^\circ \\
 D &= 30^\circ \\
 \Delta &= 65^\circ \\
 A &= 75^\circ \\
 F &= 10^\circ
 \end{aligned}$$

Calculations for value d

$$\begin{aligned}
 \frac{d}{\sin D} &= \frac{a}{\sin A} \\
 \frac{d}{\sin 30^\circ} &= \frac{600 \text{ A}^\circ}{\sin 75^\circ} \\
 \frac{d}{.5000} &= \frac{600 \text{ A}^\circ}{.966} \\
 d &= 310 \text{ A}^\circ
 \end{aligned}$$

Calculations for value δ

$$\begin{aligned}
 \sin \Delta &= \frac{\delta}{d} \\
 \sin 65^\circ &= \frac{\delta}{310 \text{ A}^\circ} \\
 .906 &= \frac{\delta}{310 \text{ A}^\circ} \\
 \delta &= 280 \text{ A}^\circ
 \end{aligned}$$